ALBERT-LUDWIGS
UNIVERSITÄT FREIBURG

HYDROLOGIE FREIBURG

Jakob Garvelmann

The Characteristic Length Scale of Stable Isotope Variation in Catchments

Chairman: Prof. Dr. Markus Weiler
Supervisor: Dr. Christoph Külls

Freiburg, February 19, 2010

ALBERT-LUDWIGS
UNIVERSITÄT FREIBURG

Jakob Garvelmann

The Characteristic Length Scale of Stable Isotope Variation in Catchments

Referent: Prof. Dr. Markus Weiler
Koreferent: Dr. Christoph Külls

Diplomarbeit unter der Leitung von
Prof. Dr. Markus Weiler

Freiburg, den 19. Februar 2010

Acknowledgements

First, I would like to thank Prof. Dr. Markus Weiler and Dr. Christoph Külls for supervising this thesis, the helpful discussions and for making this work possible.

I would like to thank also Barbara Herbstritt and Klemens Rosin for their dedicated support and their concern for the subject.

A big Thank-you goes also to my fellow students who supported me very energetic during the fieldwork and with interesting discussions.

Especially, I want to thank my family, my friends and Katja for their support and the motivation.

Contents

List of Figures

List of Tables

Abstract

The subject of the thesis presented is the variability of stable isotopes (deuterium and oxygen-18) in hydrological catchments. It was applied a various isotope profile (VIP) approach to study the isotope variability. The potential of the VIP approach for the identification of hydrological hillslope processes was secondary explored.

The study was conducted on a hillslope of a circa 1 km^2 humid catchment. Soil profiles were drilled along two hillslope catenas from near the water divide to the stream in august 2009. The soil cores were divided in soil samples. The isotope signature of the soil water of the samples was determined by water (liquid) - water (vapor) equilibration laser spectroscopy. Boxplots of the isotope data were prepared and the standard deviation was calculated in order to estimate the variability of the stable isotope profiles. Pedological soil properties were defined. The catchment area of the profile points along the hillslope and the flowpath distances within the profile catchments were derived from a digital elevation model. There are different geomorphologic situations at the two study transects. One hillslope catena is slight convex, the other slight concave. This difference is also apparent in the sampled stable isotope profiles. The variability of the profiles along the convex hillslope catena is very similar. A diversity of profile variability was observed along the concave hillslope catena. The profiles in an upslope position had comparable variabilities to the convex hillslope catena profiles. The profiles at the base of the hillslope had the lowest variability. The isotope profiles close to the stream had a higher variability again. The variability in upslope positions and along the convex catena could be explained by a conservation of the isotopic precipitation signal. These profiles have more enriched isotope values near the surface and a winter peak with isotopically depleted soil water beneath. The variability of the profiles in a hillslope foot position, could be explained by an increasing advection and dispersion due to an increase of the flowpath distances. These mechanisms would damp the input signal and thus decrease the profile variability. The increase of the variability close to the stream could be explained by the influence of streamwater.

The point with the lowest variability at the study hillslope could represent a characteristic length scale for the stable isotope variations in the upper vadose zone. There is evidence for a characteristic length scale at the study hillslope with a distance of 200 m from the water divide. The results suggest that the variability of the stable isotope profiles could depend on the flowpath distances to the profile position. Consequently, the variability of stable isotope profiles could be a proxy for the flowpath distance distribution at this point in the catchment.

Zusammenfassung

Die vorliegende Diplomarbeit beschäftigt sich mit der Variabilität von stabilen isotopen (Deuterium und Sauerstoff-18) im hydrologischen Einzugsgebiet. Um die Variabilität zu untersuchen, wurde ein Multi Isotopenprofil Ansatz gewählt. Zusätzlich wurde das Potential dieser Methode zur Identifikation von hydrologischen Hangprozessen betrachtet.

An einem Hang in einem knapp 1 km^2 Einzugsgebiet wurde im August 2009 entlang von zwei Hangcatenen mehrere Bodenprofile von unterhalb der Wasserscheide bis zum Bach gebohrt. Die Bohrkerne wurden in Bodenproben unterteil. Von diesen Bodenproben wurde die Isotopensignatur des Bodenwassers über eine laserspektroskopische Messung der Bodenluft bestimmt. Zur Abschätzung der Variabilität der Isotopenprofile wurden Boxplots der Isotopendaten erstellt und die Standardabweichungen bestimmt. Zusätzlich wurden pedologische Bodenmerkmale bestimmt, sowie die Einzugsgebietsgröße der Profilpunkte und die Fließwegdistanzen bis zu diesem Punkt aus einem digitalen Höhenmodel bestimmt. Die eine Hangkatena hat eine leicht konvexe Form, die andere ist leicht konkav. Dieser Unterschied spiegelt sich auch in den Isotopenprofilen wieder. Entlang der konvexen Hangkatena sind nur sehr geringe Unterschiede in der Profil-Variabilität zu erkennen. Beim konkaven Hangtransekt wurden jedoch sehr unterschiedliche Variabilitäten festgestellt. Die Variabilität der Profile am Oberhang ist vergleichbar mit der Variabilität der Profile am konvexen Hang. Bei den Profilen am Hangfuß wurde eine sehr geringe Variabilität festgestellt. Die Profile in Bachnähe haben wieder eine höhere Variabilität. Die höhere Variabilität der Profile am Oberhang der konkaven Hangkatena, und entlang der gesamten konvexen Hangkatena, kann auf eine Erhaltung des isotopischen Niederschlagssignals, mit isotopisch angereichertem Bodenwasser nahe der Oberfläche und einem in größerer Bodentiefe folgenden Winterpeak mit isotopisch abgereichtertem Wasser, zurückgeführt werden. Die geringere Variabilität der hangabwärtsliegenden Profile könnte mit einer zunehmenden Advektion und Dispersion durch Zunahme von längeren Fließwegen verursacht sein, die eine Dämpfung des Inputsignals bewirken. Der erneute Anstieg der Variabilität könnte mit einem Einfluss von Bachwasser erklärt werden.

Bei der Hanglage mit der geringsten Variabilität könnte es sich um eine repräsentative Länge für die Isotopenvariabilität in der oberen vadosen Zone handeln. Diese hätte, gemessen von der Wasserscheide, eine Länge von 200 m. Die Ergebnisse weisen darauf hin, dass es eine negative Korrelation zwischen der Variabilität der Isotopenprofile und der statistischen Verteilung der Fließweglängen zum jeweiligen Profil gibt. Somit könnte die Variabilität von Isotopenprofilen ein Indikator für die Fließwegdistanzenverteilung bis zu diesem Punkt im Einzugsgebiet sein.

1. Introduction

1.1. General Introduction

The stable isotopes of the water molecule, deuterium and oxygen-18, have been used as tracers in several studies to explore hydrological processes and catchment behavior (Vitvar et al., 2005). The isotopic input of precipitation has a well known characteristic scale of spatial and temporal variability that determines atmospheric boundary conditions (Dansgaard, 1964). The precipitation input signal underlies processes of selection and fractionation within the catchment. An isotopic variability of catchment water components can regularly be observed in humid environments. This variability can clearly be demonstrated by stable isotope time series of soil water, streamwater and groundwater or by hydrograph separation techniques.

Meteorological processes are modifying the isotopic water signature. There are processes affecting stable isotope signature of the water within the hydrological catchment. Pedological properties are influencing the evolution of the signal in the vadose zone. Mixing of water from different storage systems in the catchment has an influence on the isotope signal of streamwater. However, very little is known about the mechanisms and the length scale of the impacts of the catchment itself on the isotopic signature of catchment water.

1.2. Goals of the Study

The subject of this diploma thesis is the investigation of the spatial variability of stable isotopes in hydrological catchments. Since the spatial variation of the meteoric input is well known, it is very interesting to explore the spatial distribution and variability of the isotopic signature of water within the catchment. The idea is to sample soil water profiles at different positions along a study hillslope and to determine the stable isotope signature of the soil water. One precondition should be, that the study hillslope is a representative part of the catchment that covers the whole space from the water divide to the draining stream. This is a scale on which the whole extent of isotope processing should be covered.

Another precondition should be, that there is as little vegetation as possible on the study hillslope. Since interception of precipitation on vegetation covers has a fractionating impact through evaporation on the isotopic input signal reaching the soil surface. Any impact of the vegetation on the stable isotope signal will be ignored.

The aim of this study is to explore the spatial stable isotope variability by drilling soil profiles at various positions along a hillslope from the water divide to the stream. The idea is to analyze the soil samples from the profiles in a high spatial resolution for stable isotopes using laser spectrometry. The following research questions could be investigated with this approach:

- Is there a characteristic length or any other representative unit for the stable isotope variability in catchments?
- Can the variability of the soil water stable isotope profiles be used to define catchment characteristics?
- How powerfull is the approach using various isotope profiles to explore catchment properties and behavior, runoff generation processes and stable isotope variability?

The information of a characteristic length scale would be very auxiliary for designing adequate measurement campaigns. These measurement campaigns could be a powerful tool, to improve the knowledge about runoff generation processes or the quantification of catchment isotope transfer functions.

2. Basic Principles

2.1. Stable Isotopes in Hydrology

The stable isotopes deuterium and oxygen-18 are part of the water molecule. They do not undergo degradation and chemical or physical retardation within the hydrosphere. Because of this attribute, they exhibit an absolute conservative behaviour. The most important natural tracers in hydrology are the stable isotopes of oxygen (^{16}O and ^{18}O) and hydrogen (^{1}H and ^{2}H). The stable isotope species have different molecular masses. For example, deuterium (^{2}H) is heavier than protium (^{1}H) because of one more electron in the nucleus. Clark and Fritz (1997) report that the lighter isotope species of water (^{1}H and ^{16}O) are more frequent in nature than ^{18}O and ^{2}H. ^{18}O and ^{2}H have a frequency of 0.204% and 0.015%, respectively.

The differences in the molecular masses determine temperature dependent fractionation effects at phase changes (Raleigh fractionation). This can be explained because of different vapor pressures of the stable isotope species. The different vapor pressures induce an enrichment of heavy isotopes in the phase with lower energy. For example: at the phase change from water to vapor (evaporation) happens an enrichment of heavier isotopes in the liquid phase because the lighter isotopes have a stronger affinity to change the phase. Comprehensive reviews about the basic principles in stable isotope hydrology and hydrogeology can be found in Moser and Rauert (1980), Clark and Fritz (1997) and Kendall and McDonnell (1998).

Usually, values of stable isotopes are not reported in absolute concentrations. Stable isotope values are usually reported in ratios. The stable isotope ratio R, is the ratio of the infrequent to the frequent isotope. Stable isotope values can be presented in the δ notation. The δ notation (equation 2.1.1) represents a stable isotope ratio relative to a standard in per mill (‰). An international established standard is the Vienna Standard Mean Ocean Water (VSMOW). The stable isotope ratios R of VSMOW are well known and represent (155.75 ± 0.05) * 10^{-6} for deuterium and (2005 ± 0.45) * 10^{-6} for oxygen-18, respectively (Clark and Fritz, 1997).

$$\delta_{Sample} = \left(\frac{R_{Sample} - R_{Standard}}{R_{Standard}} \right) * 1000 \tag{2.1.1}$$

The fractionation factor α is a theoretical factor and is valid for isotopic equilibrium conditions at a certain temperature. α can be calculated from following equation:

$$10^3 ln\alpha = a\left(\frac{10^6}{T_K^2}\right) + b\left(\frac{10^3}{T_K}\right) + c \tag{2.1.2}$$

Whereas T_K is the temperature in kelvin. MAJOUBE (1971) published coefficients for the water-vapor system at temperatures between 0 °C and 100 °C. The coefficients are a = 24.844, b = -76.248, c = 52.612 for deuterium and a = 1.137, b = -0.4156, c = -2.0667 for oxygen-18, respectively. When the stable isotope ratios of a water-vapor system are known, it is also possible to calculate the fractionation factor α as follows:

$$\alpha = \frac{R_{Reactant}}{R_{Product}} \tag{2.1.3}$$

The isotopic signature of precipitation has a well known characteristic scale of spatial and temporal variability because of fractionation effects (DANSGAARD, 1964). The major fractionation effects are:

- **Temperature effect**: The stable isotope fractionation increases with decreasing temperature. Thus, the precipitation is isotopically lighter at high latitudes and in winter than during the summer months or at low latitudes. Furthermore, the temperature during the condensation of vapor in an airmass (warm front or cold front) determines the isotopic composition of the precipitation.
- **Altitude effect**: Mountain ranges cause an orographic uplifting and condensation of airmasses due to lower temperatures with increasing altitude. Heavy isotopes condense preferred, because of a lower vapor pressure. Moreover happens an enrichment of heavy isotopes in the liquid phase during rain. Thus, the precipitation is getting in average lighter with increasing altitude.
- **Continental effect**: The isotopic composition of the precipitation from oceanic airmasses moving over continents is getting continuously lighter with increasing distance from the ocean, because heavy isotopes are raining out first.
- **Intra storm variability**: The precipitation is getting isotopical lighter with increasing duration and intensity of a precipitation event, because of the preferred depletion of heavy isotopes.

A comprehensive review about isotopic variations in precipitation is given by INGRAHAM (1998).

Because of the mentioned fractionation processes, the stable isotope input vary in space and time. The variations of the stable isotopes in precipitation show a strong linear correlation. CRAIG (1961) published an equation for this linear correlation, that is called Global Meteoric Water Line (GMWL) with the equation:

$$\delta^2 H = 8 * \delta^{18} O + 10 \tag{2.1.4}$$

Altitude and seasonal effects as well as intrastorm and interstorm variability are the important effects to study plot scale or meso scale hydrological processes. Thus, the meteoric input has a well known characteristic with lighter (depleted) stable isotope values in winter and heavier (enriched) stable isotope values in summer. This input signal will be modified within the catchment. Catchment characteristics and the internal flow processes provide a space-time filtering by damping out the spatial and temporal variability of the stable isotope input signal (Sivapalan et al., 2001).

The damping of the seasonal meteoric stable isotope variation can be observed in the unsaturated zone with the stable isotopes of the soil water. Regularly there is observed an increased damping of the isotopic input signal with increasing soil depth. This cumulative attenuation of the input signal in the unsaturated zone can be used to calculate mean residence times of the soil water (Maloszewski et al. (1983), Stewart and McDonnell (1991), DeWalle et al. (1997), Wenninger (2007)). The approach is called sine-wave analysis or isotope damping analysis. The idea is to fit a sine-wave to the time series of stable isotopes in precipitation as well as to the isotope data of soil water time series as shown in figures 2.1.1 and 2.1.2 below. Other approaches are based on residence time distribution models (Maloszewski et al. (2002), Asano et al. (2002)). A comprehensive review about transit time modeling was published by McGuire and McDonnell (2006).

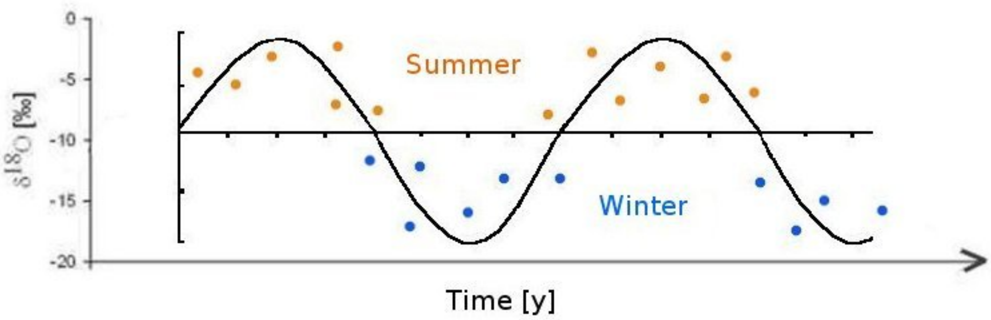

Figure 2.1.1.: Fitted sine-wave to the isotopic precipitation signal with isotopical enriched water in summer and depleted water in winter.

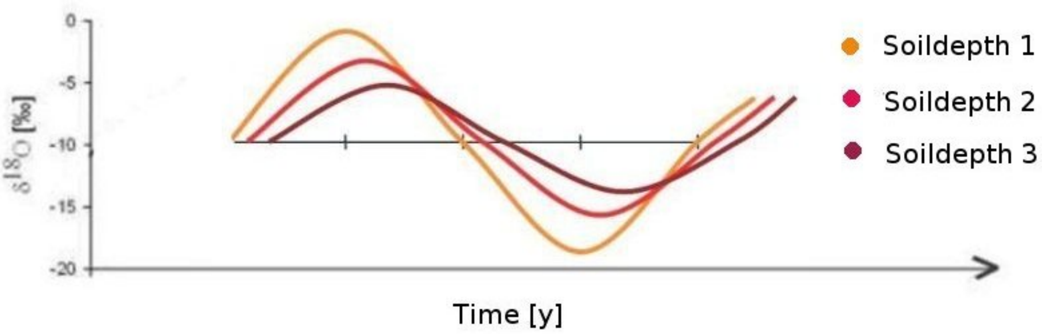

Figure 2.1.2.: Sine-waves fitted to the isotope time series in different soil depths.

The residence time can be calculated after Maloszewski et al. (1983) by using the amplitudes of the isotope sine-wave function in different soil depths:

$$T = \frac{1}{2\pi}\left[\left(\frac{a_{z2}}{a_{z1}}\right)^{-2} - 1\right]^{0.5} \tag{2.1.5}$$

Where T is the mean residence time, a_{z1} and a_{z2} are the amplitudes of the sine-wave function in soil depth 1 and soil depth 2, respectively. 2π of the sine-wave function is according to one year in the stable isotope time series.

$$T = \frac{v}{d} \tag{2.1.6}$$

Where v is the mean flow velocity of the water and d is the mean flow distance of the water. Under the conceptual assumption that the flow velocity is constant, T is proportional to the mean flow distance d. Thus, the mean residence time T can also be an indicator for flow distances within catchments.

2.2. Variability and Scales in Hydrology

The term scale describes a characteristic time or a characteristic length (Blöschl, 1996). Hydrologic processes usually have a characteristic spatial scale and a characteristic temporal scale as shown in figure 2.2.1 (Blöschl and Sivapalan, 1995).

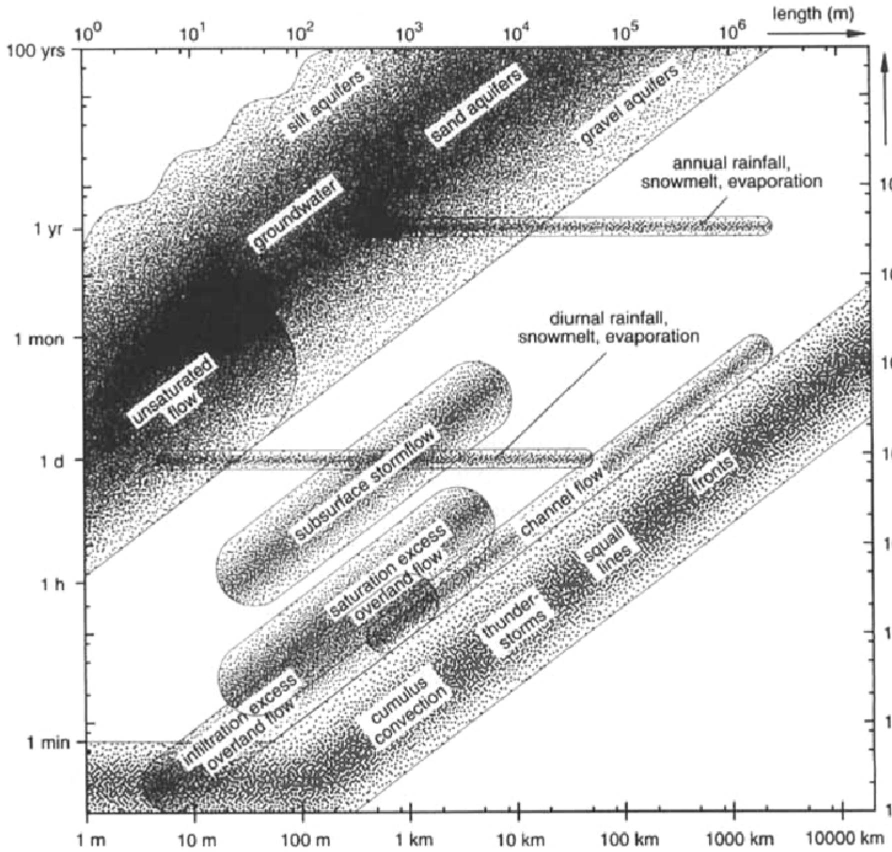

Figure 2.2.1.: Hydrological processes at a range of characteristic space scales and timescales (Blöschl and Sivapalan, 1995).

This schematic concept of characteristic space scales and timescale of hydrological processes may help to design experimental measurement campaigns. The basic consideration is that a measurement should approximately match the process of interest. On a theoretical basis the spatial as well as the temporal dimensions of measurements can be characterized by a) a spatial (temporal) extent of a data set, b) the spacing between the samples and c) the support (integration volume/time) of a sample. These three scales are called the scale triplet and are shown in figure 2.2.2 (Blöschl and Sivapalan, 1995).

The spacing of a measurement campaign refers to the distance between the sampling points or the time interval between the samples (sampling interval). The extent refers to the total plot that has been sampled or the total sampling time (length of record). The term support refers to the volume or timestep of a sample (averaging interval). The measurement of a process should be conducted on an adequate scale to gain

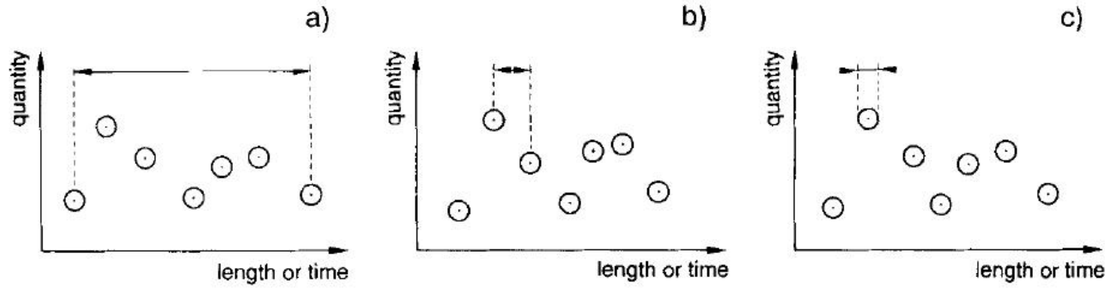

Figure 2.2.2.: Scale triplet: a) Spatial/temporal extent, b) Spacing (=resolution), c) Support (=integration volume/time) (Blöschl and Sivapalan, 1995).

information about the variability of the considered process. In reality this is not always possible, respectively the process scale is not known. Thus, measurements will not reflect the whole variability (Woods, 2005). If the spacing of the data is too large, there will be a discontinuity in the data and the small-scale variability will not be captured. If the extent of the data is too small, there will appear a trend in the data because the large-scale variability will not be captured. There can be observed a smoothing out of the variability, if the support is too large (Blöschl and Sivapalan, 1995).

In space, typical modeling or working scales are: the local (plot) scale, the hillslope scale, the catchment scale and the regional scale (Blöschl and Sivapalan, 1995). Becker (1992) distinguished between different scales: the microscale ($< 1\ km^2$), the mesoscale ($< 1000\ km^2$), and the macroscale ($> 1000\ km^2$) for a simplification. In time, there can be distinguished between the event scale (1 day), the seasonal scale (1 year), and the long-term scale (100 years) on the modeling or working scale (Blöschl and Sivapalan, 1995).

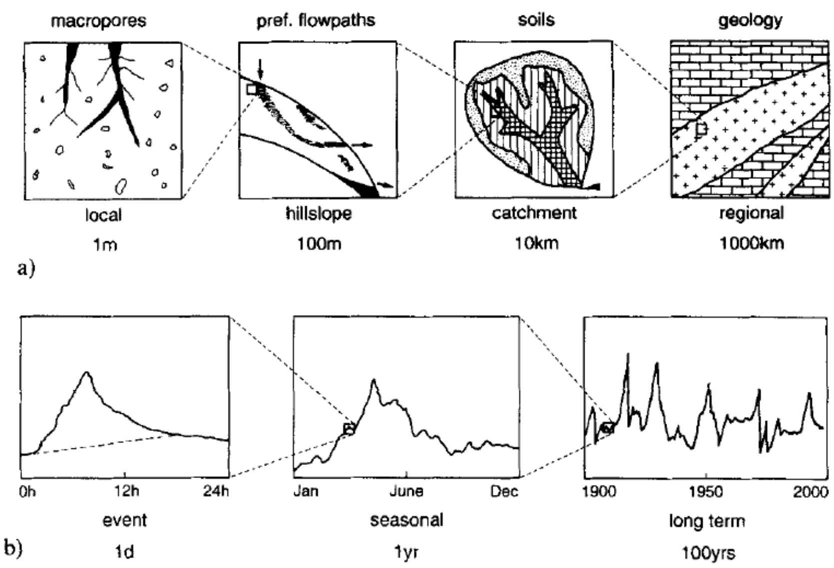

Figure 2.2.3.: Typical a) spatial and b) temporal scales in hydrology (Blöschl and Sivapalan, 1995).

A common approach in hydrological sciences is to upscale or to downscale data or process knowledge. That means that a process which was investigated, or data that was collected on the plot scale will be upscaled to a broader scale. The other way around, it is possible to downscale from larger scales. Blöschl (2005) gives a comprehensive review about statistical scaling in hydrology.

In natural catchments one can observe heterogeneity and variability in space and time. Whereas heterogeneity describes media proberties (e.g. hydraulic conductivity) that vary in space. Variability is used to describe fluxes (e.g. runoff) or state variables (e.g. soil moisture) that vary in space and/or time. Blöschl and Sivapalan (1995) defined typical scales of spacial heterogeneity (local scale, hillslope scale, catchment scale and regional scale) as well as typical scales of temporal variability (event scale, seasonal scale and long-term scale). Figure 2.2.3 shows that heterogeneity at the catchment scale may relate to different soil types and their properties. Similarly, variability in time is also present at a range of scales. Variations in time and space in hydrologic systems are typically driven by variations of physiographic factors such as climate, soils, vegetation, topography, geology and by human and animal activity. A big challenge and scientific aim is to combine temporal and spatial variability to describe space-time variability of hydrological systems (Woods, 2005).

2.3. Concepts of Dealing with Variability

Variability complicates the investigation, the theoretical analysis, the measurement, as well as the modeling and conceptualization of hydrological processes. Characteristic scales are a concept to deal with variability and heterogeneity over many orders of magnitude (e.g. Skoien et al. (2003), Woods (2005)). Instead of dealing with a spectrum of lengths and times a characteristic scale is a length or time that is representative for a process. A characteristic spatial scale is the scale over which a parameter or a process can be averaged. The idea is that the details of finer-scale heterogeneity can be neglected without losing important information about a process. Skoien et al. (2003) investigated characteristic space scales and timescales of precipitation, runoff and groundwater levels in Austria using variogramm analysis. This is a geostatistical approach to determine characteristic scales.

The representative elementary volume (REV) is a model used in fluid dynamics, soil sciences and hydrogeology. The REV is the minimum volume of a porous medium (e.g. soil sample) required from which a given soil parameter measurement becomes independent of the size of the sample. The REV is the volume over which a parameter can be statistical averaged. For homogeneous soil material the REV is smaller than for heterogeneous soil. Below a REV the parameter is not defined and the material can not be treated as a continuum (Bear, 1972). Bear and Bachmat (1984) (in VandenBygaart and Protz, 1999) concluded, that in an isotropic medium a REV is well represented by a representative elementary area (REA). That means that in two dimensions the REV can be replaced by a REA. Figure 2.3.1 shows a schematic representation of the REV/REA concept.

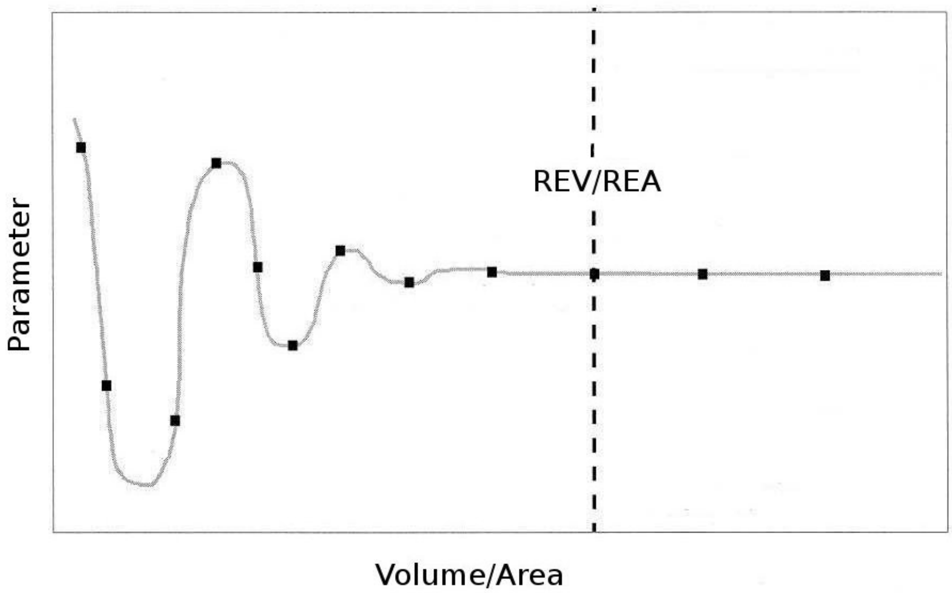

Figure 2.3.1.: Schematic illustration of the REV/REA concept (after VANDENBYGAART and PROTZ (1999)).

The REA concept has been applied to spatial heterogeneity and scale problems in catchment hydrology by WOOD ET AL. (1988). They plotted normalized subcatchment discharge versus the subcatchment area. Up to an area of approximately 1 km^2 one can observe variation in the data. The observed 1 km^2 are the minimum area of the catchment at which the average hydrological response varied minimal with increasing drainage catchment size. Thus, they concluded that this area is a REA for the investigated catchment.

The REA is strongly influenced by the subcatchment topography. The REA idea was further investigated and its utility for distributed rainfall-runoff modeling was studied (e.g. WOODS ET AL. (1995) BLÖSCHL ET AL. (1995)). WOODS ET AL. (1995) concluded that the existence and size of the REA will be specific for a particular catchment and a particular application. BLÖSCHL ET AL. (1995) suggested that the size of the REA depends on specific catchment properties and climatic conditions. DIDSZUN (2004) argues that the REA concept is a simplification of the processes within a catchment.

The idea of a representative elementary watershed (REW) for catchment modeling was presented by REGGIANI ET AL. (1998). The idea is to divide the whole watershed into smaller discrete units (REWs). The averaging of the conservation equations is carried out over the REW. The system contains a large amount of spatial variability at scales smaller than the REW. REWs are assumed to be fundamental units of discretization in space and small-scale variability can be neglected. Variability is examined only between various REWs.

3. Review

The isotopic composition of precipitation is the input signal for terrestrial stable isotope studies. The formation of precipitation determines the isotopic composition of the precipitation water. A knowledge of the temporal and spatial variations in stable isotope ratios of precipitation is important for isotope studies in hydrology (Ingraham, 1998). The basic principles and processes (section 2.1) that induce these variations are well known and provide boundary conditions for stable isotope studies.

Stable isotope profiles of soil water can be used to investigate and to determine pedohydrological processes, including infiltration, mean transit (residence) times, recharge and evaporation. The infiltration of precipitation through the unsaturated zone is an isotopical non-fractionating process. A certain enrichment of heavy isotopes of the infiltration water may occur due to evaporation. Evaporation happens during interception of precipitation on plant covers and in shallow soil depths. Evaporation has also a fractionating effect to ponding water. The extent of soil evaporation is dependend on atmospheric boundary conditions and soil characteristics (Gonfiantini et al., 1998). Transpiration is described in Zimmermann et al. (1967a) and Allison et al. (1984) (in Gehrels et al., 1998) as a non-fractionating process.

In humid and semi-arid environments the prevailing or net movement in the vadose zone is to the water table. Piston flow is an insufficient way to describe water movement in the vadose zone. In a uniform piston flow system the percolating water would preserve its isotopic signature, because dispersion and mixing is neglected. The downward velocity is usually distributed around a mean value. The distribution of the velocity depends on various factors:

- The heterogeneous grain-size distribution of soil material. This distribution controlls the tortuosity of the flowpaths.
- The vertical and horizontal permeability variation. Whereas the vertical permeability variation is more pronounced.
- Preferential flow paths and the water holding capacity of the soil

Because of these and other processes, the stratification of meteoric water input with its characteristic seasonal isotope signature can usually not be preserved in the unsaturated zone for more than one year (Gonfiantini et al., 1998).

Zimmermann et al. (1967b) showed under steady-state conditions (saturated soil column) in a sprinkling experiment with isotopical labeled water, that isotopic variations in the precipitation are damped in soil water by hydrodynamic dispersion when moving through the soil profile. They showed that the meteoric variations are traceable up to a certain soil depth. Zimmermann et al. (1967a) could also show, that the enrichment of deuterium in the soil water of the saturated soil column decreased exponentially with depth.

Stable isotope variations in soil moisture of the vadose zone are established in both, liquid and gaseous phases along vertical profiles. This is a consequence of the isotopic fractionation that happens during phase changes and the different diffusion rates of isotopic molecules (Gonfiantini et al., 1998).

Barnes and Turner (1998) explain the development of oxygen-18 and deuterium profiles. The processing of liquid phase stable isotopes moving in the unsaturated zone can be explained by convection, hydrodynamic dispersion and molecular diffusion. Water and stable isotope fluxes in the vapor phase can be described by Fick's law of diffusion for ideal gases. Fractionation of stable isotopes happens due to diffusivity differences and differences in the saturated vapor pressure between diverse stable isotope species. In arid environments or catchments with a high proportion of saturated or near-saturated areas, evaporation can have a big impact on the isotopic signature of runoff and groundwater. In humid environments the impact of evaporation on the isotopic output signal is usually small. Mixing and dispersion alter the meteoric input signal in humid environments (Barnes and Turner, 1998). These processes lead to an attenuation of the meteoric input signal with increasing soil depth in humid environments. McConville et al. (2001) note that different flow mechanisms have an impact on the formation of stable isotope profiles. Gehrels et al. (1998) showed that the seasonal cycle of isotopic composition in precipitation, characterized by lighter values in winter (winter peak) and heavier values in summer (summer peak), can be traced back in the soil to a depth of a few meters. The seasonal fluctuation moves around the mean annual isotope content of precipitation, tending closer to the average as soil depth increases. Recharge waters from successive seasons can be identified in a soil system were piston flow in vertical direction is the dominant flow mechanism. Usually there are preferential flow mechanisms and other processes in natural soils that alter the isotope signal. Gehrels et al. (1998) suggest that diffusive attenuation and dispersion of the isotope signal through preferential flow mechanisms has to be expected.

Models can simulate the behaviour of soil water isotope profiles (Braud et al., 2005). It is possible to describe and simulate the processes that generate a soil water stable isotope profile at the plot scale (Barnes and Turner, 1998). Several studies used stable isotope soil water profiles to study infiltration and recharge processes (e.g. Saxena (1984), Darling and Bath (1988), McConville et al. (2001)).

Gazis and Feng (2004) showed that soil water stable isotope profiles vary on a small scale. They published data from isotope profiles at various positions on the same hillslope and showed significant isotope variations depending on local soil characteristics (variations in soil textures, variations in soil moisture etc.).

The major aspects of isotopic exchange in soil water are well understood on the laboratory scale (Barnes and Turner, 1998). The next step is to transfer this knowledge to broader scales. Thus, to understand how these processes are integrated at the hillslope and catchment scale.

There has been several studies to explore isotopic variations at the plot scale. The situation is less clear at the hillslope scale. There are a lot of additional processes leading to a modification of the stable isotope input signal. There can be observed various mechanisms of water movement in vertical and lateral direction (e.g. unsaturated matrix flow, preferential flow, or transmissivity feedback mechanisms). Beven (2006) provide a benchmark paper collection of streamflow generation processes.

McDonnell et al. (1991) showed by means of suction lysimeter soil water stable isotope data from various topographic positions along the Maimai M8 catchment (North Westland, New Zealand) that the age of subsurface water increases considerably in downslope direction. This lateral aging of soil water happens due to a constant movement of soil water in the soil matrix between storms. The water movement in the Maimai catchment is controlled by almost unpermeable bedrock and shallow soil that induce a lateral movement of water along the hillslopes. In a small japanese catchment with weathered bedrock material, Asano et al. (2002) identified a vertical aging of water. Modeling results from Stewart and McDonnell (1991) suggest an age of more than 100 days for soil water in near stream zones and 14 days for soil water in upslope zones. The increase in soil water mean residence time in downslope direction can be explained by a continual mixing and progressive displacement of subsurface water. That was also shown by Horton and Hawkins (1965) and Zimmermann et al. (1966) with tritiated water. Stewart and McDonnell (1991) showed that deuterium variations in soil water samples were considerably delayed and damped compared to the local precipitation signal. This indicates significant storage time and mixing with soil water. Soil matrix water at shallow soil levels in unsaturated soils was relatively responsive to fresh rainfall input, but deeper soil water and water near the stream showed much less variation.

It seems that bedrock permeability and soil depth have an effect on the aging direction of unsaturated zone water (Stewart and McDonnell (1991), Asano et al. (2002), Uchida et al. (2006)). McGuire et al. (2005) could show that landscape organisation (i.e. topography) of a catchment has a greater effect on residence time than the catchment area has.

Kendall et al. (2001) explored the spatial and temporal variability of the amount and isotopic composition of soil water, groundwater and subsurface flow along the Hydrohill catchment in China. The Hydrohill catchment is an artificial catchment with extensive instrumentalization, that propose the possibility to study internal catchment processes. The study showed, that downslope transport of infiltration water through macropores, displacement of pre-event unsaturated zone water by matrix flow, and mixing of these two components cause a temporal and spatial variability in the isotopic compositions of interflow, saturated flow, groundwater, and post storm unsaturated soil water along the Hydrohill catchment.

4. Study Area

4.1. Catchment

Figure 4.1.1.: The Waldbrunnertal valley.

The study area is located about 5 km north of Freiburg im Breisgau on the foothills of the middle Black Forest, in a valley called Wildtal. The Schobbach is draining the 9.25 km^2 (WaBoa, 2007) Wildtal valley. The study was conducted in a 0.94 km^2 subcatchment of the Schobbach catchment, called Waldbrunnertal. The highest point in the Waldbrunnertal catchment is called Uhlberg (617.8 $m\,a.s.l.$) and marks the southern water divide. The lowest point of the catchment is near the farmhouse Schümperlehof at 271.3 $m\,a.s.l.$. Thus, there is a maximum vertical height of 357.8 m in the catchment. The highest point on the western divide is a castle ruin called Zähringerburg (480 $m\,a.s.l.$). The recent land use within the study catchment is 62.7% of mixed forest with mainly beech (*Fargus silvatica*), fir trees (*Abies ssp.*) and spruce (*Picea ssp.*), 35.5% grassland and meadows, 1.5% vine and about 0.3% is sealed (farmhouses of Waldbrunnerhof and Schümperlehof and street).

Contrary to most of the Black Forest area, the Wildtal valley, as well as the Waldbrunnertal valley was not formed by glacial processes. The v-shape of the valley was formed by fluvial processes at the end of the Würm glaciation (Metz, 1997).

The first settlement and agricultural use in the Wildtal area happened in the 10th or

11th century (Müller, 2008). The development of the land use between 1774 and 1998 is well documented by Abel (1998) in form of land use maps from 1774, 1888 and 1998. People startet to cultivate fruit orchards mainly with apple trees and pear trees during the 18th century. Under the trees people also practiced tillage and used the orchards as grassland. To cultivate the orchards people constructed terraces (Stufenraine) parallel to the contour lines. Nowadays some of these structures are still part of the landscape but some of them are vanished because of landscape fillings or levelling tasks. The clear structure of the terraces is also trampled down from beef and cow at some places (Abel, 1998).

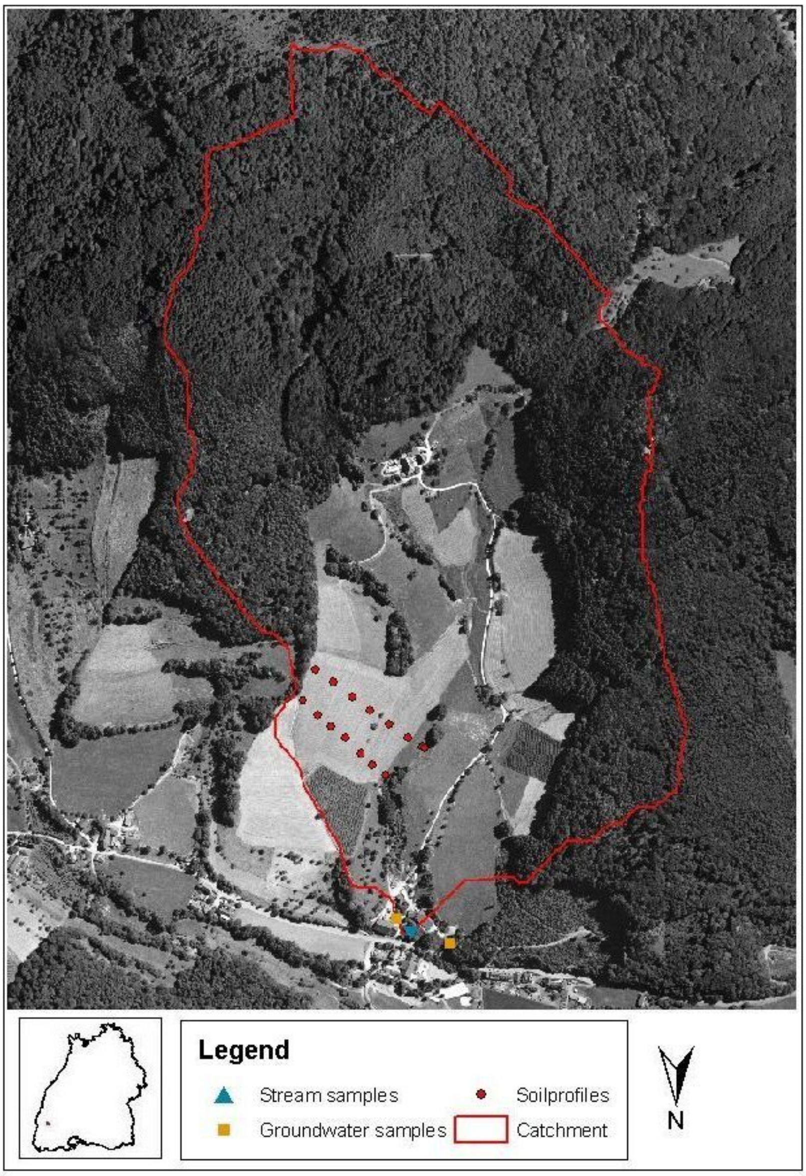

Figure 4.1.2.: Waldbrunnertal catchment with the sampling locations.

4.1.1. Climate

The study area is characterized by a temperate climate. The area is in the scope of the cyclonal westwind drift. The climate is affected by a frequent exchange of subtropical airmasses comming from west and subpolar airmasses. An increase of mean annual precipitation with altitude can be observed in the whole Black Forest area. Precipitation patterns can also be affected by local topographic effects as luv-lee effects (Uhlenbrook, 1999). The summer months are dominated by convective storms, whereas climate of the winter months is usually more affected by passing fronts.

There is a meteorological gauge in the lower Glottertal (400 $m\,a.s.l.$). A valley that is also aligned in east-west direction and about 6 km northeast from the study area. Trenkle (1988) published meteorological data from the Glottertal for the period 1931-1960. The mean annual precipitation for this period was 1069 mm with a maximum of precipitation in the months june to august. The valleys that open out into the Rhine river plaine generally have a mild climate. Because the cold air from the higher ranges can flow out of the valleys. Thus, the mean annual temperature for the Glottertal (1931-1960) is 9 $°C$. The difference between the warmest and the coolest month is 17.5 $°C$. The sunshine duration for the region ranges between 1750 and 1800 hours per year (Trenkle, 1988). Another meteorological station is located southwest about 5 km away (Freiburg-Herdern, 255 $m\ a.s.l.$) The mean annual precipitation for the period 1961-1990 is 1001 mm with a maximum of precipitation during the summer months (Mühr, 2009). Mean annual temperature for Freiburg-Herdern (1961-1990) is 10.3 $°C$. The relatively high precipitation in the study area can be explained by accumulation effects of airmasses at the mountain ranges.

It is very difficult to give a distinct information about evaporation in the study area. After WaBoa (2007) the mean annual evaporation for the area is 600 mm. The mean annual potential evapotranspiration was calculated from Mehlhorn (1998) for the Brugga catchment. The yielded value is 660 mm. Krause (1995) (in Uhlenbrook, 1999) calculated with the Penman equation a maximum evaporation rate of 8 $\frac{mm}{d}$ for south facing terrain in the Black Forest area. This rate is probably the absolute maximum because of the energy budget.

4.1.2. Geology

The Black Forest mountain range emerged during the Terciary. The Oberrhein rift valley was formed by depression, whereas the Black Forest was uplifted. The depression and the uplift caused several dislocations. The fault that divide the Black Forest bedrock and the mesozoic material of the Oberrhein rift valley runs close to the Wildtal embouchure (Groschopf and Schreiner, 1980).

The bedrock geology of the study area mainly consists of paragneiss. Rock forming geological material has been several gneiss species. The metamorphic paragneiss has been formed during the caledonian orogenesis in the Ordovician (circa 450 million years ago) by fusion of marine sediments (GEYER and GWINNER, 1991). There are also some granits and amphibolits in the catchment as well as sphalerit and iron ore in the area around the Zähringerburg (GROSCHOPF and SCHREINER, 1980). The iron ore was exhausted in the Waldbrunnertal from the 16th century through 1804 (MÜLLER, 2008).

The hydrogeology of the bedrock is determined by a system of connected fissures. These fissures are preferred flowpaths. Immobile matrix water reaches only by diffusion the mobile fissure system (STOBER, 1995). After STOBER (1995) the gneiss bedrock volumetric porosity is between 0.1% and 2.1%. The hydraulic conductivity range from 10^{-10} $\frac{m}{s}$ to 10^{-5} $\frac{m}{s}$. Baseflow components originate from the fractured bedrock and the deeper parts of the weathering zone, whereas the weathering zone and the periglazial drift covers generate fast as well as slower runoff components (UHLENBROOK, 1999).

Run-of-hill scree at the foot of steep hillslopes is not mapped for the study catchment. The valley floor is filled with alluvial clay that can have a depth of more than one meter (GROSCHOPF and SCHREINER, 1980).

4.1.3. Pedology

Typical soils in the catchment are cambisols, leptosols and alluvial soils.

Periglacial layers of debris have been formed in the Pleistocene by mechanical weathering under freezing temperatures. These layers occur at gentle to moderate sloping hillslopes in the catchment and are the basic material for soil development in this zone (HÄDRICH ET AL., 1988). The layers of debris have a thickness of 1-2 m at the hillslopes. The debris layers in the study area can be divided into three zones. Over the bedrock is a zone with grain sizes from grit to boulder, depending on the degree of physical and chemical weathering. Overlaying is a zone produced by a conclomerate of ice and soil that slid downslope in the Pleistocene. The topmost layer in the study area is an achievement of shallow melting permafrost soils whose melting water could not percolate vertically. This layer usually has a depth of 40 cm to a maximum of 150 cm. The content of bedrock material is between 10% and 40%. The remaining material is fine sand, coarse silt and Aeolian loess (HÄDRICH and STAHR, 1997).

Basic bedrock can be found at very steep, mainly south sloping hillslopes (HÄDRICH and STAHR, 1997). At these locations one can expect leptosols or leptosol-campisols.

The gentle to moderate sloping hillslopes capture the main part of the Waldbrunnertal catchment. HÄDRICH ET AL. (1988) describe the soils of this unit as cambisol-luvisols and luvisol-cambisols. These soils developed from bedrock or solifluction debris without clay or loess content or solifluction debris with a clay-loess content. This material was blown in by western winds during cool eras in the Pleistocene. In the course of the soil development the Aeolian material was decalcified and mixed with debris (HÄDRICH and STAHR, 1997). After the decalcification, the dislocation of clay took place. Nowadays these soils are acidic and they alter to cambisols. Currently they are called cambisol-luvisol with a Ah-A1-Bvt-Cv profile. The bulk density is moderate with a good budget for soil water and soil air. The nutrient budget is limited. At locations were loess is still obtained, the soils are called luvisol-cambisol with an Ah-B1v-Btv-Cv profile (Hädrich et al., 1988).

At the lower parts and the hillslope foots happened a compaction of soil material by settling and dislocation of clay. Especially during the winter and spring time precipitation and hillslope water can not infiltrate completely. Because of the deficiency of air, soils with impounded water have developed. The major soil units are pseudogleys (stagnosol with a Ah-Sw-Sd profile) and stagnosol-luvisols (Ah-SwA-SdBt-C profile). The water supply in summer is very deficient and soils become dry. The floodplain sediments in the valley floors have a sandy-loamy or sandy-loamy-gritty texture. Under phreatic conditions they evolve into oxigleys and gleys (Hädrich et al., 1988).

4.1.4. Hydrology

There exist no hydrological data for the Wildtal catchment because there is no stream gauge in the valley. Engelbrecht (2008) describe that heavy rain in the Wildtal valley can lead to floods in the Schobbbach from time to time that cause slight damages in the upper parts of the small village Wildtal. Personal observations and conversations with local farmers indicate that the Schobbach, as well as the Waldbrunnertal stream show a fast reaction to precipitation, especially when the catchment is in a condition of high antecedent moisture. The stream runs partially in an artificial pipe. This task was conducted around 1960 to obtain additional pasture land.

4.2. Study Hillslope

The study was conducted on a hillslope (figure 4.2.1) in the Waldbrunnertal catchment. The hillslope is located right hand side of the little stream in the lower part of the catchment. The hillslope is used as meadow and rangeland. There are only some trees on the divide. The remaining area of the hillslope up to the stream is grassland, except one single apple tree in the middle of the hillslope and some trees around the stream at the northern base of the hillslope. The study hillslope span from about 290 $m a.s.l.$ at the stream to about 360 $m a.s.l.$ at the water divide. That makes a difference in altitude of 70 m. The hillslope has an extent of about 250 m from the divide to the stream with a north-west aspect. The already mentioned artificial pipe in the Waldbrunnertal valley ends above the hillslope and the stream runs naturally along the study hillslope downstream.

The upper part of the study hillslope (from the trees on the water divide to the altitude of the single apple tree) is denoted in the landuse map from 1774 as rangeland

Figure 4.2.1.: Study hillslope in the Waldbrunnertal catchment.

and grassland. Between 1774 and 1888 the land use changed to tillage, because this land use form is mapped in the 1888 map. The fields were traditionally tilled parallel to the hillslope. Another land use change to rangeland and grassland happened 50 years ago. The lower part of the study hillslope was always used as rangeland or grassland. In this part, however, happened an anthropogenetic filling and levelling around 1960 (personal conversation with the Schümperlehof farmer Christoph Blattmann).

The bedrock at the study hillslope is described by GROSCHOPF and SCHREINER (1980) as bulky bright paragneiss with a fine-grained to small-grained configuration. The schistosity is often very fuzzy, but can sometimes be identified by tiny biotite aggregates. Alluvial clay is mapped around the stream at the valley floor (GROSCHOPF and SCHREINER, 1980).

5. Soil Properties

5.1. Material and Methods

5.1.1. Soil Sampling

The field work was conducted in august 2009. It was warm and sunny with no significant precipitation events during this time. There was some rain at the beginning of august and a very small thunderstorm in the night prior to the last sampling day.

Soil cores had been sampled along two hillslope transects, labeled as Wild/P1 and Wild/P2, at the study hillslope from near the water divide to the stream with a spacing of circa 40 m as shown in figure 5.1.1 below.

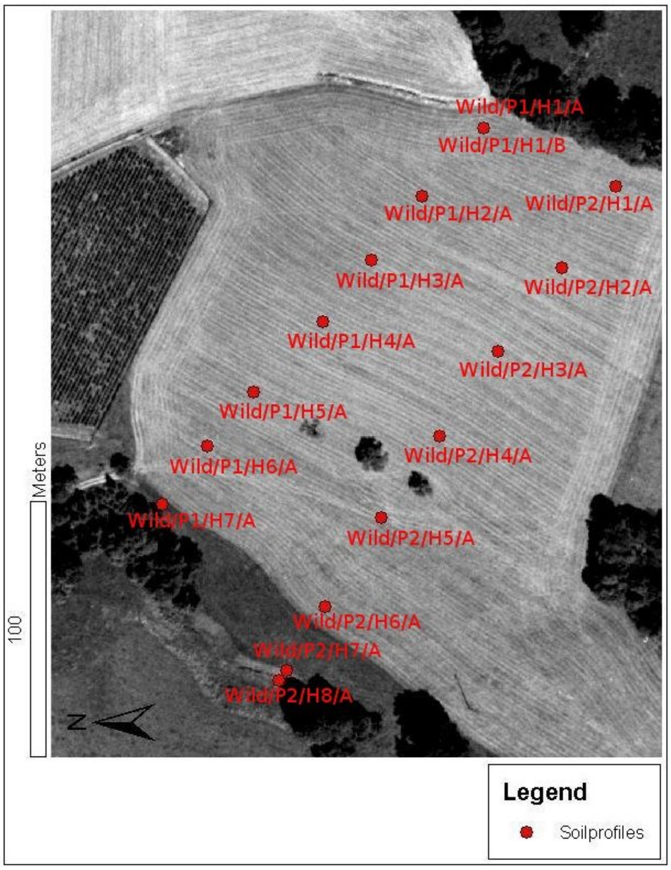

Figure 5.1.1.: Sampling points along the study hillslope.

Figures 5.1.2 and 5.1.3 show the two cross sections along the study hillslope. The two hillslope cross sections are comparable in lenght, height and mean slope. The transects differ in their geomorphology. Cross section (catena) Wild/P1 has a slight convex shape, whereas cross section (catena) Wild/P2 exhibit a concave morphology.

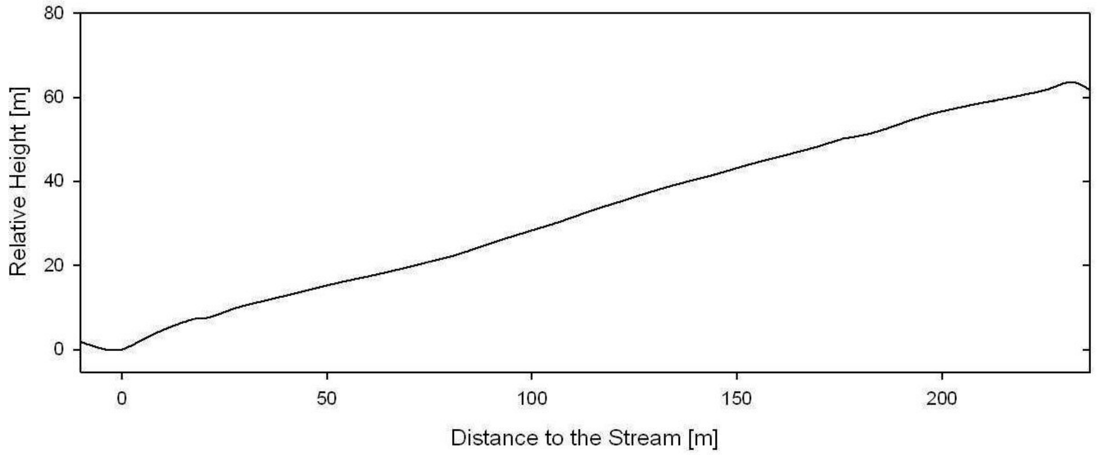

Figure 5.1.2.: Cross section Wild/P1 with distance and relative height to the stream.

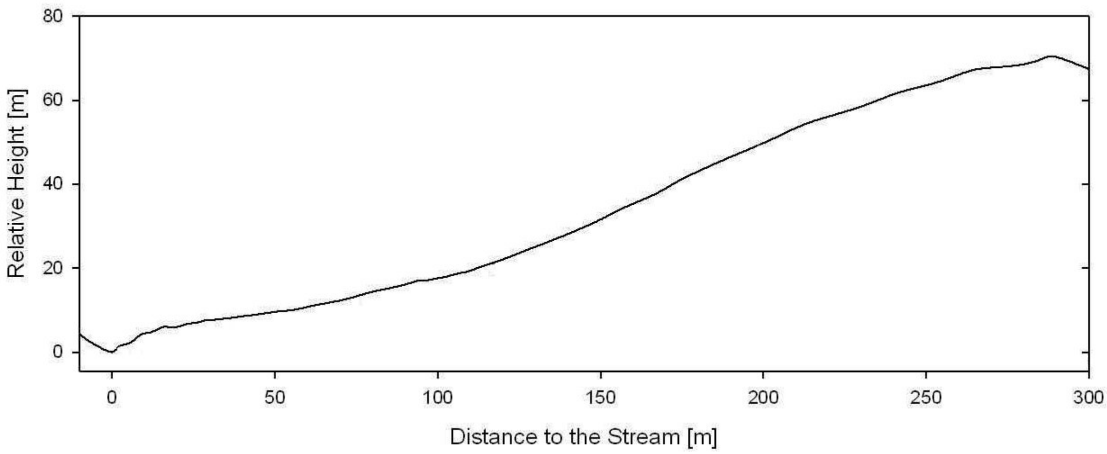

Figure 5.1.3.: Cross section Wild/P2 with distance and relative height to the stream.

The extent of the sampling campaign (distance from the stream to the water divide) was nearly 250 m for hillslope transect Wild/P1 and 280 m for Wild/P2, respectively. The profile positions on the hillslope were mapped with a GPS device. Distances from the stream to each soil profile and profile depths are shown in table A.1 added to the appendix A.

The sampled soil cores had a diameter (support) of 4.5 cm (figure 5.1.4) and were extracted using a cobra percussion drill (Typ 148, *Atlas*). The compaction of soil cores because of the drilling procedure was neglected.

The soil cores were partitioned in soil samples (soil sample lengths shown in table A.1). It was tried to divide the soil cores as accurately as possible to get identical soil sample volumes. Soil samples were subsequently packed in labeled double zipper

Figure 5.1.4.: Cobra percussion drill and soil core at profile Wild/P1/H2/A.

Ziploc bags. This procedure was done as efficient as possible to avoid evaporation. Soil characteristics of the soil cores were notedin the field book. These observations are important to identify soil types and pedophysical properties. The Ziploc bags were closed after extruding interior air. Soil cores were stored in a standard cool box for the transport to the IHF (Institute of Hydrology Freiburg) laboratory.

5.1.2. Soil Moisture

In the IHF laboratory soil samples were immediately weighted to get their moist mass ($m_{sample,wet+Ziploc}$). After the stable isotope analysis (section 7), the soil samples were dried in a drying stove at a temperature of 60 °C. The drying time of the soil samples in the stove was between 4 and 11 days. The soil samples were dried at 60 °C, instead of 105 °C, because the soil samples were dried in opened Ziplocs. A temperature of 105 °C is too high for the Ziplock plastic bags. After drying the soil samples were weighted again ($m_{sample,dry+Ziploc}$). Additionally, the weight of some empty Ziplocs was measured (m_{Ziploc}) in order to specify net weights:

$$m_{sample,wet} = m_{sample,wet+Ziploc} - m_{Ziploc} \tag{5.1.1}$$

$$m_{sample,dry} = m_{sample,dry+Ziploc} - m_{Ziploc} \tag{5.1.2}$$

The moisture of the soil samples was determined as gravimetric soil moisture. Gravimetric soil moisture can be indicated in weight percent (weight %) relative to the dry soil sample (Hartge and Horn, 2009). Gravimetric soil moisture was calculated with following equation:

$$weight\% = \frac{m_{sample,wet} - m_{sample,dry}}{m_{sample,dry}} * 100 \tag{5.1.3}$$

The volumetric soil moisture (θ) and the bulk density of a soil sample can be determined for a soil sample with a known volume. Even though, it was tried to sample equal soil volumes, the soil sample volumes vary significant. That makes an accurate identification of θ and the bulk density of the soil samples very incorrect.

5.1.3. Soil Texture

A grain size analysis is fundamental in soil sciences. The grain size distribution is a good indicator for approximate values of the water budget as well as the air budget within a soil (Hartge and Horn, 2009). The soil texture of the soil samples was determined for some samples along each soil profile.

A grain size distribution analysis is usually done with soil material having a diameter smaller than 2 mm. Thus, it was tried to seperate this material from the samples. A corrosion of organic matter with sodium-pyrophosphate ($Na_4P_2O_7$) was not arranged. Soil material smaller than 2 mm can be divided in following fractions: Sand (2-0.63 mm), Silt (0.63-0.002 mm) and Clay (0.002-63 nm). Soil textures usually are indicated in letters: T=clay, t=clayey, U=silt, u=silty, S=sand, s=sandy, L=loam, l=loamy. The soil texture can finally be determined by considering the grain size distribution. This can be done with a cumulative curve of the grains or with triangle diagrams of the grain sizes (Scheffer and Schachtschabel, 2002). The contingent of a soil fraction can be determined by filtering with different mesh sizes or sedimentation techniques. Another technique is called the finger-technique. With this technique one can determine the soil texture from criteria like plasticity, the ability to roll the sample and the coarseness of a moistened soil sample.

The grain size analysis was conducted using the finger-technique with a special triangle diagram for this technique. The analysis was performed as follows: soil material coarser than 2 mm was removed from the soil material. Thereafter, the soil material and the including soil aggregates were pestled in a mortar. This procedure can exhibit a source for errors. Because weathered bedrock material that looks like a soil aggregate can be degraded to smaller grains (Hartge and Horn, 2009). After pestling, the soil material was wetted and the soil texture was identified with the finger-technique. It has to be considered, that this is a very subjective technique providing a realistic dimension for the soil texture of a sample (Scheffer and Schachtschabel, 2002).

The characterisation of the soil, in regard to soil hydraulic properties was conducted by means of published values from Rawls and Brakensiek (1989) and AG-Boden (1994) (in Scherrer, 2006) for saturated hydraulic conductivity.

5.2. Results

The following section provides the results of the the soil moisture and soil texture analysis. A comprehensive description of soil characteristics noted during the field work is added to the appendix A. The designation of soil types is based on the observations in the field, the soil texture analysis and descriptions of Hädrich et al. (1988) and Abel (1998).

5.2.1. Soil Moisture

Soil moisture data is denoted in weight percent relative to the dry soil samples and is shown in figures 5.2.1 and 5.2.2 below.

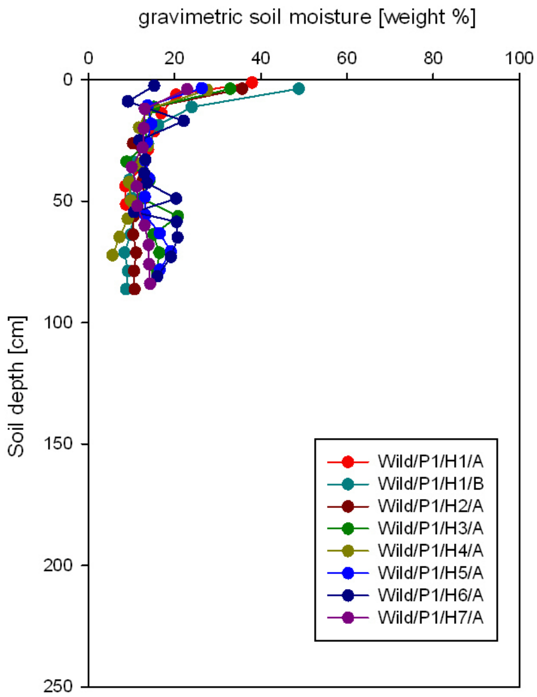

Figure 5.2.1.: Soil moisture profiles along hillslope line Wild/P1.

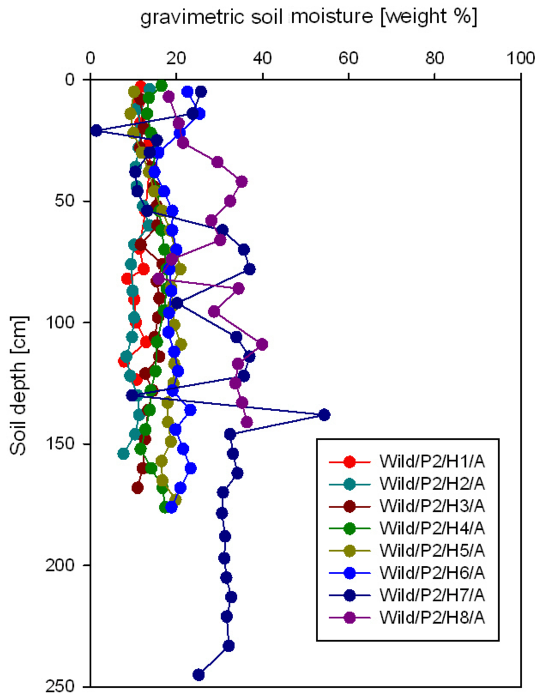

Figure 5.2.2.: Soil moisture profiles along hillslope line Wild/P2.

The gravimetric soil moisture shows similar values between 10% and 20% for most of the soil profiles. Soil profiles Wild/P2/H7/A and Wild/P2/H8/A at hillslope transect Wild/P2 have a higher gravimetric soil moisture. Figure 5.2.3 below shows the mean gravimetric soil moisture of the soil samples of each profile along the study transects.

It should be pointed out that the soil profiles along hillslope transect Wild/P1 have a depth of up to 90 *cm* below the surface, whereas the soil profiles at Wild/P2 range from 0 to 249 *cm*. The lower profile depths at transect Wild/P1 cause from an incomplete percussion drill instrument set on the first sampling day. Thus, the drill

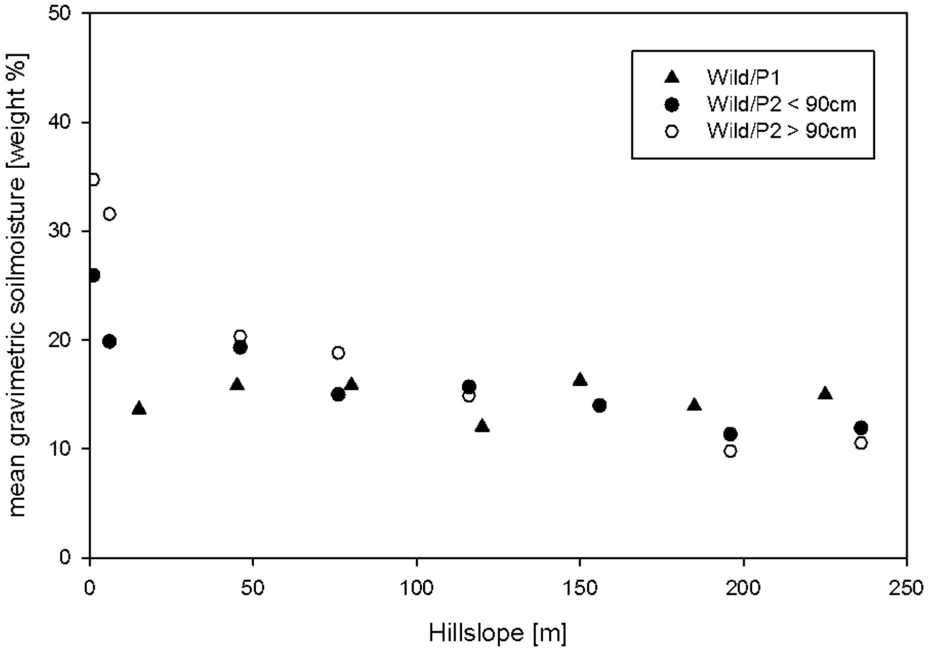

Figure 5.2.3.: Mean gravimetric soil moisture of the profiles along the study transects.

could not be extended and just a soil profile depth of 90 *cm* was possible. Because of this difference, the results of the Wild/P2 profiles are shown up to 90 *cm* and below separately, for a direct comparison of transect Wild/P1 and transect Wild/P2. Figure 5.2.3 indicate an increase of soil moisture in downslope direction at hillslope transect Wild/P2 for the mean gravimetric soil moisture of the soil profiles up to 90 *cm* and below 90 *cm*. This trend is not apparent at the Wild/P1 profiles. The Wild/P1 profiles exhibit a uniform mean gravimetric soil moisture along the whole transect.

5.2.2. Soil Texture

The results of the soil texture analysis for some soil samples at the hillslope transects are shown in figure 5.2.4 below.

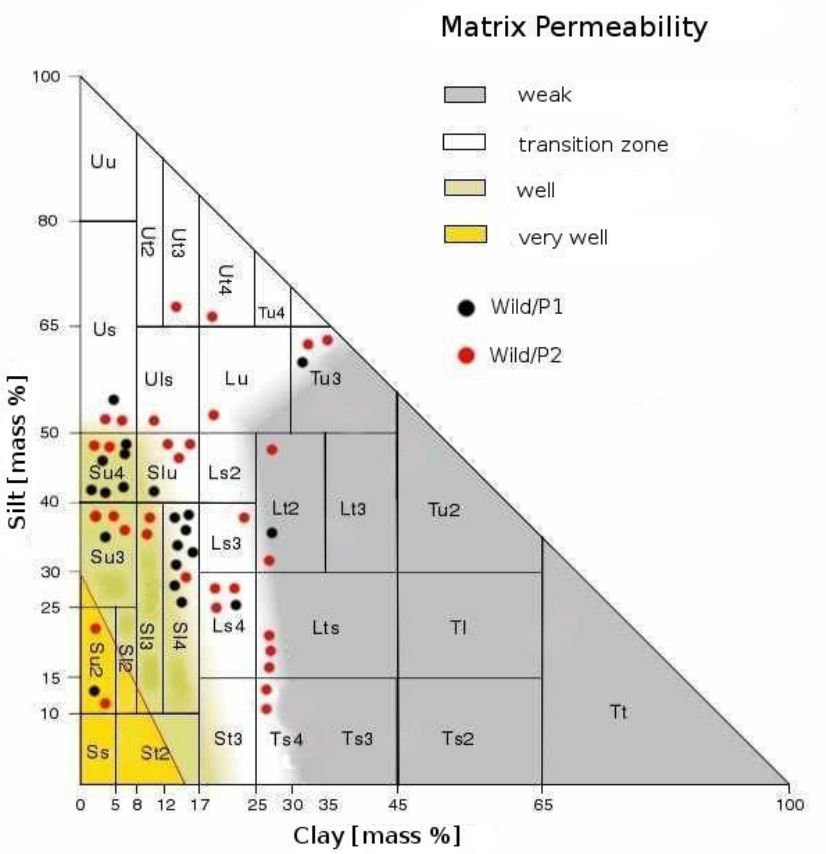

Figure 5.2.4.: Soil texture of the analyzed soil samples with the associated matrix permeability (after SCHERRER (2006)).

The soil texture of the analyzed samples are distributed over a few textures. Most of the analyzed soil samples exhibit a good matrix permeability for water due to the high content of sand.

5.2.3. Soil Types

The soil along Wild/P1 looks very similar at the first 7 soil profile locations. It was identified as a cambisol with an Ah-Bv-Cv profile. The Cv horizon is well weathered bedrock material. The soil material over the profiles at Wild/P1 is characterized by a loamy-sand or silty-sand texture. According to SCHERRER (2006) this material is well permeable for water. The last profile Wild/P1/H7/A looks slightly different, because of finer soil material in the topsoil as well as in the subsoil.

At hillslope transect Wild/P2 can be distinguished between several types of soil. The soil along the upper part of the hillslope was identified as a cambisol with an

Ah-Bv-Cv profile. The topsoil and subsoil material have a texture of loamy-sand or silty-sand that exhibit a good permeability for water. Soil profile Wild/P2/H4/A looks a little bit different from the others along the steep part of the hillslope. The topsoil is more loamy and there was a clayey-loam layer around 1 m below the surface. Below this layer the material was more sandy again. The soil material around 1 m had contingents of humous and tiny pieces of coal were found. The soil was very wet in this part of the profile. The soil material at Wild/P2/H5/A was also more loamy. The soil was wet at 50 cm and almost saturated between 70 and 160 cm. Below the soil was very dry again with a silty-loam texture that is not very well permeable. Coal pieces were found between 97 and 178 cm and the soil was reddish there. Soil profile Wild/P2/H6/A was very clayey and wet in the subsoil. Soil profiles Wild/P2/H7/A and Wild/P2/H8/A have a alluvial soil character with a silty texture, some gravel in-between and redoximorph attributes. The findings are conform to observations of Hädrich et al. (1988) who described the soil in this part of the catchment as alluvial soil. The estimated permeabilities in these two soil profiles near the stream are well permeable in the topsoil and worse permeable in the subsoil.

5.3. Discussion

There is a strong topographic control on soil moisture during wet conditions and a weak control during dry conditions (Grayson et al., 1997). There was barely precipitation in the weeks prior to the measurement campaign. The observed soil moisture pattern must be more distinct during wet conditions. Nevertheless, the increase in soil moisture in downslope direction at transect Wild/P2 could be explained by a greater increase of upslope accumulating area due to the concave morphology, compared to the convex situation along transect Wild/P1. The higher soil moisture values near the surface might be due to thaw that was observed at the soil sampling days in the morning. The almost saturated layer at Wild/P2/H5/A with the weak permeable layer below could be an indicator for lateral flow in this part of the study hillslope.

The texture of the soil material is well permeable for water actually. There could be made a clear distinction between hillslope soil with an Ah-Bv-Cv-profile and riparian zone soil with redoximorph features. Soil material along the hillslope was very sandy. The finer soil texture and the coal pieces found in the soil samples at the hillslope feet at transect Wild/P2 could be an indicator for the levelling activities 50 years ago.

A question that could not be answered is: How does it looks below the sampled profiles? Is there the same material than in the deeper parts of the soil profiles for another few decimeters? Or is there some unpermeable bedrock shortly below? This would be an important information, because the permeability of the bedrock material controls the direction of water aging (Uchida et al., 2006) and runoff generation processes (McDonnell, 1990).

6. Catchment Areas and Flowpath Analysis

6.1. Material and Methods

The calculation of the catchment area for the profile points at the hillslope and a flowpath analysis for every point was performed with the geographic information system SAGA (SAGA User Group, 2009) using a digital elevation model (DEM). The original 1 m DEM was resampled to a DEM with a spatial resolution of 5 m. A 5 m DEM, or even a 10 m, appears more susceptible to micro topographic influences and yield more realistic results for hydrological landscape analysis (Jencso et al., 2009).

The surface catchment area for the grid cell of every profile point of the sampling transects (Wild/P1 and Wild/P2) at the hillslope was calculated with the multiple flow direction (MFD) algorithm (Quinn et al., 1991) and the D-infinity (D∞) algorithm (Tarboton, 1997). A surface flowpath analysis was performed using the MFD algorithm. It was calculated the flow distance from every grid cell of the profile upslope areas to the profile location grid cell. These distances were used for flowpath length distributions for every profile location.

The D8 algorithm determines the drainage from one point on the DEM grid to one of its eight neighbor cells depending on the steepest gradient (O'Callaghan and Mark, 1984). The D∞ algorithm as well as the MFD algorithm is an advancement of the D8 algorithm and allows flow partitioning between one or two neighbor cells depending on the gradients, thus considering a bidimensional flow.

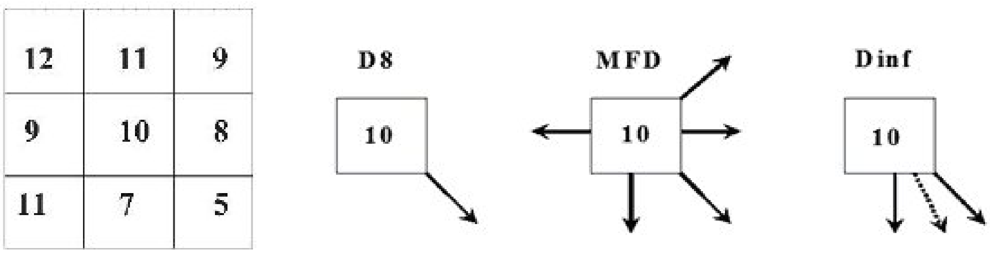

Figure 6.1.1.: Schematic illustration of the flow routing performed by the D8, MFD and D∞ algorithms based on an exemplary DEM (after Endreny and Wood (2003)).

6.2. Results

Table 6.2.1 presents the catchment areas of the isotope profile locations calculated with different algorithms. Figure 6.2.1 the catchment areas along the transects.

Table 6.2.1.: Catchment area in m^2 of the profile points calculated with the MFD algorithm and the D∞ algorithm from the 5 m DEM.

Profile	Catchment area with MFD	Catchment area with D∞
Wild/P1/H1/A+B	315.3	268.9
Wild/P1/H2/A	405.8	328.7
Wild/P1/H3/A	425.0	436.6
Wild/P1/H4/A	441.6	454.9
Wild/P1/H5/A	501.9	485.5
Wild/P1/H6/A	495.1	490.5
Wild/P1/H7/A	506.3	648.4
Wild/P2/H1/A	381.5	203.7
Wild/P2/H2/A	506.3	310.3
Wild/P2/H3/A	929.2	649.6
Wild/P2/H4/A	1605.4	1250.2
Wild/P2/H5/A	2075.1	1413.5
Wild/P2/H6/A	1665.1	1511.6
Wild/P2/H7/A	9696.5	1255.7
Wild/P2/H8/A	101441.9	927.6

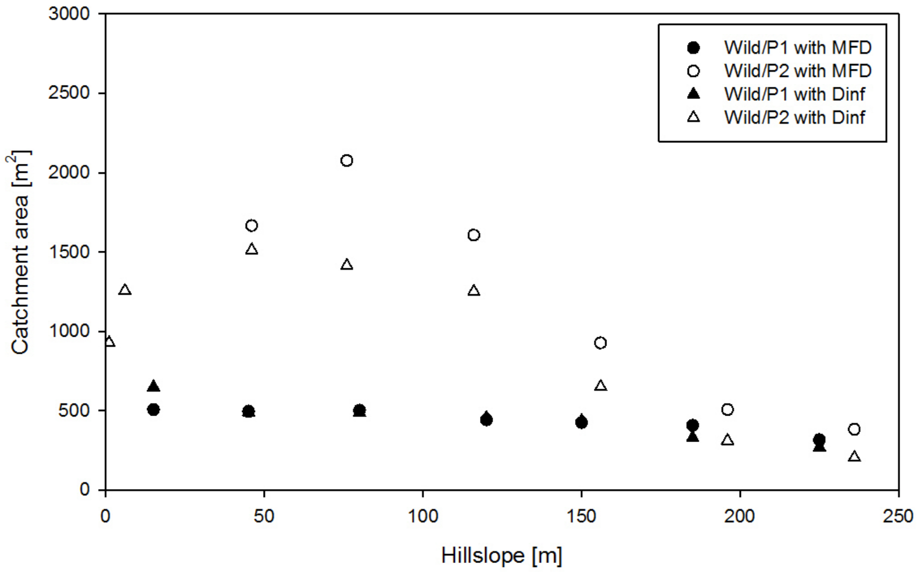

Figure 6.2.1.: Catchment area calculated with the MFD and the D∞ algorithm along the study hillslope.

The results show that the catchment area of the profile locations is increasing in downslope direction at both transects. The catchment areas at Wild/P2 are increasing much more compared to a similar position of the Wild/P1 catchments on the hillslope (figure 6.2.1). The catchment area of profile Wild/P2/H8/A calculated with the MFD algorithm had an area of 101441.9 m^2 and was not plotted on figure 6.2.1 for the benefit of clearness.

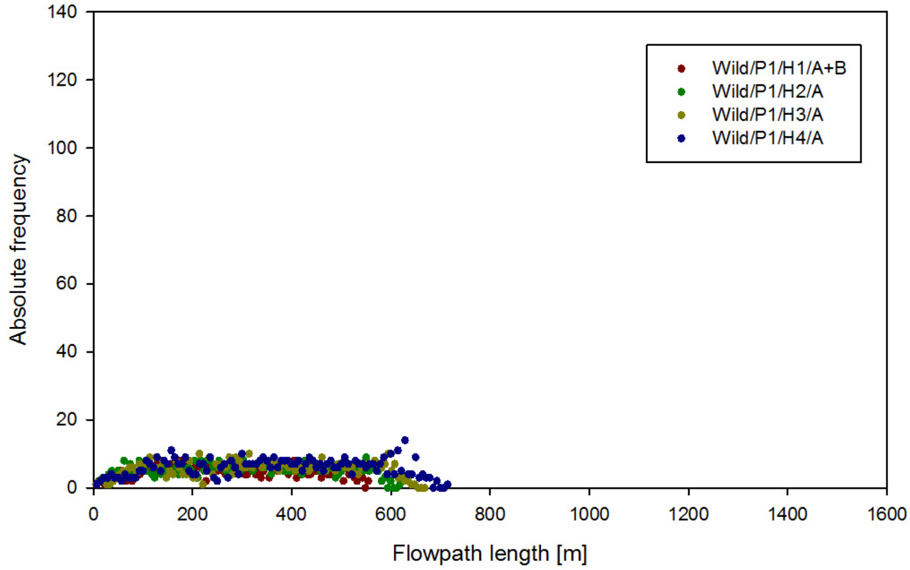

Figure 6.2.2.: Flowpath length distribution for the catchment of profile location Wild/P1/H1/A+B, Wild/P1/H2/A, Wild/P1/H3/A, Wild/P1/H4/A at study transect Wild/P1.

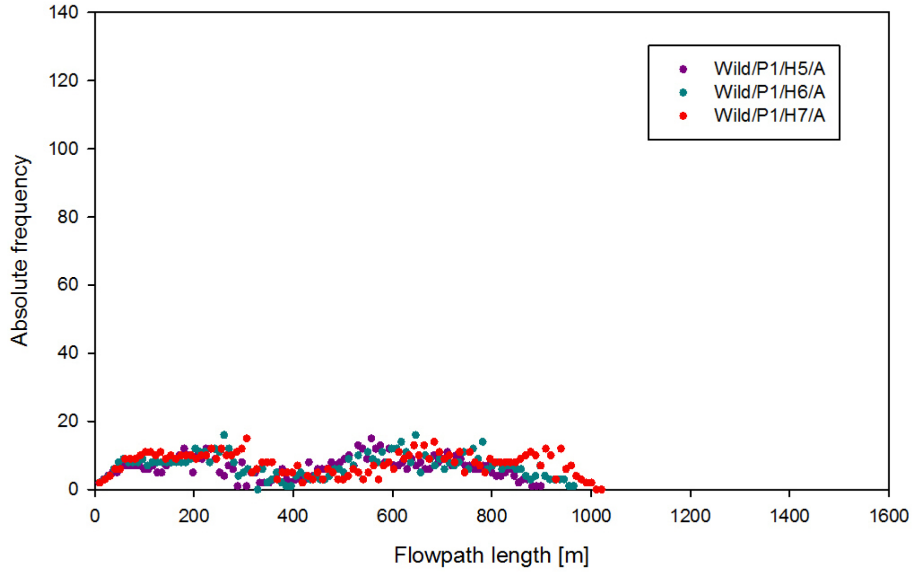

Figure 6.2.3.: Flowpath length distribution for the catchment of profile location Wild/P1/H5/A, Wild/P1/H6/A, and Wild/P1/H7/A at study transect Wild/P1.

The flowpath distribution is scattering over a wide range for all catchments. A relatively homogenous frequency of the flowpaths can be observed in figure 6.2.2. There are flowpaths with a length of up to 600 m. The Wild/P1/H5/A catchment has a maximum flowpath length of 700 m, whereas the Wild/P1/H6/A and Wild/P1/H7/A upslope areas have flowpaths with a length of up to 1000 m. The distributions exhibit two small peaks with a slightly higher frequency around a flowpath length of 200 m and 600 m. Nevertheless, there can be observed an relatively homogeneous distribution of flowpath lengths at study transect Wild/P1.

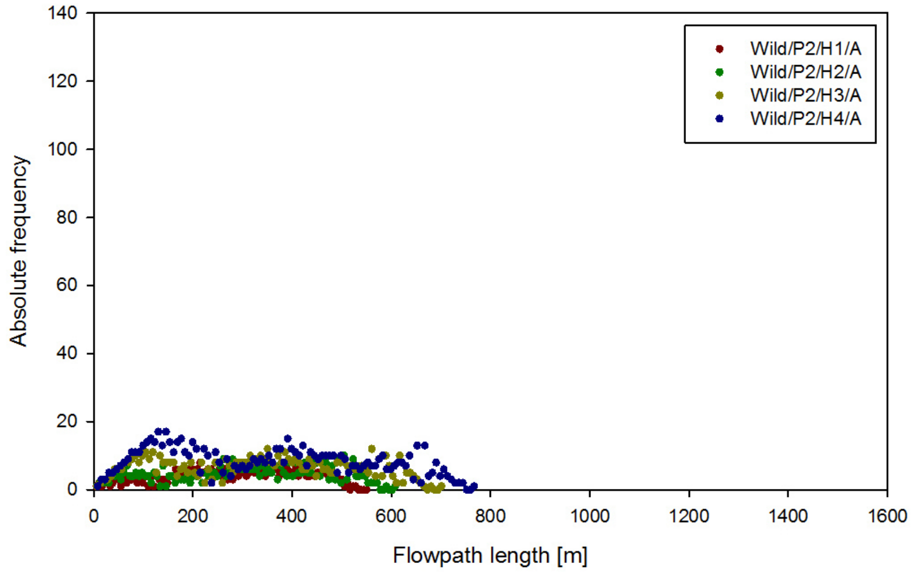

Figure 6.2.4.: Flowpath length distribution for the profile catchments Wild/P2/H1/A, Wild/P2/H2/A, Wild/P2/H3/A and Wild/P2/H4/A at the Wild/P2 transcet.

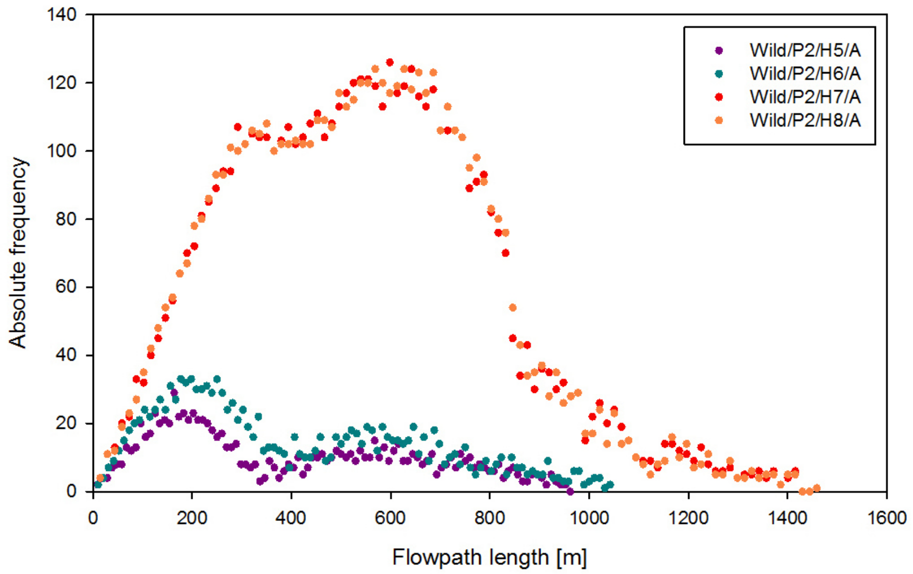

Figure 6.2.5.: Flowpath length distribution for the profile catchments Wild/P2/H5/A, Wild/P2/H6/A, Wild/P2/H7,A and Wild/P2/H8/A at study transect Wild/P2.

There can be observed a scattering of the flowpath lengths at transect Wild/P2. The longest flowpaths within the upslope areas of the first three profiles have a length between circa 600 m and 750 m. The flowpath distributions of Wild/P2/H3/A and Wild/P2/H4/A have frequency peaks at a length around 150 m and 400 m. Wild/P2/H5/A and Wild/P2/H6/A exhibit a frequency maximum around 200 m and a smaller peak around 600 m. The catchment areas of profile Wild/P2/H7/A and Wild/P2/H8/A have the highest absolute frequencies of flowpath lengths. Probably due to their catchment size. The distributions have a maximum at a flowpath length of 600 m and a smaller peak at 300 m. There can be observed longer flowpaths, especially at more downslope positions at hillslope transect Wild/P2 with higher frequencies compared to study transect Wild/P1.

Flowpath distributions for every profile position along the study transects are added to the appendix A (figure A.11 and figure A.12). The empirical distributions of the flowpath analysis for the profile catchments are dispayed on figure A.9 for Wild/P1 and figure A.10 Wild/P2 attached to the appendix A. The 90%-quantiles derived from the empirical distributions are listed in table 6.2.2 below.

Table 6.2.2.: Hillslope length and 90%-quantile of the empirical flowpath length distribution in m. Flowpath distances were calculated with the MFD algorithm for the empirical distributions.

Profile	Hillslope length	90%-quantile with MFD
Wild/P1/H1/A+B	225	479.1
Wild/P1/H2/A	185	531.6
Wild/P1/H3/A	150	570.0
Wild/P1/H4/A	120	607.5
Wild/P1/H5/A	80	753.6
Wild/P1/H6/A	45	808.4
Wild/P1/H7/A	15	883.9
Wild/P2/H1/A	236	458.0
Wild/P2/H2/A	196	503.6
Wild/P2/H3/A	156	570.9
Wild/P2/H4/A	116	628.5
Wild/P2/H5/A	76	756.5
Wild/P2/H6/A	46	770.7
Wild/P2/H7/A	6	866.9
Wild/P2/H8/A	1	852.2

The 90%-quantiles of the flowpath disributions, calculated with the MFD algorithm, are increasing in downslope direction at both study transects. There is a positive correlation between the catchment area of the sampled profiles and the 90%-quantile of the empirical flowpath length disribution (figure 6.2.6). In simply a qualitative quantification this denote an increase of the catchment size with incresing 90%-quantile of the flowpath length distribution for the catchment areas.

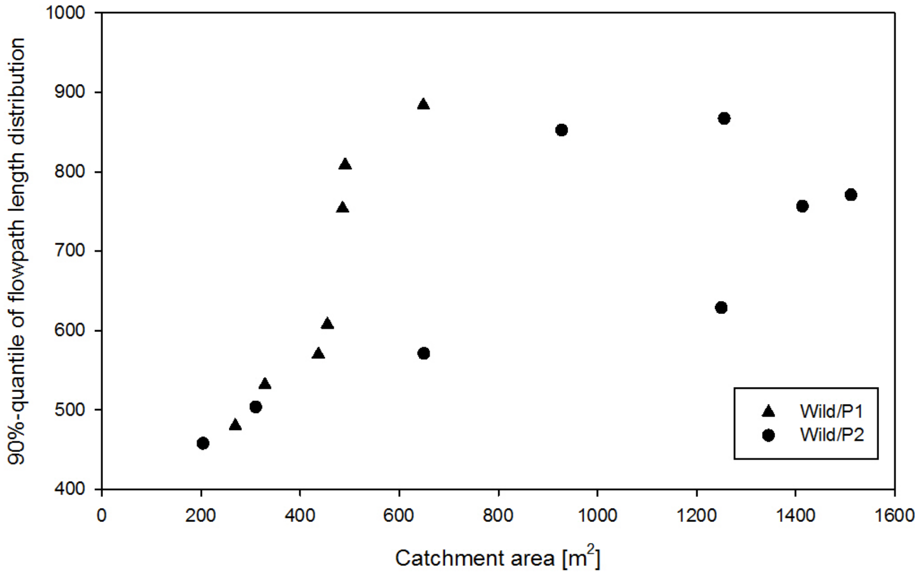

Figure 6.2.6.: 90%-quantile of the flowpath length distribution plotted against the catchment areas calculated with the D∞ algorithm.

6.3. Discussion

The increase of the profile catchment areas was more distinct at transect Wild/P2. This effect could be explained with the different geomorphologic situations at the two study transects. The morphology of the hillslope at transect Wild/P1 is convex, whereas the morphology at transect Wild/P2 has a concave shape. The largest catchment area has a distance of 1 m to the stream. This profile point (Wild/P2/H8/A) was obviously associated with a larger contributing area because of its near stream position.

The flowpath analysis was performed with the 5 m DEM, thus overland flowpaths were calculated. Subsurface flowpaths are not always determined by surface topography, but rather controlled by subsurface structures like bedrock topografy (McDonnell et al., 1996). In this study it has to be made the assumption, that surface flowpaths determined from the DEM are an indicator for subsurface flowpaths. This assumption could be supported by the soil moisture results. The soil moisture results show an increase in downslope direction, especially at transect Wild/P2. This could be associated with an increase of subsurface flowpaths, due to an increase of accumulating area.

The empirical distributions of the flowpath lengths show that there are longer flowpaths at study transect Wild/P2, especially at more downslope positions. The flowpath length distributions of the profile catchments at Wild/P2 along the upper part of the hillslope catena have a comparable distribution of flowpath lengths to study transect Wild/P1.

7. Stable Isotopes

7.1. Material and Methods

7.1.1. Soil Sampling

In order to investigate stable isotope variations along the study hillslope, soil cores had been extracted at different hillslope positions from near the divide to the stream as shown on figure 5.1.1 (section 5.1.1).

7.1.2. Stable Isotope Analysis

Soil water extraction techniques are usually applied to extract soil water from the soil material for the stable isotope analysis. There are basically four techniques for this purpose: vacuum distillaton, azeotropic distillation with parafin oil, microdistillation with zinc and centrifugation (Barnes and Turner, 1998). Walker and Woods (1991) (in Barnes and Turner, 1998) report that the extraction techniques causes errors in the range of 30‰ for deuterium and 3.5‰ for oxygen-18, respectivelly. Another technique is the extraction of soil water with suction lysimeters. Suction lysimeters had been used in several studies to sample soil water (e.g. Asano et al. (2002) and Stewart and McDonnell (1991)). In this study the approach of Wassenaar et al. (2008) was followed to determine the stable isotopes of soil water, by analyzing the stable isotopes of the soil vapor that is in isotopic equilibrium with the soil water. The technique was already successful applied by Gralher (2009) at the IHF.

The preparation of the soil samples and the stable isotope analysis was performed in the IHF stable isotope laboratory. Compressed air was transmitted through anhydrite ($CaSO_4$) to detract any moisture. The Ziplocs with the soil material inside were filled up with the dry air, closed and heat-sealed in another plastic bag. Thereafter, the samples were stored in a temperate room for at least 15 hours in order to achieve an isotopic equilibrium between the air inside the Ziplocs and the soil water of the soil material. The temperature was recorded every 5 minutes with a high precision digital thermometer (GMH 3750, *Greisinger Electronic*) during the equilibration period.

The vapor within the Ziplock bags was measured with Wavelength-Scanned Cavity Ring Down Spectroscopy (WS-CRDS). This technique was developed for continuous measuring of polyatomic gases. It was used the G1102-i laser based absorption spectrometer from *Picarro*. The WS-CRDS technique uses the effect that nearly every small gas phase molecule has a unique near-infrared absorption spectrum. At subatmospheric pressure, the spectrum consists of a series of well resolved sharp lines, each at a characteristic wavelength. Because the wavelength of the gases is well known, the concentration of any molecular species can be determined by measuring the strength of the absorption signal (Picarro, 2009).

Figure 7.1.1.: Soil vapor stable isotope analysis with the *Picarro* analyzer in the IHF laboratory.

The vapor inside the Ziplocks was measured by sticking a needle, that is connected via a plastic tube to the measuring chamber of the stable isotope analyzer, into the plastic bags. A measured value was noted manually, when there had been 12 to 15 data points with a standard deviation lower than the measurement accuracy of the analyzer. This accuracy is 0.16‰ for ^{18}O and 0.6‰ for ^{2}H, respectively. The *Picarro* analyzer measures additionally the water vapor content of the air within the Ziplock bag. This value, as well as the temperature was noted. The temperature was measured with the high precision digital thermometer next to the sample.

During the field campaign it was also sampled groundwater and streamwater in the catchment. The streamwater (SW) was sampled downstream of the study hillslope near the farm Schümperlehof. Groundwater (GW) from two drinking water wells (Farm Schümperlehof and Farm Flammhof) in the catchment was sampled. The water samples were analyzed in the IHF laboratory with the *Picarro* WS-CRDS analyzer.

7.1.3. Soil Water Stable Isotope Composition

The stable isotope data of the measured vapor had to be converted in stable isotope values of the sample soil water. Under the assumption of isotopic equilibrium, the phase change in the vapor-water system can be calculated via the fractionation factor α (section 2.1).

The results of the stable isotope analysis are δ-values relative to the interior *Picarro* standard. Since the isotope ratios R for ^{2}H and ^{18}O are not known for this intern standard, it is necessary to calibrate to the VSMOW standard whose ratios are well known. Thus, the *Picarro* vapor δ-values were calibrated to δ-values in per mill (‰) relative to VSMOW.

Since the *Picarro* analyzer measures very stable and linear, it is only necessary to use three calibration standards. Ideally, two of these calibration standards define the calibration line. Whereas a third, intermediate, point can be used for verification. The calibration points should span a representative range of values (Picarro, 2009).

The idea in this study was to produce vapor samples as standards for the calibration. For this purpose, 100 g of dry soil from different soil depths of randomly chosen locations at the study hillslope was used. The 100 g of dry soil was watered with 20 ml of water whose δ-values in per mill relative to VSMOW are well known. Two different VSMOW standard waters had been used. One standard water had δ-values of -13.93‰ for ^{18}O and -97.5‰ for ^{2}H, respectively. This water is a laboratory intern standard water sampled at a swiss glacier with the code G2005. The second standard was drinking water (DW) from the Zartener Becken with δ values of -9.3‰ (^{18}O) and -60.79‰ (^{2}H). Additionally, there had been also filled some Ziplock bags with 20 ml standard water and no soil. For calibration it was used:

- 100 g soil from profile Wild/P2/H3/A + 20 ml standard water DW
- 100 g soil from profile Wild/P2/H3/A + 20 ml standard water DW
- 100 g soil from profile Wild/P2/H3/A + 20 ml standard water G2005
- 100 g loess soil from another study + 20 ml standard water G2005
- 20 ml standard water DW
- 20 ml standard water DW
- 20 ml standard water DW
- 20 ml standard water G2005

The calibration samples were treated in the same way as the other soil samples for the stable isotope analysis. They were filled up with dry air and stored for about 15 hours for equilibration. During this time the equilibration temperature was recorded. After equilibration, the vapor within the Ziplocks was analyzed for stable isotopes with the *Picarro* analyzer.

The theoretical δ-value relative to VSMOW of the vapor of the used standard waters was calculated by using equation 2.1.2 (section 2.1) considering the equilibration temperature and the coefficients a, b and c of Majoube (1971). The theoretical values of the vapor were plotted against the measured values with the *Picarro* analyzer. Two separate plots were made, one for oxygen-18 and one for deuterium. Calibration lines were fitted for the two plots as shown in figures A.3 and A.4 attached to the appendix A. It should be mentioned that a slope of 1 for the regression equations was manually forced to have an offset as small as possible for an accurate calibration (personal communication with Dr. Külls, September 2009). The calibration lines yield an equation in the form: $y = x * a + b$, whereas a is the slope and b is the intercept of the calibration line. The yielded regression equations for ^{18}O and ^{2}H have the form:

$$\delta^{18}O_{calibrated} = \delta^{18}O_{measured} - 1.375 \tag{7.1.1}$$

and

$$\delta D_{calibrated} = \delta D_{measured} + 1.29 \tag{7.1.2}$$

With the equation 7.1.1 for ^{18}O and 7.1.2 for ^{2}H it was possible to convert the δ-vapor values measured with the *Picarro* analyzer into δ-vapor values relative to VSMOW. Based on these converted δ-vapor values it was possible to calculate with equation 2.1.1 the isotope ratio R of the vapor sample. With the fractionation factor α (equation 2.1.2) for the equilibration temperature (mean temperature of the equilibration period) it was possible to calculate via equation 2.1.3 the isotope ratio R for the soil water. This R was finally applied to equation 2.1.1 to yield the δ-values for ^{18}O and ^{2}H of the soil water in per mill relative to VSMOW.

7.1.4. Data Analysis

Second moment statistics are useful to characterize the variability of hydrological time series, space processes and time-space processes Gottschalk (2005). The standard deviation (SD) of the deuterium profile data was calculated and boxplots were prepared as statistical measurements for the variability.

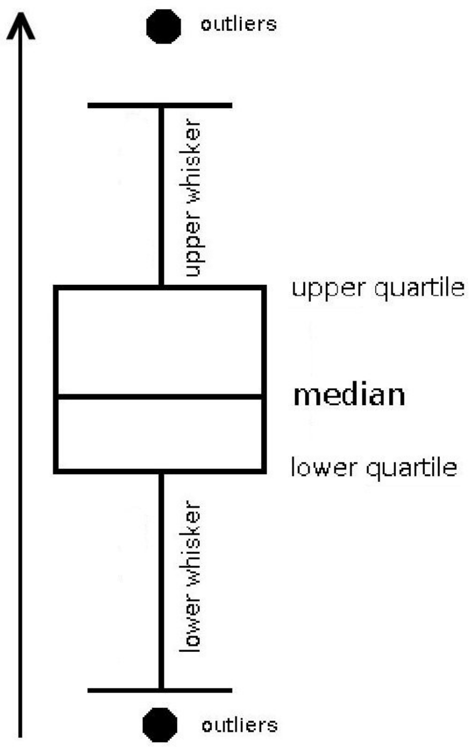

Figure 7.1.2.: Boxplot with whiskers and outliers.

The boxplot is a grafical image of the distribution of statistical data. Boxplots efficiently show the range and the frequency distribution of a dataset. The boxplot presents the median, the upper quartile, the lower quartile as well as extreme values. Outliers can be shown additionally.

The box represents 50% of the observed data. The boundaries of the box are the upper quartile (boundary farthest from zero) and the lower quartile (boundary closest to zero). The upper quartile is another notation for the 75th percentile, whereas the lower quartile is equal to the 25th percentile. Percentiles split the distribution of the data into 100 equal parts. Thus, the distribution is divided in 1 percent segments. For example, beneath the 75th percentile are 75% of the data of an observed distribution. The range between the 25th an the 75th percentile, the box, is called interquartile range (IQR) and is a mass for the diffusion of the values. The IQR can be calculated by subtraction of the lower quartile from the upper quartile. The variability of the data is characterized by the extent of the IQR. The median is the line within the box and divides the box into two parts. The position of the median within the box indicates the skewness of the distribution. For example: the distribution is right skewed if the median is in the left part of the box and inversely. Whiskers (error bars) above and below represent the data outside of the box. Whiskers indicate the 90th and the 10th percentiles. Thus, the range between the whiskers indicate 80% of the treated data (Schlittgen, 2003).

In this study the boxplots were generated with the software SigmaPlot (Systat, 2004). SigmaPlot needs a minimum number of data points to compute each set of percentiles. At least three data points are required, to compute the 25th and 75th percentiles. At least nine points are required to compute the 5th, 10th, 90th and 95th percentiles. The 5th and 95th percentiles were generated as points. These points outside the whiskers can be regarded as outliers.

7.2. Results

7.2.1. Stable Isotope Data

The results of the stable Isotope analysis of the liquid water samples are shown in table 7.2.1 below.

Table 7.2.1.: Stable isotope data of the water samples.

Sample location	Sample date	$\delta^{18}O[‰VSMOW]$	$\delta^{2}H[‰VSMOW]$
Streamwater	08/20/2009	-8.69	-58.15
Streamwater	09/18/2009	-8.45	-56.31
GW Schümperlehof	08/20/2009	-8.84	-59.47
GW Flammhof	08/20/2009	-8.69	-57.81

Figure 7.2.1 shows the $\delta^{18}O$-δ^2H plot of the stable isotope soil water data with the Global Meteoric Water Line (GMWL) added.

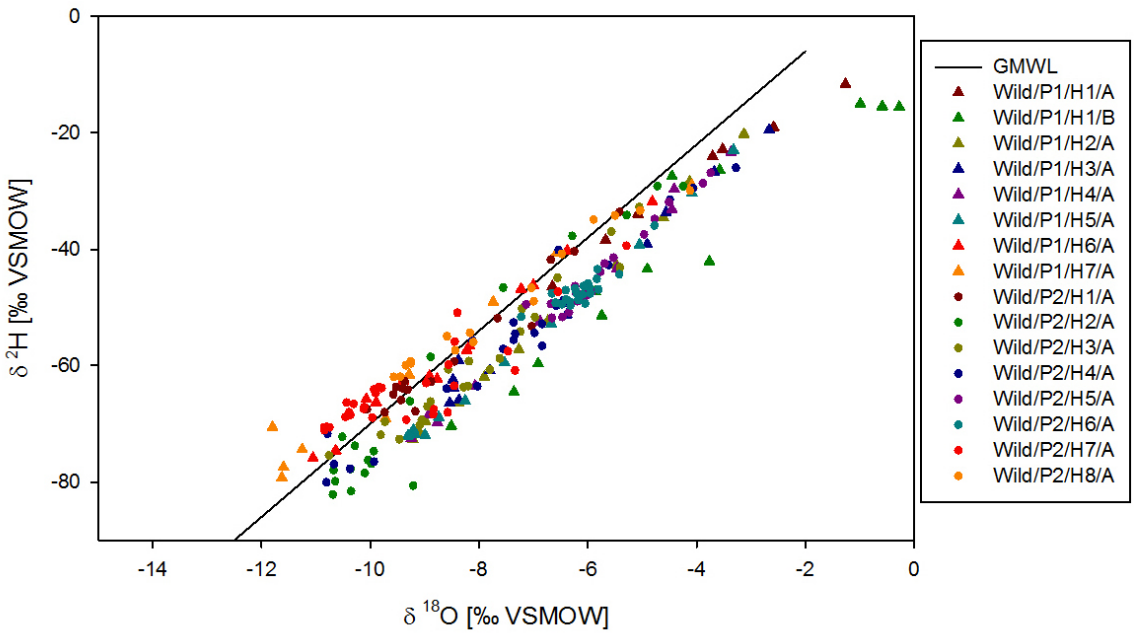

Figure 7.2.1.: $\delta^{18}O$-δ^2H plot of the soil water data and the GMWL.

The stable isotope data of the Wild/P1 profiles are depicted in triangles, whereas the Wild/P2 data is shown in scores. The samples plot very close to the GMWL and the total profile data is distributed over a wide range of values.

7.2.2. Deuterium Profiles

Figures 7.2.2 and 7.2.3 provide the stable isotope data of the soil water illustrated as deuterium profiles along the study hillslope transects. The reference on the right-hand indicate the x-axis (δ^2H values in per mill relative to VSMOW from -90 to 0) and y-axis (soil depth in *cm* from 0 at the surface to a maximum of 250) of the profiles. The dashed line at each profile represents the deuterium value of the groundwater. This reference line was added that relative differences of the profiles can be percieved easily.

The profiles at transect Wild/P1 have a maximum depth of 90 *cm*. They exhibit the same characteristic. The first values of the deuterium profiles near the surface range between -12‰ and -32‰. Below the profiles are getting continuously lighter with increasing soil depth. Deuterium profiles Wild/P1/H3/A through Wild/P1/H7/A have the lightest deuterium values (between -50‰ and -80‰) in a soil depth of 30 *cm* to 70 *cm*. After the peaks there can be observed a tendence to heavier values again.

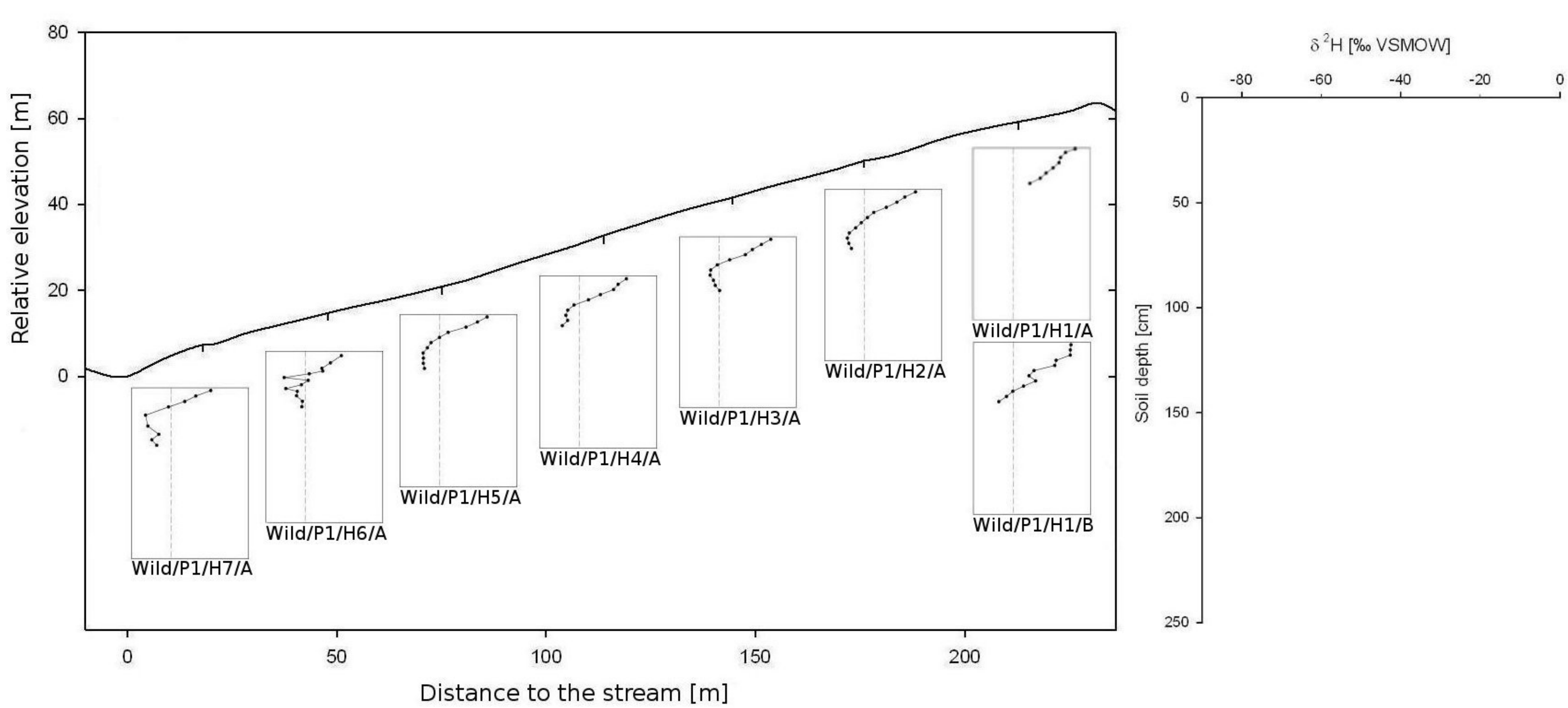

Figure 7.2.2.: Deuterium profiles along the concave hillslope transect Wild/P1. The two profiles displayed on top of each other had been drilled with a distance of 10 cm.

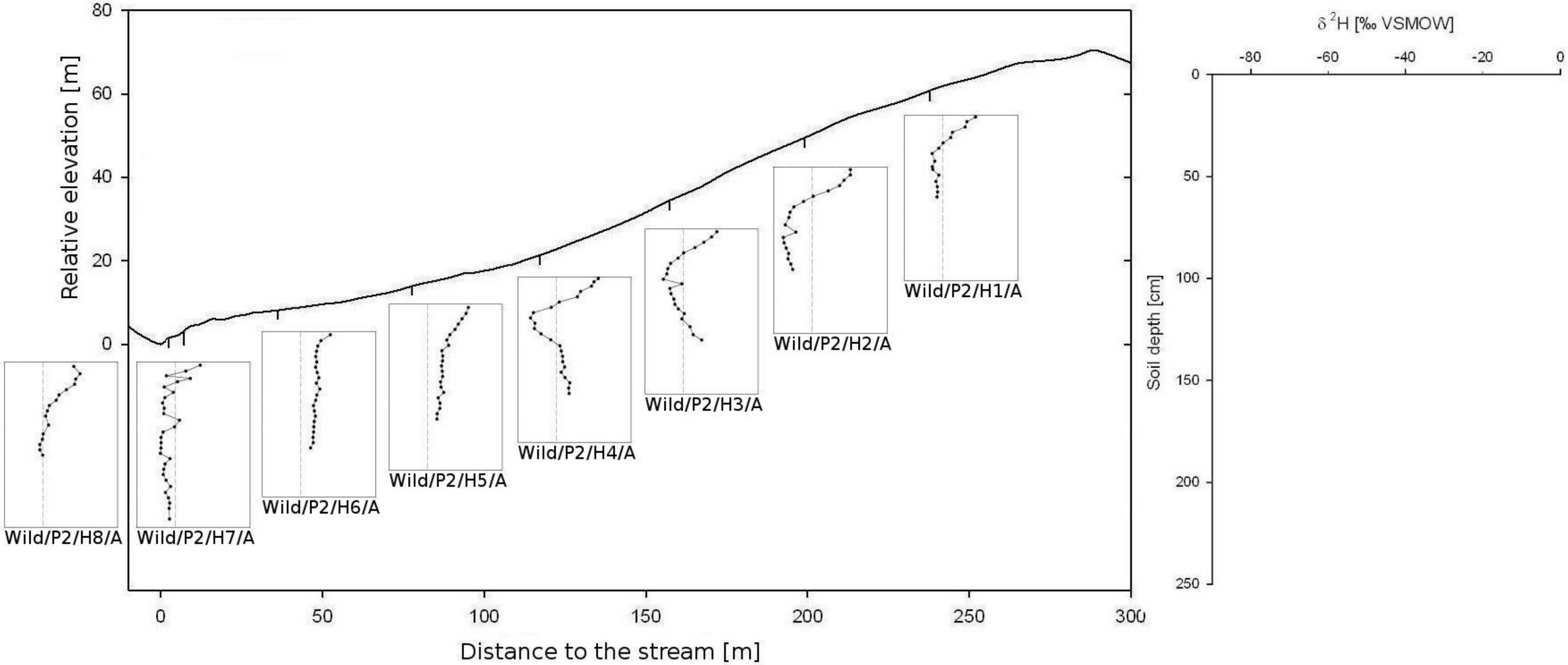

Figure 7.2.3.: Deuterium profiles along the convex Hillslope transect Wild/P2.

Figure 7.2.3 presents the deuterium profiles along hillslope transect Wild/P2. In contrast to hillslope catena Wild/P1, the profiles at Wild/P2 exhibit different characteristics. The first samples of the deuterium profiles Wild/P2/H1/A, Wild/P2/H2/A, Wild/P2/H3/A and Wild/P2/H4/A have values between -26‰ and -33‰. The values are getting continuously lighter with increasing soil depth. The lightest values are between 62 *cm* and 87 *cm* below the surface. After the peaks the values are getting heavier again. The peak is eminently pronounced at the profile Wild/P2/H3/A and Wild/P2/H4/A. Deuterium profile Wild/P2/H5/A exhibit a slight decline of the deuterium values with increasing soil depth. This decline with soil depth is even more weaker at soil profile Wild/P2/H6/A. Soil profile Wild/P2/H7/A is the deepest profile and is characterized by a very erratic behavior of the deuterium values. One can see many small peaks along the profile. The deuterium profile closest to the stream (Wild/P2/H8/A) is characterized by decreasing deuterium values with increasing soil depth.

Individual deuterium profiles as well as oxygen-18 profiles for transect Wild/P1 and transect Wild/P2 can be found in the appendix A.

7.2.3. Deuterium Variability along the Study Hillslope

Figure 7.2.4 shows the boxplots of the deuterium data for each profile along the study hillslope transect Wild/P1 and Wild/P2.

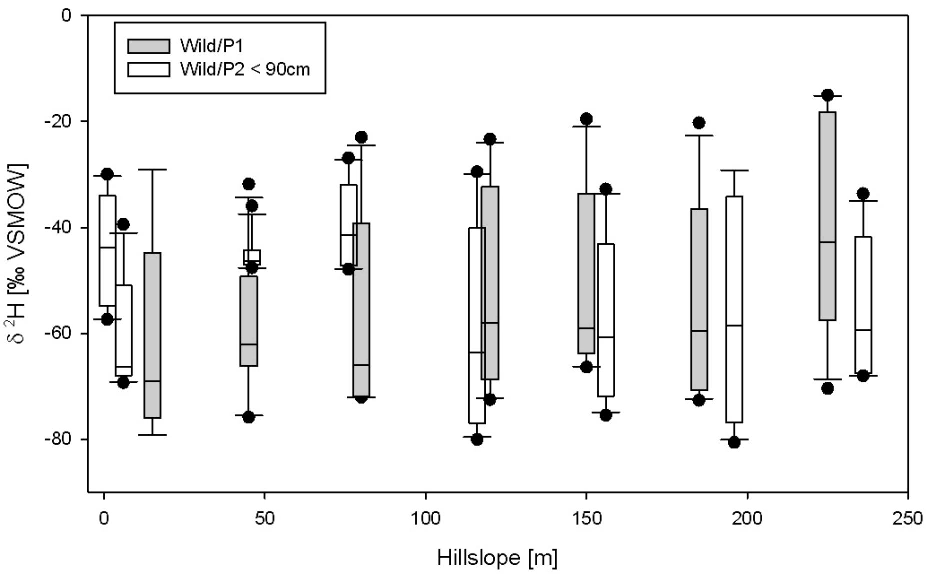

Figure 7.2.4.: Boxplots with whiskers and outliers of the deuterium profile data up to 90 *cm* below the surface for sampling transects Wild/P1 and Wild/P2.

The profiles at transect Wild/P1 were drilled to a maximum soil depth of 90 *cm*, whereas the soil profiles at Wild/P2 have a depth of up to 249 *cm*. To allow a direct comparison of the deuterium profile data from both sampling transects, only the first 90 *cm* of the Wild/P2 deuterium profile data was used to create the box plots in this figure. Figure A.15 in the appendix A shows the box plots for the Wild/P2 deuterium data below the soil depth of 90 *cm*. Figure 7.2.4 allows a direct comparison of the two sampling transects. The boxplots show very similar ranges from the water divide at about 250 *m* to a hillslope length of approximately 120 *m*. At this hillslope length the boxplots at Wild/P2 are getting smaller. Thus, the IQR is decreasing. At a hillslope length of circa 50 *m* (200 *m* from the divide) the IQR of the deuterium profile at Wild/P2 is minimal. The IQR of the Wild/P1 profile at a comparable hillslope position is also a little bit smaller. The next profiles closer to the stream show a bigger IQR again. This effect is even more pronounced on figure A.15 added to the appendix A, where the deuterium data of the Wild/P2 profiles below a soil depth of 90 *cm* is shown. A plot (A.14) showing the IQR value along the hillslope transects is added to the appendix A.

The scatter plot 7.2.5 shows the variability of the deuterium profiles by means of the standard deviation (SD) plotted against the hillslope length. To allow a direct comparison of the transects, the Wild/P2 profiles are divided at a depth of 90 *cm*.

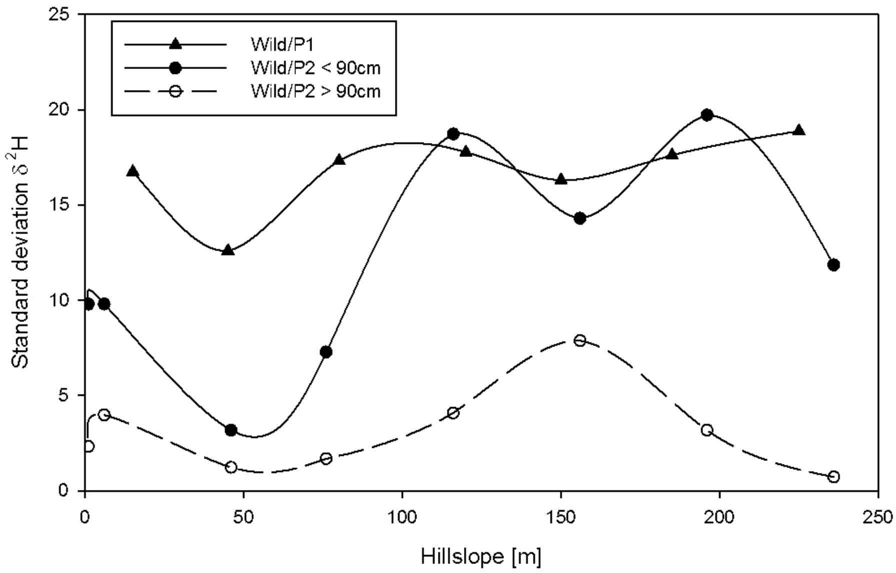

Figure 7.2.5.: Standard deviation of the deuterium profile data along the study hillslope.

Apparently there are different deuterium profile SD along the study transects. There are profiles with a higher SD and such with a lower SD. The 90 *cm* profiles of Wild/P1 and Wild/P2 have a SD between 12 and 20 along the hillslope to a length of circa 120 *m* (circa 130 *m* from the water divide). At transect Wild/P1 the profiles show a similar variability along the whole transect. The sixth profile exhibit a slight decrease in the variability and the last profile at this transect again shows a higher SD. The SD of the Wild/P2 profiles is rapidly decreasing after the hillslope length of 120 *m*. A minimum of 3.1 is evident at a distance of 46 *m* to the stream. After this distance the variability is increasing again. The deuterium profiles near the stream have a SD around 10. The development of the Wild/P2 profiles in a soil depth below

90 cm follows a wave line. With small SD followed by a peak around 8. Then the SD is decreasing again up to a hillslope length of 46 m. Where the lowest SD is apparent. The two profiles close to the stream have a standard deviation of circa 6 and 2.6 for the profile part below 90 cm.

7.2.4. Deuterium Variability and Flowpath Length Distribution

This section provides the results of the variability analysis combined with the results of the terrain analysis (section 6). Scatter plot 7.2.6 shows the SD of the deuterium profiles against the 90%-quantile of the empirical flowpath length distribution.

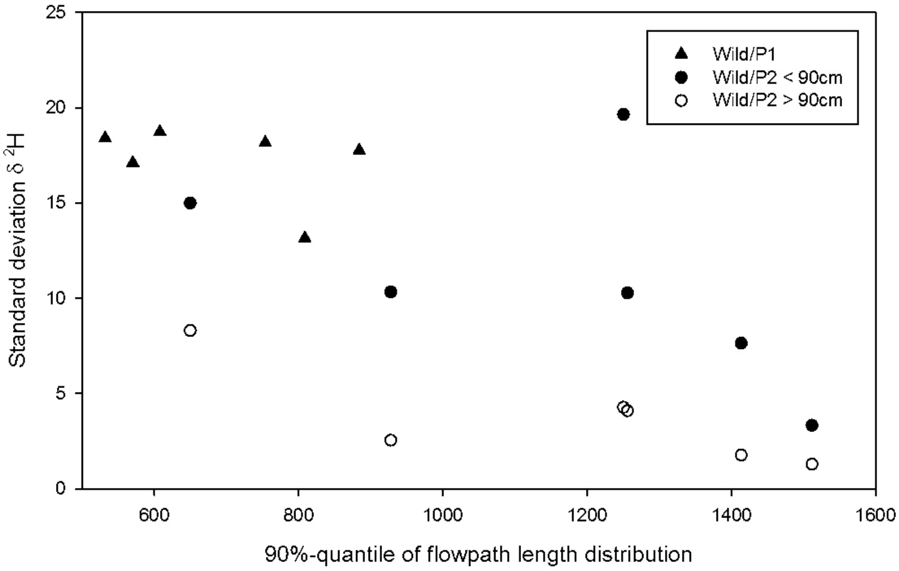

Figure 7.2.6.: Standard deviation of the deuterium profiles plotted against the 90%-quantile of the empirical flowpath length distributions.

Figure 7.2.6 illustrates a negative correlation between the SD of the deuterium data and the 90%-quantile of the empirical flowpath length distribution. This means that the SD of the deuterium profiles is lowest, when the 90%-quantile of the empirical flowpath length distribution has the highest value and vice versa.

7.3. Discussion

7.3.1. Characteristic Length Scale of Stable Isotope Variation

Soil profiles were sampled from near the water divide to the stream in order to investigate the stable isotope variability along the hillslope. The various isotope profile (VIP) approach was accomplished in order to cover the whole extent of stable isotope processing of soil water in the catchment. The spatial scale triplet for the VIP setting was about 40 m spacing, 250 m extent and 4.5 cm support.

At the hillslope scale fractionation effects of the meteoric input signal due to altitude and the temperature should be minimal. Thus, a very similar input signal can be expected along the whole hillslope. In a flat environment with identical soil properties and only vertical water movement, all deuterium profiles should be equal. This behavior was not observed on the study hillslope. This implies that the variations observed among the isotope profiles at different positions must derive from processes on the hillslope. Influences on the isotope signature of the profiles could be: lateral components, geomorphology or soil properties.

The deuterium and oxygen-18 data of the streamwater samples (table 7.2.1 and figure A.13) indicate that the catchment was in baseflow condition, because streamwater and groundwater had very similar stable isotope values. This would imply that no fast runoff components were contributing to the streamflow during the soil sampling activities.

Looking on the deuterium profiles (figures 7.2.2 and figures 7.2.3 or A.5 and A.6 in the appendix A), profiles with a seasonal shape (Wild/P2/H1/A, Wild/P2/H2/A, Wild/P2/H3/A and Wild/P2/H4/A), characterized by isotopical enriched summer water at the soil surface and a winter peak (lightest value) with isotopical depleted water below, could be identified. For transect Wild/P1 it is difficult to make a final statement, because of the slight profile depths. The shape of these profiles suggests a conservation of the seasonal isotope variation in precipitation, with light (depleted in ^{2}H or ^{18}O) values in winter and heavy (enriched in ^{2}H or ^{18}O) values in summer. The soil samples were extracted in summer. The stable isotope values near the soil surface indicate summer water. Then the stable isotope values are getting more depleted with increasing soil depth. After the peak with the lightest values, the stable isotope signature is getting isotopical enriched again. It seems that the deuterium profiles at transect Wild/P1 exhibit this seasonal shape. A direct comparison of the two study transects is possible to a soil depth of 90 cm. The variability of the Wild/P1 profiles is very similar along the whole hillslope. At study transect Wild/P2 the seasonal shape of the deuterium profiles is apparent to a certain hillslope length. Profile Wild/P2/H5/A and, in particular, profile Wild/P2/H6/A does not show a seasonal shape. Especially at profile Wild/P2/H6/A it seems that the seasonality of the input signal is strongly damped over the entire profile depth. This damping is indicated by a low IQR (figures 7.2.4 and A.15) and the decreased SD (7.2.5) of this profile. Profile Wild/P2/H7/A shows an erratic distribution of the deuterium values and no clear seasonal characteristic. When ignoring the erratic behavior, the profile could also show the averaged shape of profile Wild/P2/H6/A. But in fact, the variability of the profile has increased again. The last profile close to the stream has no seasonal shape and again a higher variability.

The deuterium profile variability is decreasing after a hillslope length of circa 120 m distance from the water divide. This effect is particularly pronounced at transect Wild/P2. Profile Wild/P2/H6/A has the lowest variability with a distance of 200 m from the water divide. Taking in to account the considerations above, this minimum of variability could be an evidence for a characteristic length scale of the stable isotope variations along the study hillslope in the Waldbrunnertal catchment. On the plot scale a vertical characteristic length scale could be assumed at the depth were the input signal variations are averaged. At the hillslope and catchment scale vertical and lateral components have to be assumed and the identified distance could be an evidence for a characteristic length scale at the hillslope or even catchment scale.

7.3.2. Isotope Profile Variability as an Indicator for Flowpath Lengths

Why is the decrease of the deuterium profile variability more distinct at study transect Wild/P2? The morphology of the hillslope and/or the predominat flow direction and flowpath length in the vadose zone could be an explanation. This was explored by accomplishing a terrain anlysis. The upslope (catchment) area of every profile point (table 6.2.1) and the flowpath length distribution within this areas (figures A.11 and A.12) was calculated. There is a much greater catchment area increase in downslope direction at the concave transect (figure 6.2.1). The empirical flowpath distribution suggests that the flowpaths of the concave Wild/P2 transect are longer than at the convex (Wild/P1) transect.

Tetzlaff et al. (2009) used the ratio of the standard deviation of oxygen-18 in streamwater to the ratio of standard deviation of oxygen-18 in precipitation as a proxy for the mean residence time of the water in catchments. The idea here is, that the variability (SD or IQR) of the deuterium profiles could be used as a proxy for the flowpath lengths, and therefore transit times in catchments.

The soil along the hillslope exhibits a good permeability for water. Profiles at positions along the hillslope where flowpaths seems to be short, vertical movement is propably the dominant direction of water flow. These profiles exhibit a higher variability than deuterium profiles which can be associated with a bigger upslope area and thus longer flowpaths. Short flowpaths imply little dispersion of the stable isotope tracer input, whereas longer flowpaths imply a higher dispersion. The variability of the deuterium profiles could be determined by the degree of seasonality apparent in the profile (see equation 2.1.5 and 2.1.6 in section 2.1). A high variability would imply little dispersion due to a shorter travel distance to the profile point and a small variabilty higher dispersion due to a longer flow distance to the profile point.

The stable isotope signal at every profile point would be the integral of the isotope signal contributions from each point in the catchment area of this point (Kirchner et al., 2001). It seems that the seasonal signal is damped at hillslope positions where the flowpath distances are longer and the lateral component could be more pronounced due to a higher flow accumulation. The almost saturated soil layer with a weak permeable layer below observed at the profile at the base of the hillslope (Wild/P2/H5/A) could be an indicator for a lateral flow component. The damping could be supported by a mixing of waters with different transit times within the catchment. The interpretation of profile Wild/P2/H7/A and Wild/P2/H8/A in the manner outlined above fails. The profiles have a higher variability, longer flowpaths and a bigger upslope area, compared to profile Wild/P2/H6/A upslope. The increased variability of Wild/P2/H8/A could be explained with the distance to the stream. The isotope signature of this profile could be influenced by streamwater. The same could be relevant for profile Wild/P2/H7/A. The erratic form of this profile could also originate from preferential flowpaths, return flow and/or systematic or analytical measurement errors. Under the assuption that the peaks would not be present, the shape would be comparable to profile Wild/P2/H6/A. If so, profile Wild/P2/H7/A would sustain the considerations above.

The variability of isotope profiles could be an indicator for flowpath lengths within catchments according to the accomplished considerations.

7.3.3. Various Isotope Profile Approach to Explore Hillslope Processes

Figure A.17 in the appendix A is an attempt to use the VIP approach as a tool to specify dominant processes at the hillslope scale. The deuterium profiles at transect Wild/P2 were used for this purpose. They provide more information than the Wild/P1 profiles due to their depth. The first four profiles exhibit a seasonal shape as discussed above. The seasonality of these profiles could indicate a vertical movement as the major flow direction of soil water (signified with blue dashed arrows in figure A.17). The winter peaks were identified in an average depth of 80 cm. Because the soil profiles were drilled in summer, this would imply an unsaturated vertical percolation of 160 cm per year. This corresponds to a velocity of $3 * 10^{-3}$ mm/s for the unsaturated vertical percolation.

Profile Wild/P2/H4/A seems to have the seasonal shape of the upslope profiles in the upper profile part and the damped characteristic of profile Wild/P2/H5/A and Wild/P2/H6/A below a profile depth of circa 1 m (marked with a red oval). This characteristic could be an indicator for temporary lateral hillslope flow (signified with blue errors). Profile Wild/P2/H7/A shows a very erratic isotope signature. The sharp peaks in the upper part could be caused by return flow. Return flow could be a realistic process at this hillslope position. The following peaks could mark measurement errors. Influences of streamwater or groundwater, indicated by redoximorph attributes observed at this profile, could be another option. Wild/P2/H8/A was sampled 1 m close to the stream. The position near the stream and the redoximorph properties of this profile likely indicate an influence of streamwater or groundwater.

The sharp and tiny peaks signified with small orange cycles could be recognized as indicators for flow mechanisms like preferential flow and return flow or as measurement errors due to the applied preparation and equilibration technique. Another explanation could be a systematic error emerging from the soil sampling with the drill pipe. A systematic error seems to be the most realistic reason. A contamination of soil material from shallower soil layers falling into the bore hole when extending the drill could be the answer. This soil material would be associated with a deeper soil layer and thus present a systematic error. An evidence for this possibility is the sampling drill length of 90 cm and the small peaks appearing at this depth.

7.3.4. Ideas to Improve the Various Isotope Profile Approach

The data show that the accomplished method is working and provides usefull results. Nevertheless, there are some ideas for an improvement of the approach. First: the sampling procedure could be improved. The sampled soil should be stored from the sampling moment, during the preparation for the isotope analysis, the equilibration period and the stable isotope analysis under the temperature prevailing in the soil. This would avoid a condensation as observed in the Ziplock plastic bags due to temperature differences. The soil samples could be vacuum heat-sealed with an adequate instrument immediately in the field to avoid a contamination of the sample with atmospheric air. This improvement would also include the use of preferably diffusion free bags. Second: a perfect calibration procedure. Instead of the presented approach (section 7.1.3), a standard conversion identity as presented by Craig (1957) (in Criss, 1999) could be used. This convention can be applied, when it is necessary to convert the δ-value of a sample measured relative to one isotopic standard, to the δ-value which would be measured relative to a second standard.

The soil profiles were drilled along two transects. Alternatively to the conducted sampling strategy, the profiles could be drilled randomly distributed over the whole study hillslope. In a following study, one could think about reducing the number of soil profiles. Deeper soil profiles would yield even more information. The study hillslope was rather dry since there was marginal precipitation in the weeks prior to the sampling camgaign. The approach should be applied under different hydrological conditions. Additionally after intense rainfall or during a snowmelt event, for example.

Soil water extracted from different soil depths over a certain period has been used as stable isotope time series (e.g. Asano et al. (2002) and Stewart and McDonnell (1991)). It seems that stable isotope profiles presented in this study provide a time series information in a point measurement conducted at one certain moment. This would alleviate the investigation of hillslope processes and catchment behavior.

8. Conclusions

The subject of this thesis was the investigation of stable isotope variations along a hillslope from the water divide to the stream in a 1 km^2 Black Forest catchment. There are various aspects and questions related to this subject. How powerful is the applied approach? Is there a characteristic length scale or any other representative unit for the stable isotope variability in the upper vadose zone? Is the variability of stable isotopes an adequate appliance to explore catchment characteristics and process behavior?

The approach could be accomplished succesfully and usefull results could be obtained. The results demonstrate a variability of the soil water deuterium profiles along the study hillslope. It seems that different hillslope positions as well as the geomorphological landscape situation (concave, convex) and the related hydrological behaviour have an impact on the variability of the stable isotope signature of soil water. A characteristic length scale for the stable isotope variability at the concave hillslope catena could be in the dimension of 200 m distance from the water divide. The variability of the stable isotope profiles of soil water could be used as an indicator for flowpath distances to this point in the catchment. Indicated by a low stable isotope profile variability at hillslope positions with a dominance of long flowpaths, and a high stable isotope profile variability at hillslope positions associated with short flowpaths prevailing. The VIP approach has potential for the investigation of hydrological hillslope and catchment processes.

This study was a first attempt to investigate stable isotope variations by means of soil profiles along a hillslope in a high spatial resolution. A couple of ideas to improve the approach could be identified. The improvements are related to an improved sampling procedure and preparation technique. In order to establish general principles concerning a characteristic length scale of stable isotope variation in catchments or the use of stable isotope profile variability as a proxy for flowpath distances, the approach should be applied at other hillslopes.

A. Appendix

Table A.1.: Distances between soil profiles and stream, profile depths and soil sample lengths at transects Wild/P1 and Wild/P2.

Soil profile	Distance to the stream	Profile depth	Soil sample length
Wild/P1/H1/A	225.1 *m*	55 *cm*	7.5 *cm*
Wild/P1/H1/B	225 *m*	90 *cm*	7.5 *cm*
Wild/P1/H2/A	185 *m*	90 *cm*	7.5 *cm*
Wild/P1/H3/A	150 *m*	90 *cm*	7.5 *cm*
Wild/P1/H4/A	120 *m*	76 *cm*	7.5 *cm*
Wild/P1/H5/A	80 *m*	82 *cm*	7.5 *cm*
Wild/P1/H6/A	45 *m*	85 *cm*	8.0 *cm*
Wild/P1/H7/A	15 *m*	88 *cm*	8.0 *cm*
Wild/P2/H1/A	236 *m*	127 *cm*	8.0 *cm*
Wild/P2/H2/A	196 *m*	158 *cm*	8.0 *cm*
Wild/P2/H3/A	156 *m*	172 *cm*	8.0 *cm*
Wild/P2/H4/A	116 *m*	180 *cm*	8.0 *cm*
Wild/P2/H5/A	76 *m*	177 *cm*	8.0 *cm*
Wild/P2/H6/A	46 *m*	180 *cm*	8.0 *cm*
Wild/P2/H7/A	6 *m*	249 *cm*	8.0 *cm*
Wild/P2/H8/A	1 *m*	145 *cm*	8.0 *cm*

The geographic coordinates of the soil profile positions were located with an GPS device in the field. The distances between the soil profiles were measured with a measuring tape. These distances were verified with the geographic information system ArcGIS and the distances to the stream were calculated.

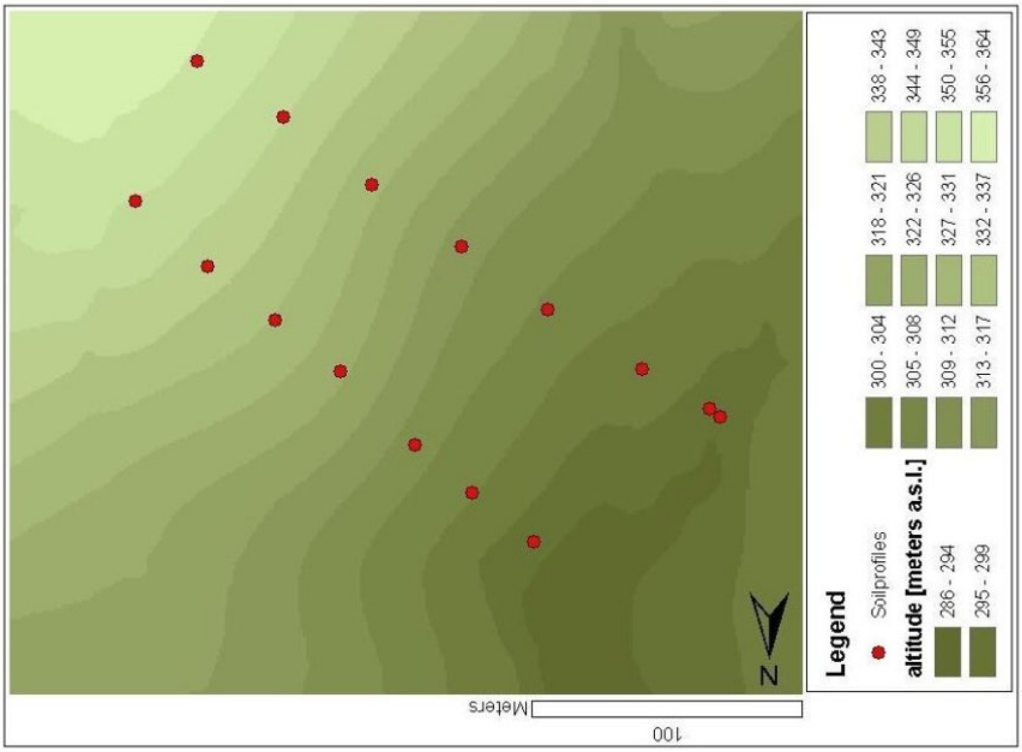

Figure A.1.: Altitude along the study hillslope.

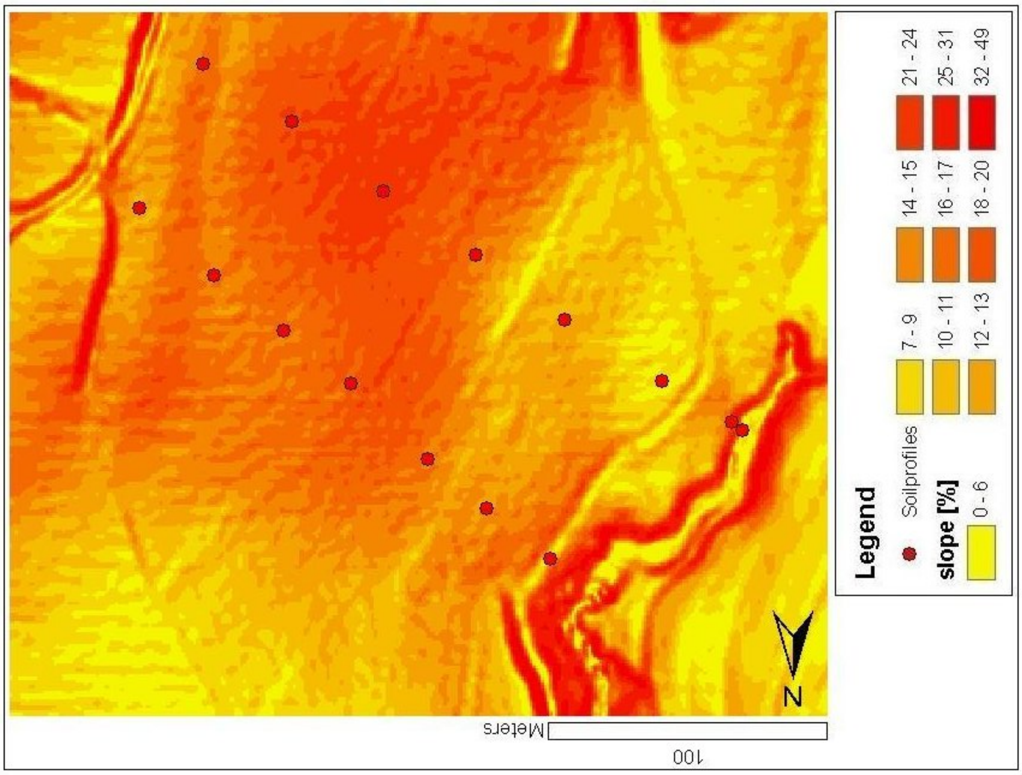

Figure A.2.: Slope along the study hillslope.

Table A.2.: Soil properties observed at the soil cores in the field.

Soil profile	Observations
Wild/P1/H1/A	Ah horizon was identified for the first 15 *cm*. Bv horizon was found between 15 and 50 *cm*. Below 50 *cm* weathered bedrock with loam material in-betweeen.
Wild/P1/H1/B	The humous topsoil was identified for the first 25 *cm*.
Wild/P1/H2/A	Fine roots and humous was found up to 23 *cm* soil depth.
Wild/P1/H3/A	First signs of colluvium. More clay content in the subsoil and thus more soil moisture. Below 90 *cm* reddish coloration.
Wild/P1/H4/A	The topsoil was for the first 16 *cm* rich in humous (Ah horizon). Fine roots were observed up to 24 *cm*. The subsoil was rather sandy and not really wet. At the lower edge of the profile was colluvium with claycutans on it. Claycutans are a sign that water is flowing in this soil depth. The colluvium showed signs of solifluction (rounded edges of the stones).
Wild/P1/H5/A	Fine roots and humous topsoil was found in the first 22 *cm* followed by a Bv and a Cv horizon.
Wild/P1/H6/A	Topsoil with humous and fine roots were observed up to 21 *cm* (Ah horizon). Between 21 and 80 *cm* is Bv and below that depth Cv.
Wild/P1/H7/A	This soil profile shows a 30 *cm* Ah horizon. Below this layer no distict horizons. The material was finer than in the overlying soil profiles.
Wild/P2/H1/A	Ah horizon of about 15 *cm*, Bv horizon of approximately 35 *cm* depth and a Cv horizon below.
Wild/P2/H2/A	Ah horizon of about 15 *cm*, Bv horizon of approximately 35 *cm* depth and a Cv horizon below.
Wild/P2/H3/A	Ah horizon of about 15 *cm*, Bv horizon of approximately 35 *cm* depth and a Cv horizon below.
Wild/P2/H4/A	Ah horizon of about 15 *cm*, Bv horizon of approximately 35 *cm* depth and a Cv horizon below.
Wild/P2/H5/A	The soil material in the profiles above was very dry. This profile was for the first 60 *cm* also very dry. Between 60 and 150 *cm* the soil was almost saturated. Below 150 *cm* the soil material was rather dry than wet.
Wild/P2/H6/A	Fine roots were found up to 20 *cm* depth. The subsoil was very clayey and wet. No gravel material or grit was found along the profile. Little coal pieces were found distributed over the whole profile.
Wild/P2/H7/A	The humous topsoil was identified up to 18 *cm*. The soil material had a reddish-greyish coloration between 92 and 174 *cm*. Below 220 *cm* the soil material was just reddish. The red color (iron and manganese) is an evidence for redoximorph processes under sporadic saturation.
Wild/P2/H8/A	Topsoil with humous up to 20 *cm*. Redoximorph attributes.

Table A.3.: Soil sample textures and associated matrix permeability.

Soil profile	Sample depth [cm]	Soil texture	Matrix permeability (Scherrer,2006)	Ks [m/s] (AG Boden, 1994)	Ks [m/s] (Rawls and Brakensiek, 1989)
P1/H1/B	10	Su4	well permeable	4,7*10^-6	7,2*10^-6
	47,5	Sl4	well permeable/transition zone	5*10^6	7,2*10^-6
	85	Sl4	well permeable/transition zone	5*10^6	7,2*10^-6
P1/H2/A	15	Su4	well permeable	4,7*10^-6	7,2*10^-6
	52,5	Sl4	well permeable/transition zone	5*10^6	7,2*10^-6
	90	Sl4	well permeable/transition zone	5*10^6	7,2*10^-6
P1/H3/A	15	Su4	well permeable	4,7*10^-6	7,2*10^-6
	52,5	Sl4	well permeable/transition zone	5*10^6	7,2*10^-6
	90	Sl4	well permeable/transition zone	5*10^6	7,2*10^-6
P1/H4/A	16	Su4	well permeable	4,7*10^-6	7,2*10^-6
	38,5	Su3	well permeable	8,7*10^-6	7,2*10^-6
	76	Sl4	well permeable	5*10^6	7,2*10^-6
P1/H5/A	22	Su4	well permeable	4,7*10^-6	7,2*10^-6
	44,5	Ls4	transition zone	2,3*10^-6	7,2*10^-6
	82	Sl4	well permeable/transition zone	5*10^6	7,2*10^-6
P1/H6/A	21	Su4	well permeable	4,7*10^-6	7,2*10^-6
	53	Slu	well permeable/transition zone	4,7*10^-6	1,8*10^-6
	85	Su2	very well permeable/well permeable	1,8*10^-6	1,7*10^-5
P1/H7/A	16	Us	transition zone	2,5*10^-6	3,6*10^-6
	48	Lt2	barely permeable	1,5*10^-6	6,3*10^-7
	88	Ts3	barely permeable	1,5*10^-6	3,3*10^-7
P2/H1/A	14	Slu	well permeable/transition zone	4,7*10^-6	1,8*10^-6
	14 - 147	St3/Sl4/Ls4	well permeable/transition zone	5*10^-6 – 2,3*10^-6	1,8*10^-6
P2/H2/A	24	Sl3	well permeable	5,4*10^-5	7,2*10^-6
	48	Su4	well permeable	4,7*10^-6	7,2*10^-6
	48 – 158	St3/Sl4/Ls4	well permeable/transition zone	5*10^-6 – 2,3*10^-6	1,8*10^-6
P2/H3/A	20	Sl3	well permeable	5,4*10^-5	7,2*10^-6
	50	Su4	well permeable	4,7*10^-6	7,2*10^-6
	50 – 150	St3/Sl4/Ls4	well permeable/transition zone	5*10^-6 – 2,3*10^-6	1,8*10^-6
P2/H4/A	18	Ts4	transition zone/barely permeable	-	1,2*10^-6
	52	Ls4	transition zone	2,3*10^-6	1,8*10^-6
	82	Ls3	transition zone	1,5*10^-6	1,8*10^-6
	100	Lt2	barely permeable	1,5*10^-6	6,3*10^-7
	140	Su3	well permeable	8,7*10^-6	7,2*10^-6
	180	Su3	well permeable	8,7*10^-6	7,2*10^-6
P2/H5/A	18	Ts4	barely permeable	8,7*10^-6	1,2*10^-6
	42	Ls4	transition zone	2,3*10^-6	1,2*10^-6
	50	Lts	barely permeable	1,4*10^-6	1,2*10^-6
	97	Lts	barely permeable	1,4*10^-6	1,2*10^-6
	145	Lts	barely permeable	1,4*10^-6	1,2*10^-6
	178	Tu3	transition zone/barely permeable	3,1*10^-8	4,1*10^-7
P2/H6/A	18	Slu	well permeable/transition zone	4,7*10^-6	1,8*10^-6
	50	Slu	well permeable/transition zone	4,7*10^-6	1,8*10^-6
	92	Lu	transition zone	3*10^-6	3,6*10^-6
	140	Tu3	barely permeable	3,1*10^-6	4,1*10^-7
	180	Su3	well permeable	8,7*10^-6	7,2*10^-6
P2/H7/A	18	Sl4	well permeable/transition zone	5*10^-6	7,2*10^-6
	50	Su2	very well permeable	1,8*10^-6	1,7*10^-5
	102	Ls4	transition zone	2,3*10^-6	1,8*10^-6
	150	Ut4	transition zone	3,6*10^-6	3,6*10^-6
	201	Us	transition zone	4*10^-6	3,6*10^-6
	249	Ut3	transition zone	4,4*10^-6	3,6*10^-6
P2/H8/A	18	Lt2	barely permeable	1,5*10^-6	6,3*10^-7
	58	Su2	well permeable	1,8*10^-6	1,7*10^-5
	113	Us	transition zone	2,5*10^-6	3,6*10^-6
	145	Uls	transition zone	4,1*10^-6	3,6*10^-6

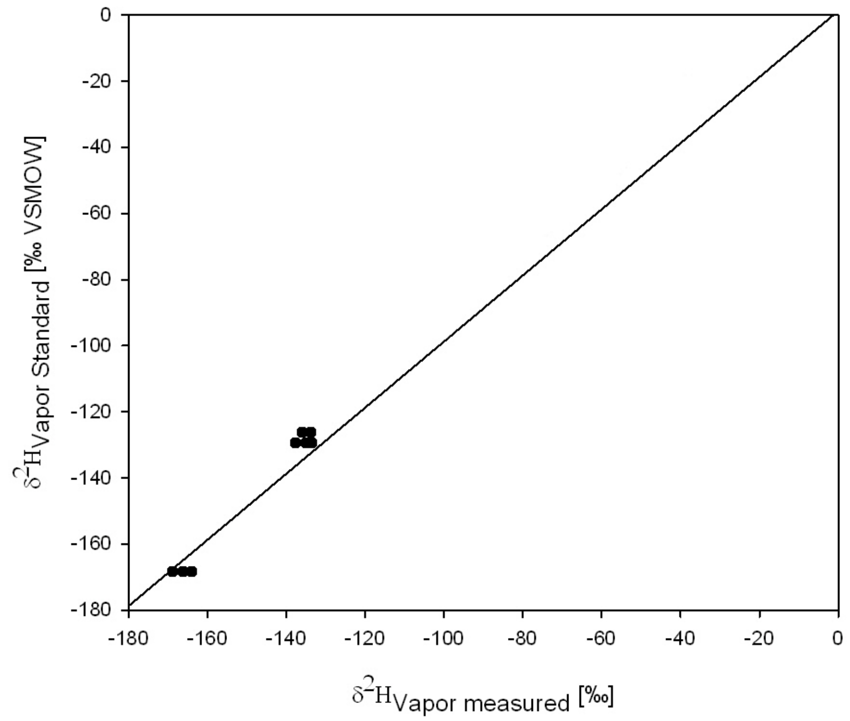

Figure A.3.: Measured ^{2}H vapor data versus standard ^{2}H vapor data.

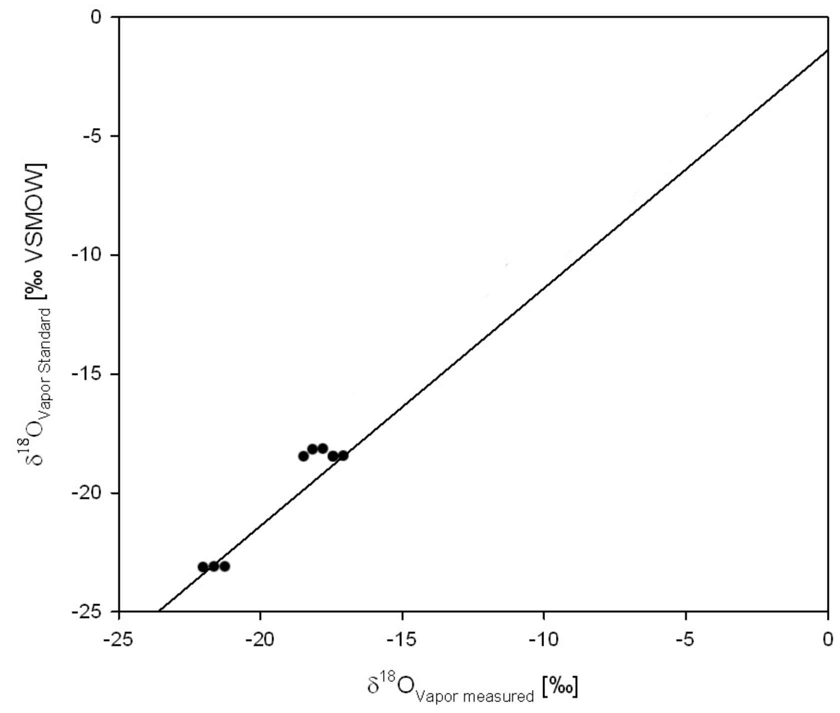

Figure A.4.: Measured ^{18}O vapor data versus standard ^{18}O vapor data.

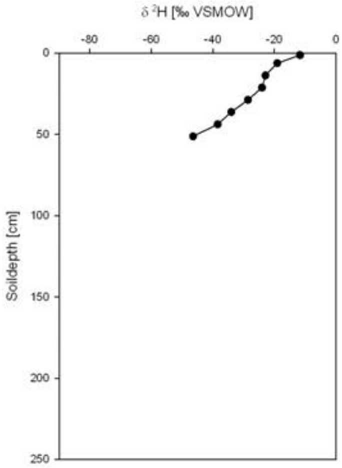

(a) Wild/P1/H1/A

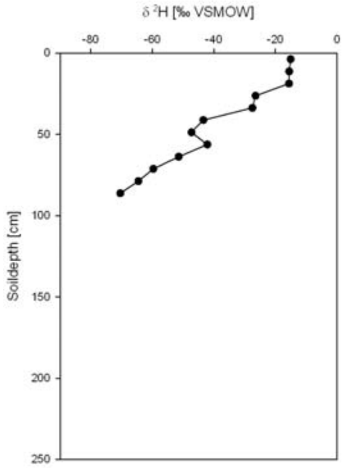

(b) Wild/P1/H1/B

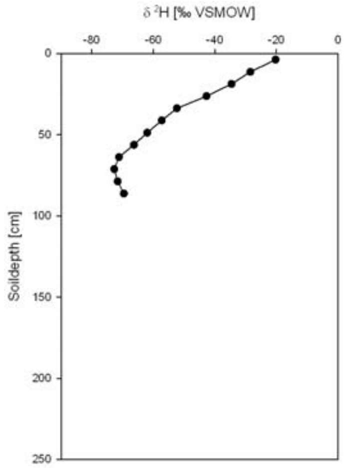

(c) Wild/P1/H2/A

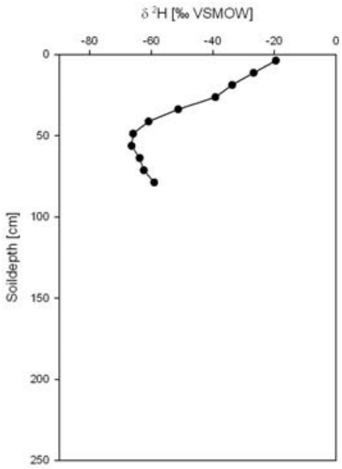

(d) Wild/P1/H3/A

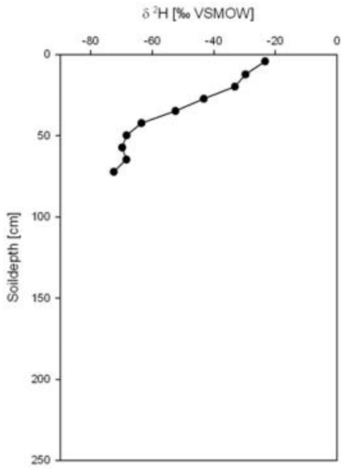

(e) Wild/P1/H4/A

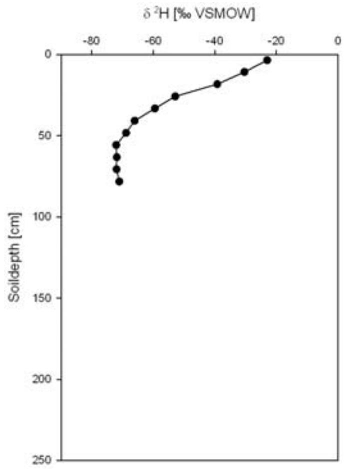

(f) Wild/P1/H5/A

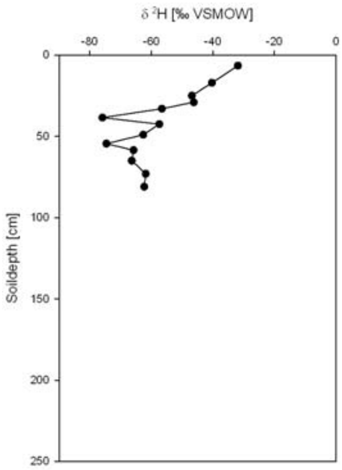

(g) Wild/P1/H6/A

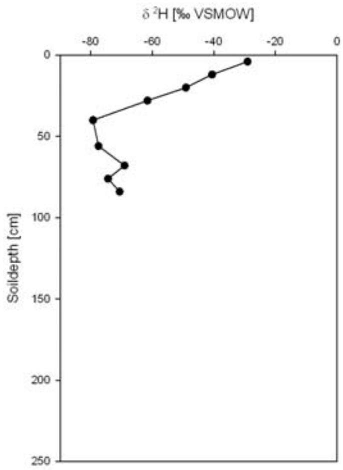

(h) Wild/P1/H7/A

Figure A.5.: $\delta^2 H$ profiles at hillslope transect Wild/P1.

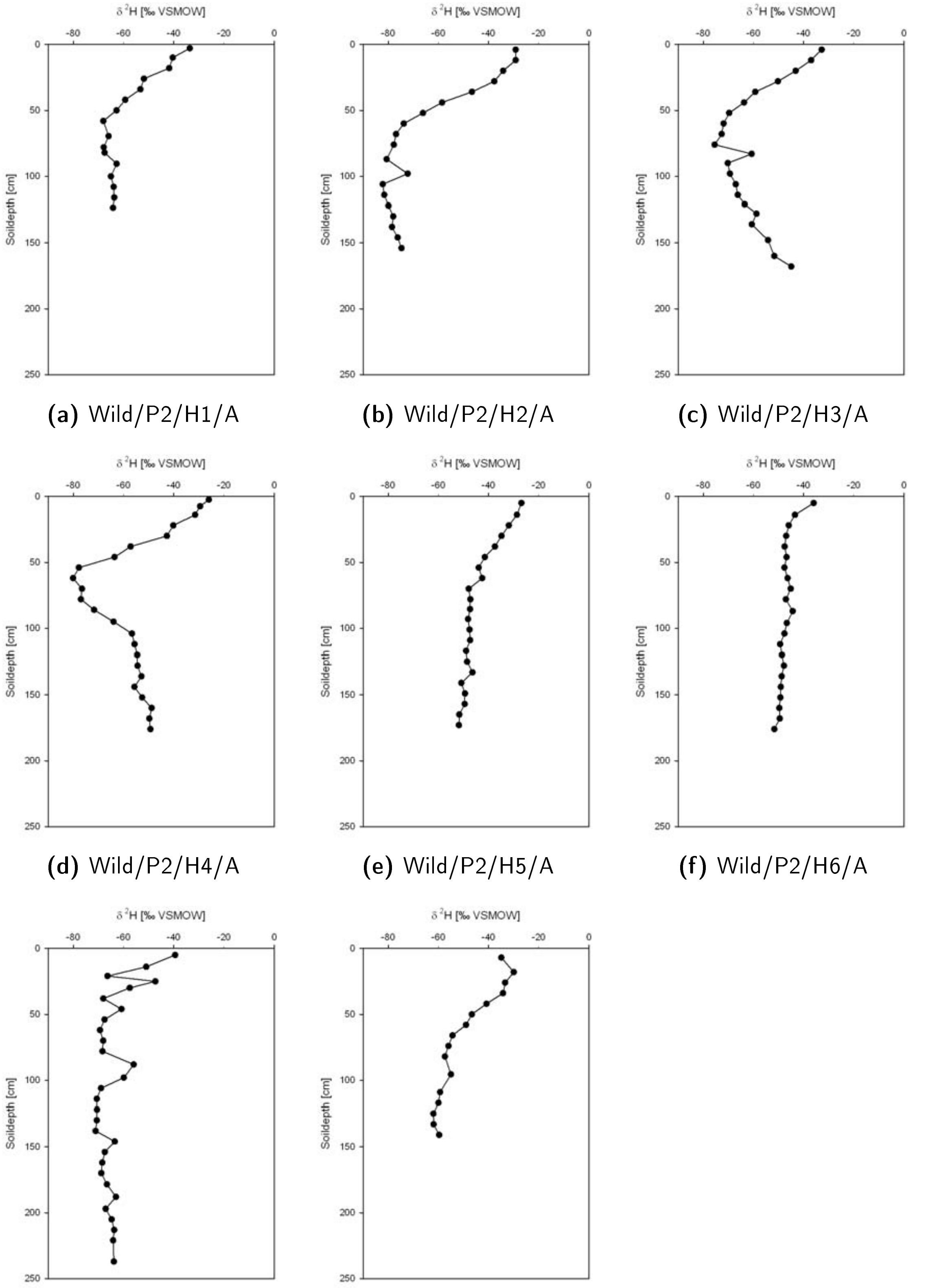

(a) Wild/P2/H1/A (b) Wild/P2/H2/A (c) Wild/P2/H3/A

(d) Wild/P2/H4/A (e) Wild/P2/H5/A (f) Wild/P2/H6/A

(g) Wild/P2/H7/A (h) Wild/P2/H8/A

Figure A.6.: $\delta^2 H$ profiles at hillslope transect Wild/P2.

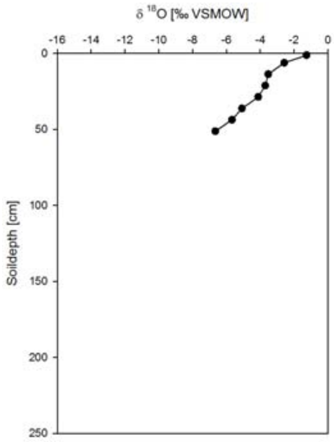

(a) Wild/P1/H1/A

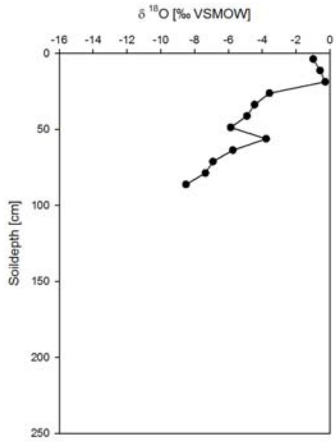

(b) Wild/P1/H1/B

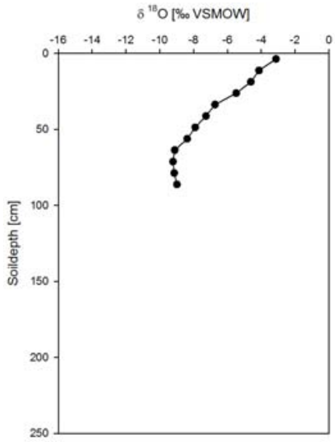

(c) Wild/P1/H2/A

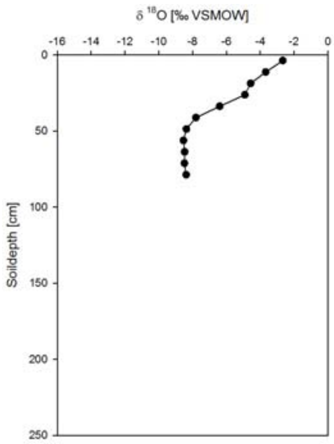

(d) Wild/P1/H3/A

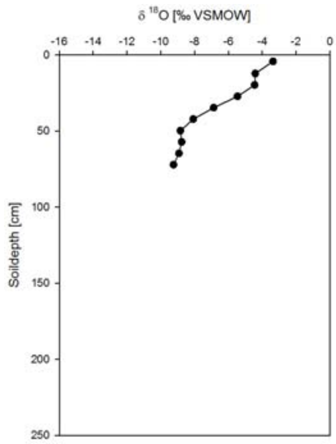

(e) Wild/P1/H4/A

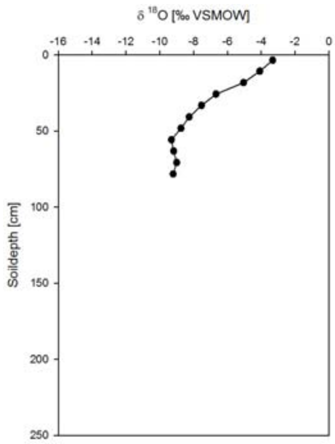

(f) Wild/P1/H5/A

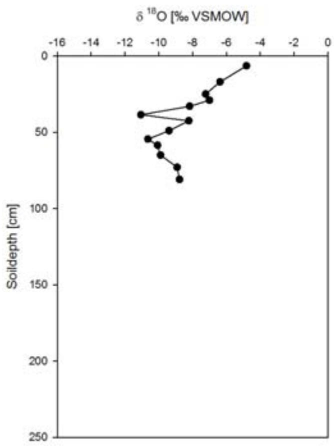

(g) Wild/P1/H6/A

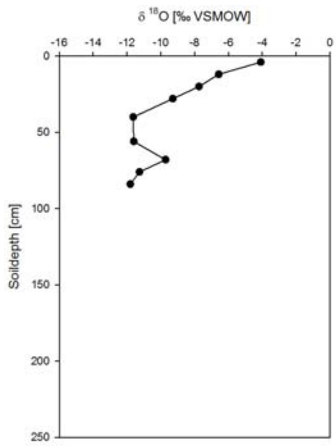

(h) Wild/P1/H7/A

Figure A.7.: $\delta^{18}O$ profiles at hillslope transect Wild/P1.

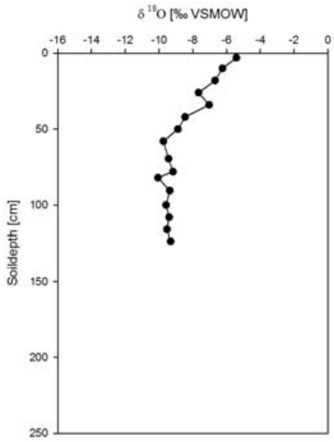

(a) Wild/P2/H1/A

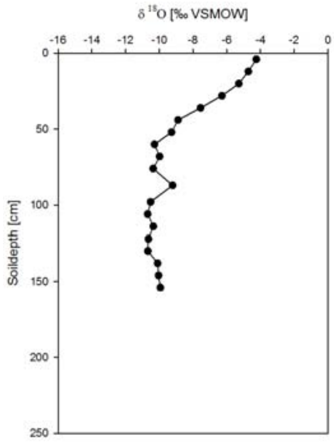

(b) Wild/P2/H2/A

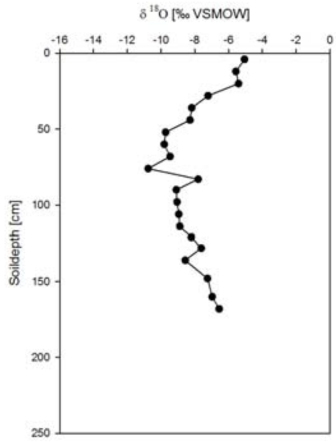

(c) Wild/P2/H3/A

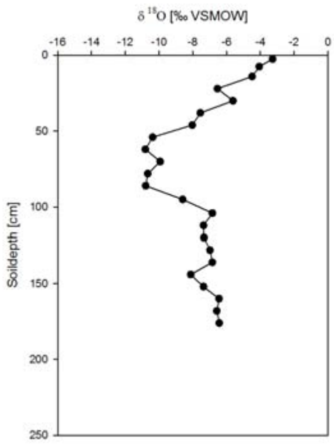

(d) Wild/P2/H4/A

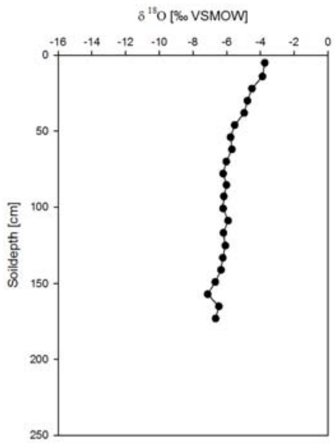

(e) Wild/P2/H5/A

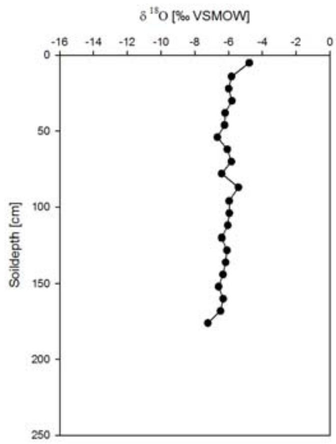

(f) Wild/P2/H6/A

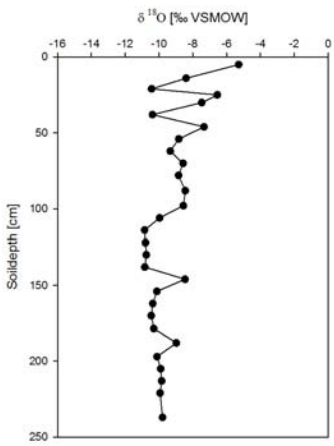

(g) Wild/P2/H7/A

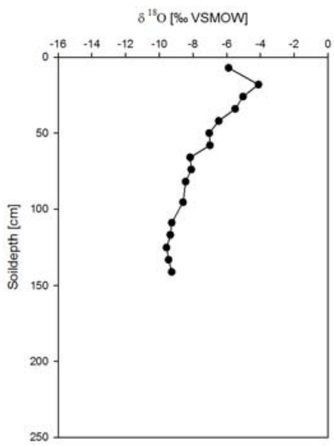

(h) Wild/P2/H8/A

Figure A.8.: $\delta^{18}O$ profiles at hillslope transect Wild/P2.

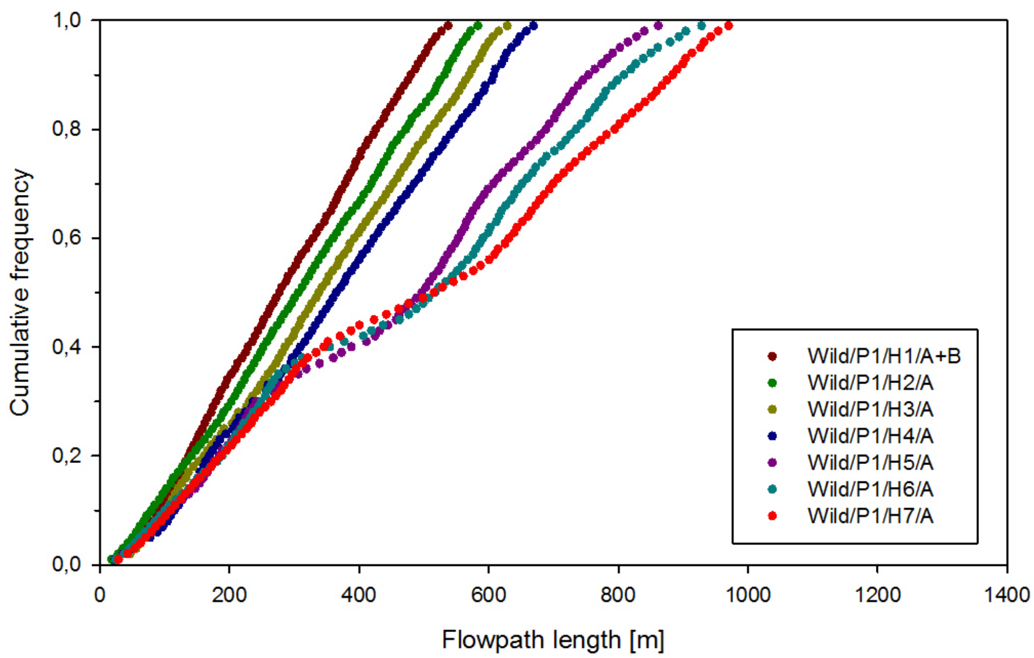

Figure A.9.: Empirical flowpath length distribution for the flowpath distances of the isotope profile catchments at hillslope transect Wild/P1. On the x-axis are the flow path lengths in m. On the y-axis the cumulative frequency F(x).

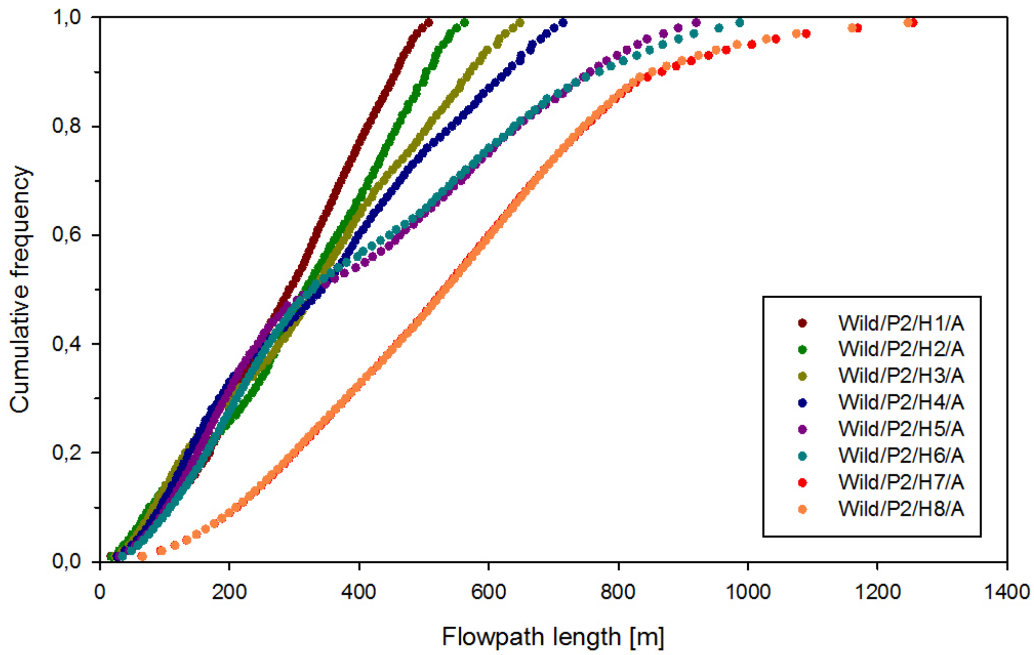

Figure A.10.: Empirical flowpath length distribution for the flowpath distances of the isotope profile catchments at hillslope transect Wild/P2. On the x-axis are the flow path lengths in m. On the y-axis the cumulative frequency F(x).

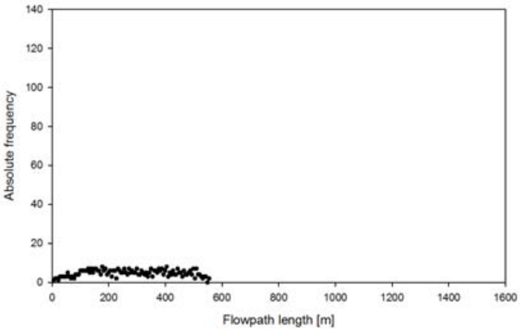

(a) Wild/P1/H1/A+B

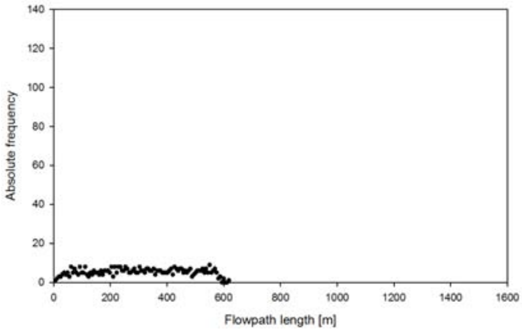

(b) Wild/P1/H2/A

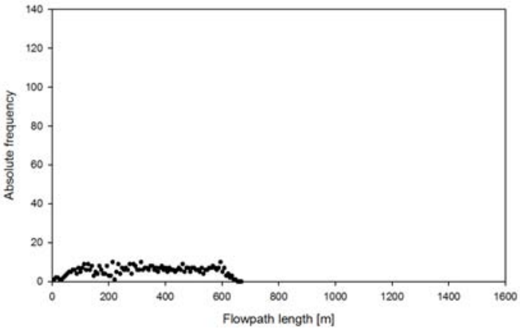

(c) Wild/P1/H3/A

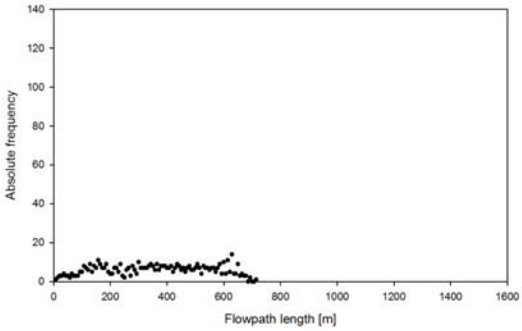

(d) Wild/P1/H4/A

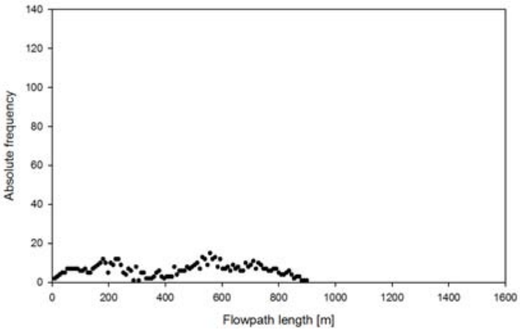

(e) Wild/P1/H5/A

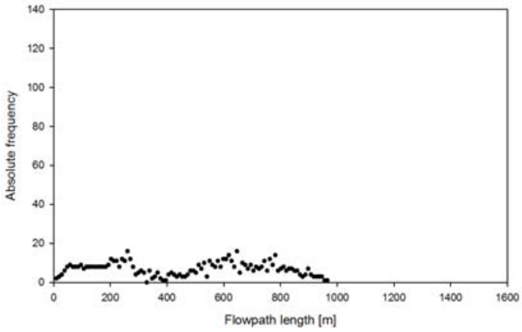

(f) Wild/P1/H6/A

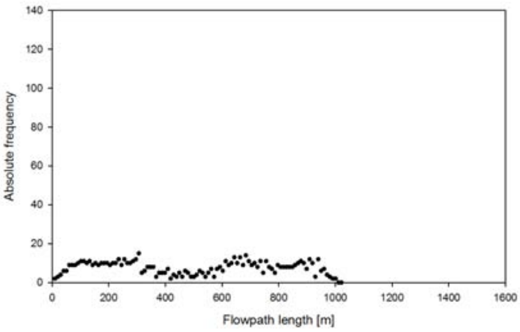

(g) Wild/P1/H7/A

Figure A.11.: Flowpath length distributions of the profile catchments at study transect Wild/1.

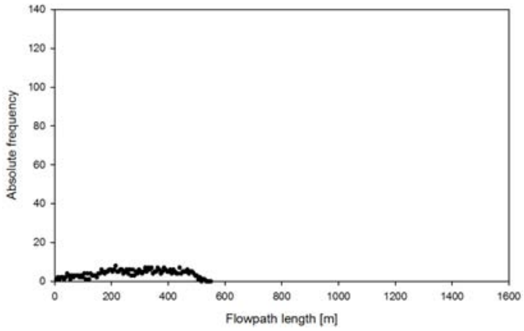

(a) Wild/P2/H1/A

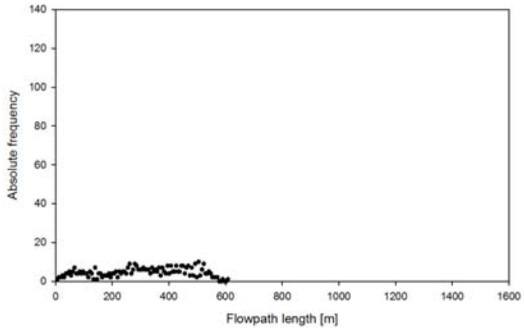

(b) Wild/P2/H2/A

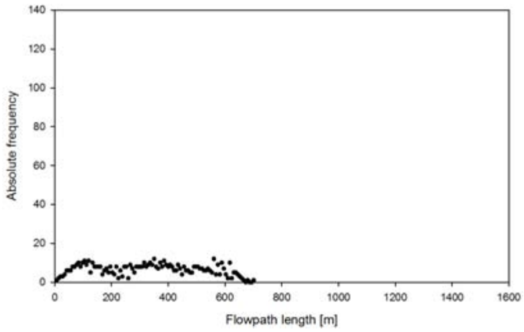

(c) Wild/P2/H3/A

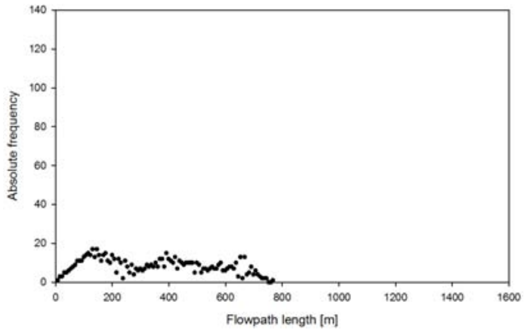

(d) Wild/P2/H4/A

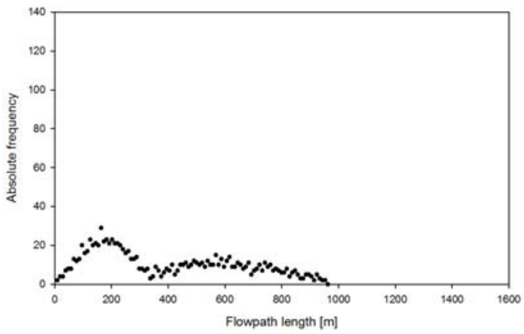

(e) Wild/P2/H5/A

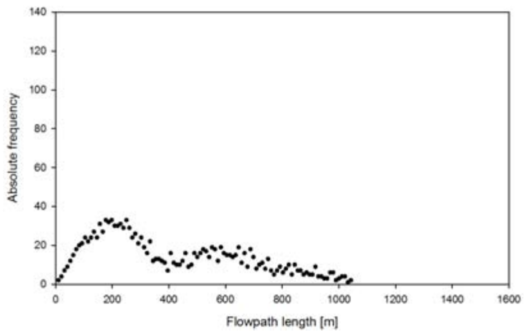

(f) Wild/P2/H6/A

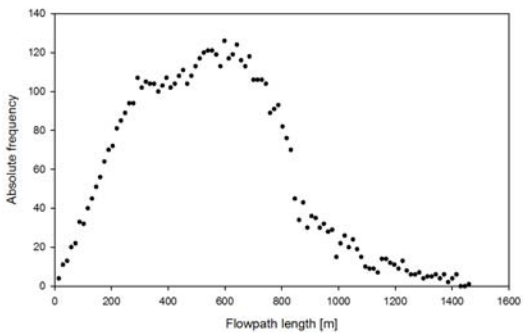

(g) Wild/P2/H7/A

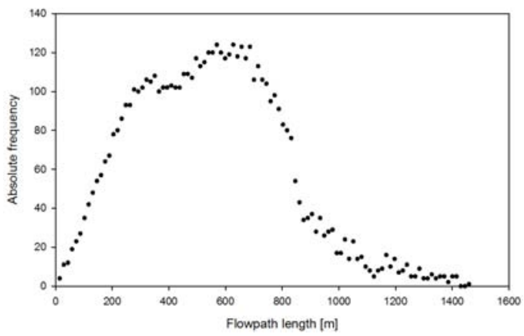

(h) Wild/P2/H8/A

Figure A.12.: Flowpath length distributions of the profile catchments at study transect Wild/2.

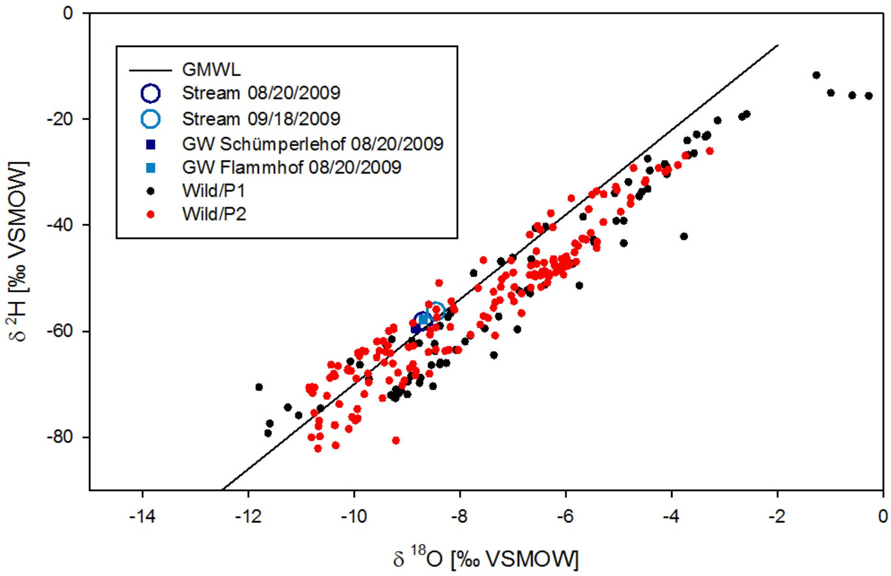

Figure A.13.: $\delta^{18}O$-$\delta^{2}H$ plot of the soil water at transects Wild/P1 and Wild/P2, streamwater and groundwater with the GMWL.

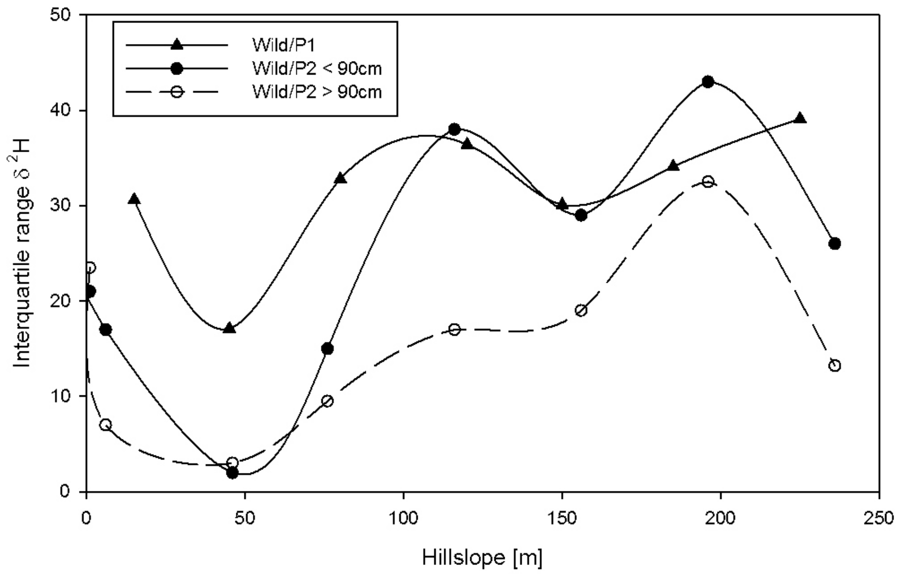

Figure A.14.: Interquartile range (IQR) of the deuterium profile data along the study hillslope.

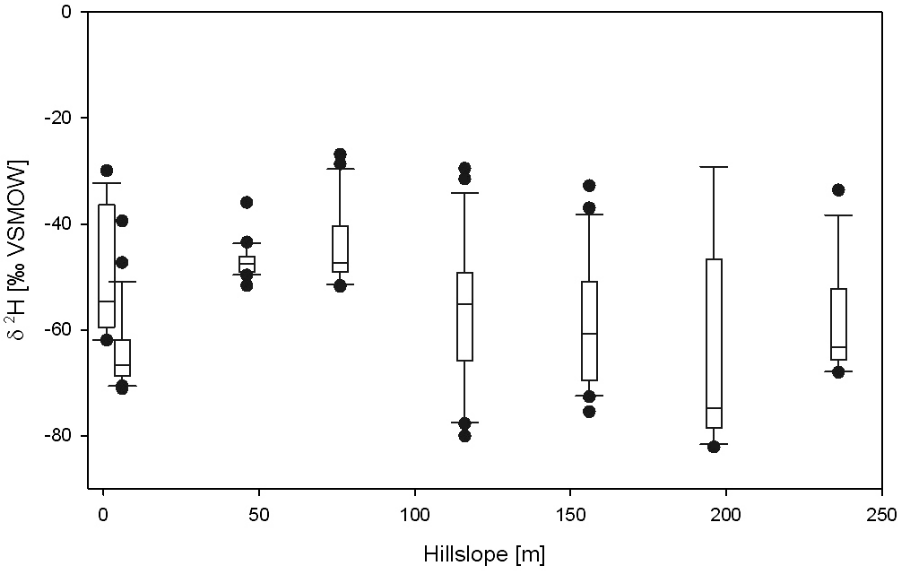

Figure A.15.: Boxplot with whiskers and outliers of the deuterium profile data sampled deeper than 90 cm below the surface along hillslope transect Wild/P2.

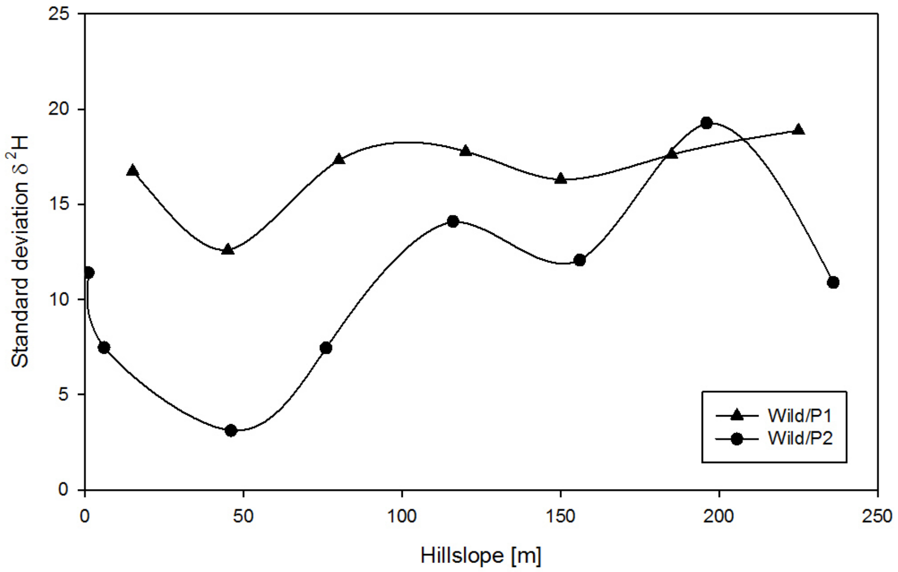

Figure A.16.: Standard deviation (SD) of the Wild/P1 profiles and the Wild/P2 profiles considered are the entire profile depths. Because of the differences in profile depths between the two transects, a direct comparison based on this figure is not possible.

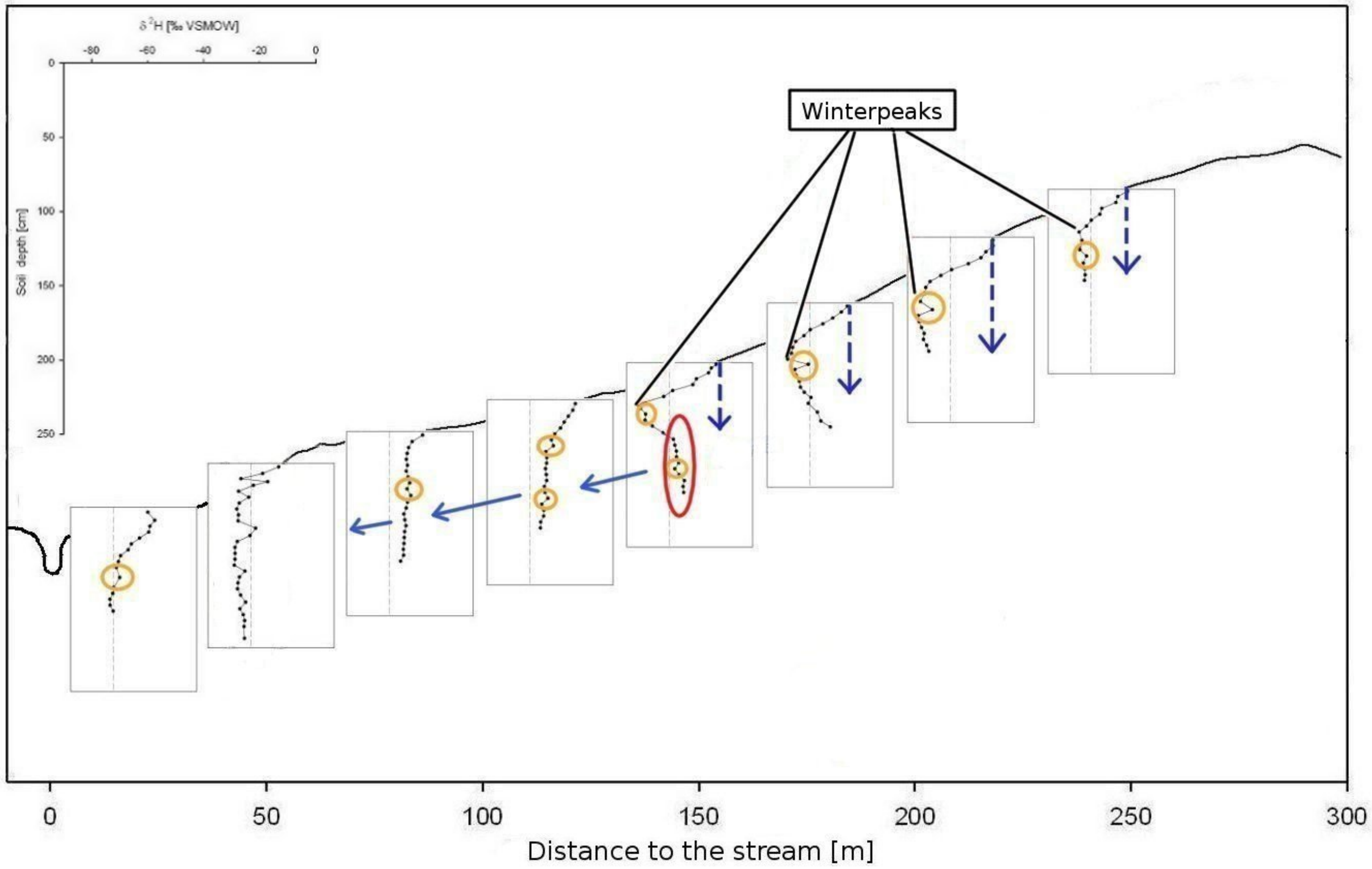

Figure A.17.: Conceptual illustration of possible hydrological processes on hillslope catena Wild/P2 based on the results of the various isotope profile (VIP) approach.

Bibliography

Abel U. (1998). Genese und Vegetation morphologischer Kleinstrukturen im Wildtal/Mittlerer Schwarzwald, Master's thesis, Institut für Landespflege der Albert-Ludwigs Universität, Freiburg i. Br.

AG-Boden (1994). Bodenkundliche Kartieranleitung, 4. Auflage, E. Schweizerbart'Sche Verlagsbuchhandlung, Hannover, 392 pp.

Allison G.B., Barnes C.J., Hughes M.W., Leaney F.W.J. (1984). Effect of climate and vegetation on oxygen-18 and deuterium profiles in soils, In: IAEA (ed.), Proceedings of the IAEA Symposium on Isotope Hydrology 1983, IAEA, Vienna, Austria, pp. 105–122.

Asano Y., Uchida T., Ohte N. (2002). Residence times and flow paths of water in steep unchaneled catchments, Tanakami, Japan, Journal of Hydrology, vol. 261 (1-4), pp. 173–192.

Barnes C.J., Turner J.V. (1998). Isotopic Exchange in Soil Water, In: C. Kendall, J.J. McDonnell (eds.), Isotope Tracers in Catchment Hydrology, Elsevier, Amsterdam, Lausanne, New York, Oxford, Shannon, Singapore, Tokyo, pp. 137–163.

Bear J. (1972). Dynamics of fluids in porous media, Elsevier, Mineola, New York, USA, 784 pp.

Bear J., Bachmat Y. (1984). Transport phenomena in porous media - basic equations, In: J. Bear, M.Y. Corapeioglu (eds.), Fundamentals of Transport Phenomena in Porous Media, M. Nijhoff, Dordrecht, The Netherlands, p. 1003.

Becker A. (1992). Methodische Aspekte der Regionalisierung, In: DFG: Regionalisierung hydrologischer Parameter, VCH-Verlag, Weinheim, pp. 16–32.

Beven K. (2006). Streamflow Generation Processes - Selection, Introduction and Commentary by Keith J. Beven, Benchmark Papers in Hydrology, IAHS Publications, Vienna, Austria, 431 pp.

Blöschl G. (1996). Scale and scaling in hydrology, Wiener Mitteilungen Band 132, Selbstverlag Institut für Hydraulik, Gewässerkunde und Wasserwirtschaft der Technischen Universität, Wien, 346 pp.

Blöschl G. (2005). Statistical Upscaling and Downscaling in Hydrology, In: M.G. Anderson, J.J. McDonnell (eds.), Encyclopedia of Hydrological Sciences, John Wiley & Sons, Ltd., The Atrium, Southern Gate, Chichester, West Sussex, England, pp. 135–154.

Blöschl G., Grayson R.B., Sivapalan M. (1995). On the representative elementary area (REA) concept and its utility for distributed rainfall-runoff modelling, Hydrological Processes, vol. 9, pp. 313–330.

Blöschl G., Sivapalan M. (1995). Scale issues in hydrological modelling: A review, Hydrological Processes, vol. 9, pp. 251–290.

Braud I., Bariac T., Vauclin M., Boujamlaoui Z., Gaudet J.P., Biron P., Richard P. (2005). SiSPAT-Isotope, a coupled heat, water and stable isotope transport model for bare soil. Part II. Evaluation and sensitivity tests using two laboratory data sets, Journal of Hydrology, vol. 309 (1-4), pp. 301–320.

Clark I.D., Fritz P. (1997). Environmental Isotopes in Hydrogeology, Lewis Publishers, Boca Raton, New York, 328 pp.

Craig H. (1957). Isotopic standards for carbon and oxygen and correction factors for mass-spectrometric analysis of carbon dioxide, Geochimica et Cosmochimica Acta, vol. 12, pp. 133–149.

Craig H. (1961). Variations in Meteoric Waters, Science Journal, vol. 133 (3465), pp. 1702–1703.

Criss R.E. (1999). Principles of Stable Isotope Distribution, Oxford University Press, 254 pp.

Dansgaard W. (1964). Stable isotopes in precipitation, Tellus, vol. 16, pp. 436–468.

Darling W.G., Bath A.H. (1988). A stable isotope study of recharge processes in the English chalk, Journal of Hydrology, vol. 101, pp. 31–46.

DeWalle D.R., Edwards P.J., Swistock B.R., Aravena R., Drimie R.J. (1997). Seasonal isotope hydrology of three Appalachian forest catchments, Hydrological Processes, vol. 11 (15), pp. 1895–1906.

Didszun J. (2004). Experimentelle Untersuchungen zur Skalenabhängigkeit der Abflussbildung, Freiburger Schriften zur Hydrologie Band 19, Selbstverlag Institut für Hydrologie der Albert-Ludwigs Universität, Freiburg i. Br., 234 pp.

Endreny T.A., Wood E.F. (2003). Maximizing spatial congruence of observed and DEM-delineated overland flow networks, International Journal of Geographical Information Science, vol. 17 (7), pp. 699–713.

Engelbrecht D.L.W. (2008). Natürliche Grundlagen von Gundelfingen und Wildtal, In: Gundelfingen und Wildtal - Die Geschichte beider Orte zum 1000jährigen Jubiläum Gundelfingens, Freiburger Grafische Betriebe, Freiburg i. Br., pp. 9–28.

Gazis C., Feng X. (2004). A stable isotope study of soil water: evidence for mixing and preferential flow paths, Geoderma, vol. 119 (1-2), pp. 97–111.

Gehrels J.C., Peeters J.E.M., de Vries J.J., Dekkers M. (1998). The mechanism of soil water movement as inferred from oxygen-18 stable isotope studies, Hydrological Sciences Journal, vol. 43 (4), pp. 579–594.

Geyer O.F., Gwinner M.P. (1991). Geologie von Baden-Württemberg, E. Schweizerbart'Sche Verlagsbuchhandlung, Stuttgart, 482 pp.

Gonfiantini R., Fröhlich K., Araguas-Araguas L., Rozanski K. (1998). Isotopes in Groundwater Hydrology, In: C. Kendall, J.J. McDonnell (eds.), Isotope Tracers in catchment Hydrology, Elsevier, Amsterdam, Lausanne, New York, Oxford, Shannon, Singapore, Tokyo, pp. 203–245.

Gottschalk L. (2005). Methods of Analyzing Variability, In: M.G. Anderson, J.J. McDonnell (eds.), Encyclopedia of Hydrological Sciences, John Wiley & Sons, Ltd., The Atrium, Southern Gate, Chichester, West Sussex, England, pp. 94–122.

Gralher B. (2009). Isotopenprofile in der flüssigen und gasförmigen Phase im Boden: Messung und Auswertung, Master's thesis, Institut für Hydrologie der Albert-Ludwigs Universität, Freiburg i. Br.

Grayson R.B., Western A.W., Chiew F.H.S., Blöschl G. (1997). Preferred states in spatial soil moisture patterns: Local and nonlocal controls, Water Resources Research, vol. 33 (12), pp. 2897–2908.

Groschopf R., Schreiner A. (1980). Geologische Karte von Baden-Württemberg 1:25000 - Erläuterungen zu Blatt 7913 Freiburg i. Br. - NO, Landesvermessungsamt Baden-Württemberg, Stuttgart, 112 pp.

Hädrich F., Moll W., Stahr K. (1988). Bodenentwicklung und Bodentypen, In: Breisgau-Hochschwarzwald: Land vom Rhein über den Schwarzwald zur Baar, Schillinger Verlag GmbH, Freiburg i. Br., pp. 53–69.

Hädrich F., Stahr K. (1997). Die Böden in der Umgebung von Freiburg i. Br., In: R. Mäckel, B. Metz (eds.), Schwarzwald und Oberrheintiefland - Eine Einführung in das Exkursionsgebiet um Freiburg im Breisgau, Selbstverlag Institut für Physische Geografie der Albert-Ludwigs Universität, Freiburg i. Br., pp. 137–212.

Hartge K.H., Horn R. (2009). Die physikalische Untersuchung von Böden, 4. Auflage, E. Schweizerbart'Sche Verlagsbuchhandlung, Stuttgart, 179 pp.

Horton J.H., Hawkins R.H. (1965). Flowpath of rain from the soil surface to the water table, Soil Science Journal, vol. 100, pp. 377–383.

Ingraham N.L. (1998). Isotopic Variation in Precipitation, In: C. Kendall, J.J. McDonnell (eds.), Isotope Tracers in Catchment Hydrology, Elsevier, Amsterdam, Lausanne, New York, Oxford, Shannon, Singapore, Tokyo, pp. 87–117.

Jencso K.G., McGlynn B.L., Gooseff M.N., Wondzell S.M., Bencala K.E., Marshall L.A. (2009). Hydrologic connectivity between landscapes and streams: Transferring reach- and plot-scale understanding to the catchment scale, Water Resources Research, vol. 45 (W04428).

Kendall C., McDonnell J.J. (1998). Isotope Tracers in Catchment Hydrology, Elsevier, Amsterdam, Lausanne, New York, Oxford, Shannon, Singapore, Tokyo, 839 pp.

Kendall C., McDonnell J.J., Gu W. (2001). A look inside black box hydrograph separation models: a study at the Hydrohill catchment, Hydrological Processes, vol. 15, pp. 1877–1902.

Kirchner J.W., Feng X., Neal C. (2001). Catchment scale advection and dispersion as a mechanism for fractal scaling in stream tracer concentrations, Journal of Hydrology, vol. 254, pp. 82–101.

Krause P. (1995). Auswahl eines repräsentativen Standortes einer Klimamessstation zur Datenaufnahme für die Modellierung der potentiellen Gebietsverdunstung im Bruggaeinzugsgebiet, Master's thesis, Institut für Hydrologie der Universität, Freiburg i. Br.

Majoube M. (1971). Fractionement en oxygene-18 et en deuterium entre l´eau et sa vapeur, Journal of Chemical Physics, vol. 68, pp. 1423–1436.

Maloszewski P., Rauert W., Stichler W., Hermann A. (1983). Application of flow models in an alpine catchment area using tritium and deuterium data, Journal of Hydrology, vol. 140 (1-4), pp. 343–360.

Maloszewski P., Stichler W., Zuber A., Rank D. (2002). Identifying the flow systems in a karstic-fissure-porous aquifer, the Schneealpe, Austria, by modelling of environmental oxygen-18 and tritium isotopes, Journal of Hydrology, vol. 256, pp. 48–59.

McConville C., Kalin R.M., Johnston H., McNeil G.W. (2001). Evaluation of recharge in a small temperate catchment using natural and applied oxygen-18 profiles in the unsaturated zone, Ground Water, vol. 39, pp. 616–623.

McDonnell J.J. (1990). A Rationale for Old Water Discharge Through Macropores in a steep, Humid Catchment, Water Resources Research, vol. 26 (11), pp. 2821–2832.

McDonnell J.J., Freer J., Hooper R., Kendall C., Burns D.A., Beven K. (1996). New method developed for studying flow on hillslopes, EOS, vol. 77 (47), pp. 465–472.

McDonnell J.J., Stewart M.K., Owens I.F. (1991). Effect of Catchment-Scale Subsurface Mixing on Stream Isotopic Response, Water Resources Research, vol. 27 (12), pp. 3065–3073.

McGuire K., McDonnell J.J. (2006). A review and evaluation of catchment transit time modeling, Journal of Hydrology, vol. 330 (3-4), pp. 543–563.

McGuire K.J., McDonnell J.J., Weiler M., Kendall C., Welker J.M., McGlynn B.L., Seibert J. (2005). The role of topography on catchment-scale water residence time, Water Resources Research, vol. 41 (W05002).

Mehlhorn J. (1998). Tracerhydrologische Ansätze in der Niederschlags-Abfluß-Modellierung, Freiburger Schriften zur Hydrologie Band 19, Selbstverlag Institut für Hydrologie der Albert-Ludwigs Universität, Freiburg i. Br., 148 pp.

Metz B. (1997). Glaziale Formen und Formungsprozesse im Schwarzwald, In: R. Mäckel, B. Metz (eds.), Schwarzwald und Oberrheintiefland - Eine Einführung in das Exkursionsgebiet um Freiburg im Breisgau, Selbstverlag Institut für Physische Geografie der Albert-Ludwigs Universität, Freiburg i. Br., pp. 51–74.

Moser H., Rauert W. (1980). Isotopenmethoden in der Hydrogeologie, Gebrüder Bornträger, Berlin, Stuttgart, 400 pp.

Mühr B. (2009). Klimadiagramme.
URL `http://www.klimadiagramme.de/rrnn.html(9/18/2009)`

Müller F. (2008). Die Landwirtschaft in Gundelfingen und Wildtal, In: Gundelfingen und Wildtal - Die Geschichte beider Orte zum 1000jährigen Jubiläum Gundelfingens, Freiburger Grafische Betriebe, Freiburg i. Br., pp. 29–37.

O'Callaghan J.F., Mark D.M. (1984). The extraction of drainage networks from digital elevation data, Computer Vision, Graphics and Image Processing, vol. 28, pp. 323–344.

Picarro (2009). Picarro Manual.
URL `http://www.Piccaro.com/assets(8/5/2009)`

Quinn P.F., Beven K., Chevallier P., Planchon O. (1991). The prediction of hillslope flow paths for distributed hydrological modeling using digital terrain models, Hydrological Processes, vol. 5, pp. 59–79.

Rawls W.J., Brakensiek D.L. (1989). Estimation of soil water retention and hydraulic conductivity, In: H.J. Morel-Sytoux (ed.), Unsaturated flow and hydrologic modeling - Theory and Practice, Kluver Academic Publishers, pp. 275–300.

Reggiani P., Sivapalan M., Hassanizadeh S.M. (1998). A unifying framework for watershed thermodynamics: balance equations for mass, momentum, energy and entropy, and the second law of thermodynamics, Advances in Water Resources, vol. 22 (4), pp. 367–398.

SAGA User Group (2009). SAGA GIS - System for Automated Geoscience Analyses.
URL `http://www.saga-gis.org/en/index.html(12/2/2009)`

Saxena R.K. (1984). Seasonal variations of oxygen-18 in soil moisture and estimation of recharge in esker and moraine formations, Nordic Hydrology, vol. 15, pp. 235–242.

Scheffer F., Schachtschabel P. (2002). Lehrbuch der Bodenkunde, 15. Auflage, Spektrum Akademischer Verlag, Heidelberg, Berlin, 593 pp.

Scherrer S. (2006). Bestimmungsschlüssel zur Identifikation hochwasserrelevanter Flächen, Landesamt für Umwelt, Wasserwirtschaft und Gewerbeaufsicht Rheinland-Pfalz (LUWG), Oppenheim, 126 pp.

Schlittgen R. (2003). Einführung in die Statistik - Analyse und Modellierung von Daten, 10. Auflage, Lehr- und Handbücher der Statistik, Oldenbourg Wissenschaftsverlag GmbH, München, 520 pp.

Sivapalan M., Kumar P., Harris D. (2001). Nonlinear propagation of multi-scale dynamics through hydrologic subsystems, Advances in Water Resources, vol. 24, pp. 935–940.

Skoien J.O., Blöschl G., Western A.W. (2003). Characteristic space scales and timescales in hydrology, Water Resources Research, vol. 39 (10).

Stewart M.K., McDonnell J.J. (1991). Modeling Base Flow Soil Water Residence Times from Deuterium Concentrations, Water Resources Research, vol. 27 (10), pp. 2681–2693.

Stober I. (1995). Die Wasserführung des kristallinen Grundgebirges, Ferdinand-Enke-Verlag, Stuttgart, 191 pp.

Systat (2004). SigmaPlot User´s Guide 9.0.
URL `http://www.physiol.ox.ac.uk/Computing/Online.../sigmaplot/spw8user.pdf(12/16/2009)`

Tarboton D.G. (1997). A new method for the determination of flow directions and upslope areas in grid digital elevation models, Water Resources Research, vol. 33 (2), pp. 309–319.

Tetzlaff D., Seibert J., McGuire K.J., Laudon H., Burns D.A., Dunn S.M., Soulsby C. (2009). How does landscape structure influence catchment transit time across different geomorphic provinces?, Hydrological Processes, vol. 23, pp. 945–953.

Trenkle H. (1988). Das Klima, In: Breisgau-Hochschwarzwald - Land vom Rhein über den Schwarzwald zur Baar, Schillinger Verlag GmbH, Freiburg i. B., pp. 83–95.

Uchida T., McDonnell J.J., Asano Y. (2006). Functional intercomparison of hillslopes and small catchments by examining water source, flowpath and mean residence time, Journal of Hydrology, vol. 327 (3-4), pp. 627–642.

Uhlenbrook S. (1999). Untersuchung und Modellierung der Abflussbildung in einem mesoskaligen Einzugsgebiet, Freiburger Schriften zur Hydrologie Band 10, Selbstverlag Institut für Hydrologie der Albert-Ludwigs Universität, Freiburg i. Br., 201 pp.

VandenBygaart A.J., Protz R. (1999). The representative elementary area (REA) in studies of quantitative soil micromorphology, Geoderma, vol. 89 (3-4), pp. 333–346.

Vitvar T., Aggarwal P.K., McDonnell J.J. (2005). A Review of Isotope Applications in Catchment Hydrology, In: P.K. Aggarwal, J.R. Gat, K.F.O. Froehlich (eds.), Isotopes in the Water Cycle: Past, Present and Future of a Developing Science, Springer, Dordrecht, The Netherlands, pp. 151–169.

WaBoa (2007). Wasser und Bodenatlas Baden-Württemberg, Digitale Version im Arbeitsmaßstab 1:200.000.

Walker G.R., Woods P.H. (1991). Inter-laboratory comparison of methods to determine the stable isotope composition of soil water, In: IAEA (ed.), Proceedings of the IAEA Symposium on Isotope Techniques in Water Resources Development, 11-15 March 1991, IAEA, Vienna, Austria, pp. 509–517.

Wassenaar L.I., Hendry M.J., Chostner V.L., Lis G.P. (2008). High resolution pore water delta deuterium and oxygen-18 measurements by water (liquid)-water (vapor) equilibration laser spectroscopy, Environmental Science and Technology, vol. 42 (24), pp. 9262–9267.

Wenninger J. (2007). Prozesshydrologische Untersuchung im System Boden-Vegetation-Atmosphäre, Freiburger Schriften zur Hydrologie Band 25, Selbstverlag Institut für Hydrologie der Albert-Ludwigs Universität, Freiburg i. Br., 151 pp.

Wood E.F., Sivapalan M., Beven K., Band L. (1988). Effects of spatial variability and scale with implications to hydrologic modeling, Journal of Hydrology, vol. 102 (1-4), pp. 29–47.

Woods R.A. (2005). Hydrologic Concepts of Variability and Scale, In: M.G. Anderson, J.J. McDonnell (eds.), Encyclopedia of Hydrological Sciences, John Wiley & Sons, Ltd., The Atrium, Southern Gate, Chichester, West Sussex, England, pp. 23–40.

Woods R.A., Sivapalan M., Duncan M.J. (1995). Investigating the representative elemetary area concept: an approach based on field data, Hydrological Processes, vol. 9, pp. 291–312.

Zimmermann U., Ehhalt D., Munnich K.O. (1967a). Soil-water movement and evapotranspiration: changes in the isotopic composition of the water, In: IAEA (ed.), Proceedings of the IAEA Symposium on Isotope Hydrology, IAEA, Vienna, Austria, pp. 567–585.

Zimmermann U., Münich K.O., Roether W. (1967b). Downward Movement of Soil Moisture Traced by Means of Hydrogen Isotopes, In: E.S. Glenn (ed.), Isotope Techniques in the Hydrologic Cycle, William Byrd Press, Inc., Richmond, Virginia, USA, p. 199.

Zimmermann U., Munnich K.O., Roether W., Kreuzt W., Schubach K., Siegel O. (1966). Tracers determine movement of soil moisture and evaporation, Science Journal, vol. 152, pp. 346–347.

Ehrenwörtliche Erklärung

Hiermit erkläre ich, dass die Arbeit selbständig und nur unter Verwendung der angegebenen Hilfsmittel angefertigt wurde.

Ort, Datum Unterschrift